

**Effects of perturbation of gut microbiota on host physiology:
In C57BL/6 and BALB/c mice models.**

By

Pratikshya Ray

LIFE11201404008

National Institute of Science Education and Research (NISER), Bhubaneswar.

A thesis submitted to the Board of studies in Life Sciences

In partial fulfillment of requirements for the Degree of

DOCTOR OF PHILOSOPHY

Of



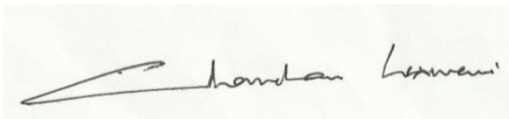
HOMI BHABHA NATIONAL INSTITUTE

December, 2020

Homi Bhabha National Institute

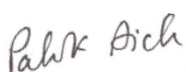
Recommendations of the Viva Voce Committee

As members of the Viva Voce Committee, we certify that we have read the dissertation prepared by Ms. Pratikshya Ray entitled "Effects of perturbation of gut microbiota on host physiology: In C57BL/6 and BALB/c mice models" and recommend that it may be accepted as fulfilling the thesis requirement for the award of Degree of Doctor of Philosophy.



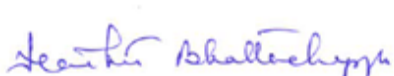
Chairman—Dr.ChandanGoswami

Date:17/05/2021



Guide/Convener—Dr.PalokAich

Date:17/05/2021



Examiner—Dr.MaitreeBhattacharyya

Date:17/05/2021



Member1—Dr.AsimaBhattacharyya

Date:17/05/2021



Member2—Dr.RamanujanSrinivasan

Date:17/05/2021



Member3—Dr.ShantibhusanSenapati

Date:17/05/2021

Final approval and acceptance of this thesis is contingent upon the candidate's submission of the final copies of the thesis to HBNI.

I/We hereby certify that I/we have read this thesis prepared under my/our direction and recommend that it may be accepted as fulfilling the thesis requirement.

Date: 17/05/2021

Place: NISER, Jatni



Dr. Palok Aich (Thesis Supervisor)

Publications in Refereed Journal:

Publications pertaining to thesis

a. Published

- **Pratikshya Ray**, Uday Pandey, and PalokAich. Comparative analysis of beneficial effects of Vancomycin treatment on Th1- and Th2-biased mice and the role of gut microbiota. *Journal of Applied Microbiology* published: 21 September 2020 (<https://doi.org/10.1111/jam.14853>)
- **Pratikshya Ray**, Uday Pandey, Debasmita Das, and PalokAich. Vancomycin induced changes in host immunity and behavior: Comparative genomic and metagenomic analysis in C57BL/6 and BALB/c mice. *Digestive Diseases and Sciences*. published: 1 January 2021 (<https://doi.org/10.1007/s10620-020-06729-x>)

b. Communicated:

- **Pratikshya Ray** and PalokAich. Effects of treatment with three antibiotics, AVNM, neomycin or vancomycin on C57BL/6 mice - A comparative analysis. (Communicated)

c. In preparation:

- **Pratikshya Ray**, Salila Pradhan and PalokAich. Cecal microbiota transplantation can confer young immunity into older mice.

Publications not pertaining to thesis

- Biswaranjan Pradhan, Dipanjan Guha, Krushnachandra. Murmu, Abhinav Sur, Pratikshya Ray, Debasmita Das, and PalokAich. Comparative efficacy analysis of anti-microbial peptides, LL-37 and indolicidin upon conjugation with CNT, in human monocytes.JNanobiotechnology;15:44,2017.

<https://jnanobiotechnology.biomedcentral.com/articles/10.1186/s12951-017-0278-1>

- Biswaranjan Pradhan, Dipanjan Guha, Pratikshya Ray, Debasmita Das, and PalokAich. Comparative Analysis of the Effects of Two Probiotic Bacterial Strains on Metabolism and Innate Immunity in the RAW 264.7 Murine Macrophage Cell Line. Probiotics Antimicrob Proteins: 2016. 1-12. 10.1007/s12602-016-9211-4.

<https://www.ncbi.nlm.nih.gov/pubmed/27038159>

Other Publication:

Conference Proceedings

- **Pratikshya Ray**, Debasmita Das and PalokAich. Effects of perturbation of gut microbiota on host physiology: Emphasis on metabolism and innate immunity; Poster no: NRSM/2017/0078, 13th NRSM, ACTREC, Mumbai , India,14th-15th December 2017.

• **Pratikshya Ray**, and PalokAich. Effects of treatment of antibiotics on gut microbiota and physiology of mice;Poster no: 299 – 6,AIIMS-ASM Conference "Antibiotic Resistance: Renewed Fight", New Delhi, India, 07th-08th September 2020

• **Pratikshya Ray**, Uday Pandey and PalokAich* A comparative analysis of different antibiotics treatment on gut microbiota. Conference on “INFECTIOUS DISEASE, MICROBIOME and PUBLIC HEALTH IN THE CURRENT SCENARIO”, NISER, Bhubaneswar, Odisha, India, 10th- 11thAugust, 2020.

A handwritten signature in blue ink that reads "Pratikshya Ray". The signature is fluid and cursive, with "Pratikshya" on the first line and "Ray" on the second line.

Signature of Student:

Date: 03-12-2020

STATEMENT BY AUTHOR

This dissertation has been submitted in partial fulfillment of requirements for an advanced degree at Homi Bhabha National Institute (HBNI) and is deposited in the library to be made available to borrowers under the rules of the HBNI.

Brief quotations from this dissertation are allowable without any special permission, provided that accurate acknowledgment of the source is made. Requests for permission for extended quotation from or reproduction of this manuscript in whole or in part may be granted by the competent authority of HBNI when in his or her judgment the proposed use of the material is in the interests of the scholarship. In all other instances, however, permission must be obtained from the author.

A handwritten signature in blue ink that reads "Pratikshya Ray". The signature is fluid and cursive, with "Pratikshya" on the top line and "Ray" on the bottom line.

Pratikshya Ray

Dt: 02-01-2021

DECLARATION

I, hereby declare that the investigation presented in the thesis has been carried out by me. The work is original and has not been submitted earlier as a whole or in part for a degree/diploma at this or any other Institution / University.

A handwritten signature in blue ink that reads "Pratikshya Ray". The signature is fluid and cursive, with "Pratikshya" on the first line and "Ray" on the second line.

Pratikshya Ray

Dt: 02-01-2021

DEDICATION

With great respect, I dedicate this thesis to my beloved parents who have been the source of inspiration and motivated me to pursue the Ph. D. program. Their guidance and endless support gave me the strength to achieve my goal.

ACKNOWLEDGEMENT

I am expressing my deepest gratitude to my Ph.D. supervisor Dr. PalokAich for his continuous support, valuable guidance, and constructive criticism that endured my enthusiasm for the completion of this project. His valuable suggestions and motivational advice throughout these years have made me believe in myself and brought out the best in me. He had given me sufficient freedom during my Ph.D. period that led tothe development of creative thinking and a sense of responsibility in me.

I would also avail this opportunity to express my sincere thanks to the director of NISER, Prof. Sudhakar Panda, for allowing me to work in this institute. I am very much gratified to my doctoral committee members Dr. Chandan Goswami, Dr. Asima Bhattacharyya, Dr. Ramanujan Srinivasan, and Dr.Shantibusan Senapati for their critical evaluation and valuable suggestions during every annual progress meeting.

I am thankful to my lab members Dr. SushriPriyadarhinee, Dr. Biswa Ranjan Pradhan, Ms. Debasmita Das, Dr. Dipanjan Guha, Ms. SohiniMukhopadhay, Mr. Raktim Mukherjee, Mr. Uday Pandey, Mr. Dhyanendra Chauhan, Ms. Salila Pradhan, and Ms. Swati Panda for their continuous help and inspiration in completing this work. I appreciate all my batch mates for their constant support, interactive discussions, and motivational words throughout the work which kept me going. I am grateful to all the faculty members and staff of SBS for their blessings and encouragement. I acknowledge the central instrumentation facilities, Animal house staff, library staff, and timely help received from the academic, non-academic staff at NISER. My parents are the greatest motivational force behind me in completing my work and perhaps no word of acknowledgment is sufficient for them. I am highly indebted to my husband Mr. Sasanka Sekhar Lenka for his constant support, encouragement, and inspiration duringthe difficult phase of my life. A special thanks to my Younger brothers and sister for their encouragement and support. With lots of Love, I would like to appreciate my daughter Shivanshi for her unconditional love and affection.

Table of Contents

1.1 Gut microbiota	24
1.2 Constitution of the gut microbiota in the mammal:	25
1.3 Development of gut microbiota:	28
1.4 Functions of gut microbiota in host:	30
1.5 Role of gut microbiota in immune homeostasis:	32
1.5.1 Various functions of gut microbes in the evolution of the innate immune system	32
1.5.2 Role of gut microbiota in adaptive immune homeostasis:	34
1.6 Gut microbiota regulates the different metabolism and production of various metabolites of the host.	36
1.6.1 Function of gut microbiota for the production of different Short-chain fatty acids.....	36
1.6.2 Function of gut microbiota during different metabolic diseases of the host.	40
1.7 Gut microbiota regulates the production of different hormones.....	41
1.8 Role of gut microbiota on stress and behavior of host (HPA axis).....	43
1.9 Different ways to perturb the gut microbiota:	46
1.10 Use of BALB/c and C57BL/6 mice as model organisms for the gut microbiota perturbation study.	49
1.11 Restoration of gut microbiota	50
1.12 Fecal microbiota transplantation	50
1.13 Different methods to study gut microbiota:	59
Chapter: 2	62
Materials and Methods	62
2.1 Animals Used in the study:.....	63
2.2 Vancomycin treatment	63
2.3 Restoration procedure.....	63
2.4 Sample collection	64
2.5 Cecal Sample plating.....	65
2.6 Genomic DNA extraction	63
2.7 16S-rRNA sequencing (V3-V4 Metagenomics) of gut microbiota	65
2.8 RNA extraction	66
2.9 cDNA preparation from extracted RNA.....	67

2.10 Real-time PCR (qRT-PCR)	67
2.11 Cytokine Analysis at the protein level	67
2.12 Serum collection.....	68
2.13 Measurement of Cecal index	68
2.14 Gut permeability test by FITC dextran.....	68
2.15 Cecal Microbiota Transplantation (CMT).....	68
2.16 Oral Glucose tolerance test (OGTT)	69
2.17 Sample preparation and NMR data acquisition for metabolomics study	69
2.18 Metabolomic Analysis of NMR data.....	70
2.20 Endotoxin detection assay from serum:	70
2.21 Acetate detection assay in serum:	70
2.22 Hormonal assay:	71
2.23 Elevated plus maze test:	71
2.24 Forced swim test (FST):	72
2.25 Open field (OF) test:.....	73
2.26 Animals Used in the CMT study:.....	74
2.27 <i>Salmonella Typhimurium</i> (ST) culture and dose standardization:	75
2.28 Cecal microbiota transplantation (CMT):.....	75
2.29 Grouping and Sample collection of mice:	77
2.30 Treatment with other antibiotics	77
2.31 Statistical Analysis	78
Chapter: 3	79
Results and Discussion.....	79
Chapter 3.1: Perturbation of gut microbiota through Vancomycin and its effect on the physiology of Th1- and Th2-biased mice.....	80
3.1.1 Introduction:.....	80
3.1.2 Results:	81
3.1.3 Discussion.....	107
Chapter 3.2: Restoration kinetics of gut microbiota following the cessation of vancomycin treatment and its consequence on the physiology of Th1- and Th2- biased mice.....	113
3.2.1 Introduction:.....	113

3.2.2 Results:	115
3.2.3 Discussion.....	137
Chapter 3.3 Comparative study of different antibiotics treatment on gut microbiota and immune system of the host.....	141
3.3.1 Introduction:.....	141
3.3.2 Results:	143
3.3.3 Discussion:.....	156
Chapter 3.4: Effect of Cecal microbiota transplantation from younger to older mice following antibiotic-induced gut microbial dysbiosis.....	160
3.4.1 Introduction:.....	160
3.4.2 Results:	161
3.4.3 Discussion:.....	173
Chapter: 4	175
Summary and Conclusions	175
Chapter: 5	184
References	184

List of Figures and Tables

Chapter 1: General Introduction& Review of Literature.

Figure 1.1: Schema showing the development of gut bacteria with age from the gestation period to old age [64,65].	29
Figure 1.2: Major functions of gut microbiota in the host.	31
Figure 1.3: Gut microbiota-produced SCFAs (Acetate, propionate, butyrate) in regulating the immune system of the host [131].....	39
Figure 1.4: The two-way relationship between gut-microbiota and gut-brain axis [203]. Gut microbes communicate with the gut-brain-axis through endocrine, immune, neuronal, and hormonal pathways [203]......	45
Figure 1.5: Different ways to perturb and restore the gut microbiota.....	46
Figure 1.6: Schematic diagram of the 16s rRNA gene.	60

Table 1.1: The organization of the gut microbiota at various portions of the gastrointestinal tract of mammals [11]......	26
Table 1.2: Alteration in the gut bacterial population during different metabolic diseases.	40
Table 1.3: Alteration pattern of gut microbiota following different antibiotics treatment.	52
Table 1.4: Altered profile of gut bacteria following different cocktails of antibiotics treatment..	54
Table 1.5: Altered gut microbiota profile during antibiotics therapy and subsequent recovery period.....	56

Chapter 2: Materials and methods

Figure 2.1: A schema of the experimental protocol for perturbation and restoration of gut microbiota is shown below.....	64
Figure 2.2: An image of elevated plus-maze instrument.....	72
Figure 2.3: An image of forced swim test.....	73
Figure 2.4: An image of open field test.....	74
Figure 2.5: Timeline of the experimental procedure for Cecal microbiota transplantation from younger to older mice and other host physiology related study.....	76.

Chapter3.1: Perturbation of gut microbiota through vancomycin and its effect on the physiology of Th1- and Th2-biased mice.

Figure 3.1.1: Kinetic of perturbation of gut microbiota following different antibiotics treatment in Th1- and Th2- biased mice.....	82
Figure 3.1.2: Phylum level changes in the gut microbiota.....	86
Figure 3.1.3: Metagenomic analysis of genus-level variation of gut microbiota in vancomycin treated and its respective control group of mice.....	89
Figure 3.1.4: Transcriptional gene expression profile of different immune genes	93
Figure 3.1.5: Protein level gene expression and comparative analysis of qRT PCR and ELISA..	95
Figure 3.1.6: Measurement of intestinal integrity of BALB/c and C57BL/6 mice following treatment with Vancomycin.....	98
Figure 3.1.7: Glucose and SCFA level in the serum of mice	101

Figure 3.1.8: Alteration in the concentration of select hormones during vancomycin treatment.....	105
Figure 3.1.9: Graphical representation of vancomycin induced perturbation of gut microbiota and its effect on the physiology of BALB/c and C57BL/6 mice.	112
Table 3.1.1: Measurement of the cecal index and cecal liquid content at different time points in BALB/c and C57BL/6 mice.	87
Table 3.1.2: 16S qPCR detection of <i>A. muciniphila</i> bacteria abundance in cecal samples of treated and control mice.	90
Table 3.1.3: The abundance of various SCFAs and associated metabolites in untreated (control) and vancomycin treated BALB/c and C57BL/6.	103
Table 3.1.4: Sequences of forward (_F) and reverse (_R) primers for PCR studies to confirm the presence and expression level of various genes used in this study.	106

Chapter 3.2: Restoration kinetics of gut microbiota following the cessation of vancomycin treatment and its consequence on the physiology of Th1- and Th2- biased mice.

Figure 3.2.1: Composition of gut microbiota at phylum level during perturbation and restoration period.....	118
Figure 3.2.2: Behavioral studies following treatment with vancomycin	125
Figure 3.2.3: Transcriptional profile of different genes in the brain of mice.	128
Figure 3.2.4: Transcriptional profile (by qRT-PCR) of various immune genes and tight junction genes in the colonic tissue of mice during vancomycin perturbation and restoration period.	131

Figure 3.2.5: The alteration patterns of Shannon diversity index of gut microbiota and IgA level were compared.....	134
---------------------------------------------------------------------------------------------------------------------	-----

Table 3.2.1: Percent abundance of major phyla of gut microbiota during vancomycin perturbation and restoration.....	118
Table 3.2.2: Percent abundance of major phyla of gut microbiota during vancomycin perturbation and restoration.....	120
Table 3.2.3: Measurement of the cecal index at different time points of perturbation and restoration periods in BALB/c and C57BL/6 mice.....	132
Table 3.2.4: Comparison of Firmicutes to Bacteroidetes ratio (F/B) at different time points of BALB/c and C57BL/6 mice.....	134
Table 3.2.5: Sequences of forward (_F) and reverse (_R) primers for qRT-PCR studies to confirm the presence and expression level of various genes used in this study.....	135

Chapter 3.3: Comparative study of different antibiotics treatment on the gut microbiota and immune system of the host.

Figure 3.3.1: Alteration of the gut microbiota following antibiotic treatment.....	144
Figure 3.3.2: Effect of antibiotic treatment on the diversity of gut microbial composition.....	146
Figure 3.3.3: Transcriptional profile of different immune regulatory genes in the colon of mice following antibiotics.....	148
Figure 3.3.4: The abundance of select metabolites in the serum of mice by chemometric1H-NMR studies.....	150

Figure 3.3.5: Comparative relationship between anxiety and gut Proteobacteria level in mice. 152

Table 3.3.1: Percent abundance of major phyla of gut microbes in the untreated control and different antibiotics treated mice.	153
Table 3.3.2: Sequences of forward (_F) and reverse (_R) primers for PCR studies to confirm the expression of various genes used in this study.	154
Table 3.3.3: Bodyweight of mice during antibiotic treatment.....	154
Table 3.3.4: Daily Fluid consumption (ml/day) of mice during AVNM treatment.....	155

Chapter3.4: Effect of Cecal microbiota transplantation from younger to older mice following antibiotic-induced gut microbial dysbiosis.

Figure 3.4.1: The survivability rate of mice at different ST doses..	162
Figure 3.4.2: Pie chart showing gut microbial composition at the phylum level.	166
Figure 3.4.3: Gut microbial diversity and cecal index of mice	168
Figure 3.4.4: Expression of immune and tight junction protein genes in the colon of mice following antibiotic treatment and restoration period.	170
Figure 3.4.5: Pathway analysis of different metabolites following antibiotic treatment and restoration period.	172

Chapter: 4

Summary and Conclusions

The present work concludes a few significant outcomes of the study. The study aimed to understand the role of gut microbiota following treatment with select antibiotics. We treated immunologically different Th1- and Th2-biased mice models with various antibiotics. Since host genetics is the most critical factor in controlling gut microbiota composition (388), we used C57BL/6 (Th1 biased) and BALB/c (Th2-biased) mice. C57BL/6 and BALB/c are two genetically different inbred strains with other characteristics, a) immunological bias and b) baseline microbiota compositions (226,227,229). Perhaps because of different immune biases and varied gut microbial composition, C57BL/6 and BALB/c mice behaved differently following treatment with antibiotics and Microbiota transplantation. Both perturbation and restoration efficiency and pattern of gut microbiota varied significantly between two strains of mice at the same dose and duration of antibiotic treatment.

A comparative analysis of Th1- and Th2-biased animals is essential to understand a) the roles of inflammatory (Th1) and tolerogenic (Th2) bias of the animal and their responses against a challenge or disease. We also know those asthmatic individuals or conceives are more Th2-biased immunologically than normal healthy states. By comparing Th1- and Th2- biased mouse models, one can understand the host's differential genetic and microbial contributions to a threat or environmental changes. The current study established the microbial bias of Th1- over Th2-biased animals and vice-versa. This information is essential to understand and maintain health.

Gut microbes could produce metabolites like acetate, propionate, and butyrate that belong to SCFAs by metabolizing various dietary fibers in the host (100). Firmicutes, specifically the Clostridium group present in the gut, produce short-chain fatty acids like acetate, butyrate, propionate from complex carbohydrate foods (100). Bacteria of Instentimonas genus (Firmicutes phylum) produces butyrate from lysine, and Bacteroidetes produces propionate from threonine in

the gut (101,102). Butyrate is one of the essential SCFAs that supplies energy to the host's colonocytes and helps maintain intestinal homeostasis via stimulating the production of regulatory T cells and anti-inflammatory cytokines (111). SCFAs in the gut suppress the LPS and pro-inflammatory cytokines like TNF- α , IL-6 level and increased the production of anti-inflammatory cytokines like IL-10 (103,104). Butyrate enhanced the anti-inflammatory effects of the intestinal mucosa by inhibiting the histone deacetylases (HDACs) and stimulating the G protein-coupled receptors (GPCRs) present in intestinal epithelial cells (IECs) of the host (100). In the colon tissue, we observed that butyrate caused inhibition of the lipopolysaccharide-induced activation of NF- κ B through GPR109A and I κ B α degradation (112,349,389). During the dysbiosis of gut microbiota, the increase in the pathogenic Gram-negative group of bacteria caused a rise in the blood endotoxin level through their LPS which enhanced the production of various pro-inflammatory cytokines by activating different Toll-Like Receptors (TLR4) of the gut epithelial cells (105–107,169,170). The Increased level of inflammatory cytokine s was associated with the higher gut permeability in the host by repressing the expression of tight junction proteins like occludin and claudin 1 (126,127). SCFA, butyrate, in particular, has a vital role in maintaining gut integrity (123,124)

it was observed that during obesity and diabetes, metabolic endotoxemia condition commonly appeared in the host where endotoxin (LPS) level increased in the blood, causing inflammation and impaired glucose metabolism (169,170). In the current study, the increased glucose and serum insulin level following antibiotic treatment were associated with the higher abundance of Proteobacteria and endotoxin level of the host, however, decreased glucose level associated with the abundance of *A. muciniphila* bacteria.

The long-term use of antibiotics disrupted the diversity and composition of the gut microbiota, which affects the pathogenesis of inflammatory bowel disease (390). A significant increase in specific opportunistic pathogens, resistant bacteria like *Clostridium difficile*, and a decrease in beneficial butyrate-producing bacteria like *Roseburia hominis*, *Faecalibacterium prausnitzii*, and *Eubacterium rectale* were observed in IBD patient compared to healthy individuals (391).

The fecal sample of IBD and long-term antibiotic usage patients contained a significantly less amount of SCFA, which could be associated with a higher range of inflammation in the host (100,333,392). The restoration of gut microbiota following long-term antibiotic therapy was a time taking incomplete process (234).

The advantage of using mice models is their small size and can be easily maintained and inbred to study various human diseases. Nearly 85% of mice and the human genome is conserved, and specifically, the regulatory networks of transcription factors are strongly conserved between them. Though the anatomical, histological and physiological characters of mice and human intestinal tract and the composition of gut microbiota were shared, many differences were observed, which limit the translation of the results from the mice to human (26).

The current study revealed that the perturbation of gut microbiota is an effective way to understand the role of the gut microbiome. The study elucidated the efficacy of select antibiotics in perturbing the gut microbiota and how the different gut microbiota compositions following perturbation could affect the host immunity and metabolism to regulate health. The present work also unveiled the pertaining effects of various factors like the age and genetics of the host, types, and duration of antibiotic treatment on the perturbation and restoration patterns of the gut

microbiota. The current study addresses specific potential ideas on how gut microbial perturbation patterns following treatment with various select antibiotics directly affect dynamics of different host physiology. We found both beneficial and adverse effects of gut microbial dysbiosis in the host depending on the types of microbes and their presence or absence in the gut during various antibiotic treatments.

The key findings are listed below for a quick review.

Key findings

- ❖ The healthy gut of C57BL/6 and BALB/c mice contained mainly Firmicutes and Bacteroidetes phyla and a meager percentage of Proteobacteria phylum. However, the abundance of each major phylum of gut microbiota varied between these two strains of mice. Variation in the host genetics caused the difference in the constitution of gut microbiota of Th-1 (C57BL/6) and Th2- (BALB/c) biased mice before antibiotic treatment.
- ❖ Effects following treatment with vancomycin
 - Vancomycin treatment caused a time-dependent alteration pattern of gut microbiota. Initial doses caused a decrease in the abundance of Firmicutes, Bacteroidetes, and an increase in pathogenic Proteobacteria phyla, while later doses reduced the Proteobacteria abundance and increased the Verrucomicrobia phylum.
 - The pathogenic Proteobacteria phylum mainly contained *E.coli* and *Shigella*, while the Verrucomicrobia phylum mainly contained *Akkermansiamuciniphila* bacteria.

- The changes in gut microbiota altered the host physiology in a time-dependent manner. Vancomycin treatment for the first four days significantly enhanced Pro-inflammatory gene expression and gut permeability. The anxiety and depressive behavior of mice also increased with the altered expression of stress-related genes in mice's brains during this period.
- Continued treatment with vancomycin beyond day 4 reduced the abundance of Proteobacteria and enhanced the abundance of *A. muciniphila* of Verrucomicrobia phylum. Enhanced *A. muciniphila* conferred beneficiary effects such as an increased anti-inflammatory gene expression in the gut and brain and decreased gut permeability. The stress level of mice also reduced on the sixth day of vancomycin treatment. However, the beneficial effects were more prominent in C57BL/6 mice than BALB/c mice as the percentage of Verrucomicrobia is higher in C57BL/6 mice than the BALB/c mice.
- Glucose metabolism was associated with the abundance of *A. muciniphila* bacteria of Verrucomicrobia phylum; the bacteria enhanced glucose metabolism and decreased the blood glucose level efficiently in C57BL/6 mice compared to BALB/c mice.
- Vancomycin treatment caused a decrease in different short-chain fatty acid levels in the serum of mice. It also altered various hormones such as insulin, PYY, and Leptin in the serum.
- Maximum gut microbiota restored within 15 days of cessation of vancomycin treatment. On day 60 of restoration, all the major phyla were restored, and the

composition and diversity of gut microbiota were similar to untreated control mice. BALB/c mice had greater efficiency of restoration of gut microbiota compared to C57BL/6 mice.

- With the successful restoration of gut microbiota, most of the altered physiology of the host also normalized and became similar to the control mice. Different host physiology like the expression of immune genes and stress-related genes, behavioral changes, gut permeability, SCFA levels were restored with the restoration of gut microbiota.
 - The perturbation and restoration patterns of gut microbiota were different between the BALB/c and C57BL/6 mice to reveal the effect of host genetics on gut microbiota composition.
- ❖ Treatment with other antibiotics (Neomycin and AVNM)
- Neomycin treatment caused a significant increase in the *Bacteroides* genus of Bacteroidetes phylum. This caused an increase in the expression of both IFN- γ and IL-10 genes and an elevated level of propionate and acetate level in the serum.
 - AVNM treatment caused a dramatic increase in the Pathogenic Proteobacteria like *E.coli*, *Shigella*, and a decrease in the Clostridia group of bacteria. This alteration in the gut microbial profile caused the increase of pro-inflammatory cytokine genes like in TNF- α gene expression. Serum of AVNM treated mice showed a significant reduction in the concentrations of three SCFAs, such as acetate, propionate, and butyrate.

- The cecal index was considerably increased for vancomycin, and AVNM treated mice, while no significant change was observed in neomycin treated mice.
- ❖ Cecal Microbiota Transplantation (CMT)
 - Mice that received CMT restored both the diversity and composition of gut microbiota more efficiently following antibiotic treatment than non-CMT recipient mice.
 - CMT recipient mice showed a higher survivability rate during Salmonella infection compared to non-CMT recipient mice. The efficient recovery of the cecal index was observed in CMT recipient mice following AVNM treatment.
 - CMT recipient mice showed altered expressions of immune and tight junction protein genes in the colon of mice compared to non-CMT recipient mice, which were earlier perturbed due to antibiotic treatment. CMT restoration alleviated the expression of a pro-inflammatory gene like TNF- α and increased anti-inflammatory genes like TGF- β and IL10 in the gut. During AVNM treatment, expression of occludin, claudin-like tight junction protein genes decreased significantly; however, after the CMT procedure, their expression increased considerably, maintaining gut integrity.
 - Carbohydrate (glucose, starch, and sucrose) and aromatic amino acids (phenylalanine, tyrosine, and tryptophan) metabolism pathways were primarily affected in the AVNM treated and CMT restored mice. AVNM treatment caused a significant increase in the level of above three aromatic amino acids in the serum. Both CMT was restored, and the control group of mice had a similar AAA level in the serum.

Future potentials and limitations of the study

We found a better understanding of host-microbiome crosstalk and specific microbes in regulating the distinct physiologies of the host during the current study. Different reports previously showed that the antibiotic treatments caused many adverse effects in the host by increasing pathogenic bacteria and decreasing commensal bacteria. This study also gave us similar results with the previous reports; however, it also revealed some new beneficial effects of antibiotics treatment in the host — the appearance of *A.muciniphila* and *B. fragilis* gave many beneficial effects vancomycin and neomycin treatment. The significant increase in the abundance of *A.muciniphilla* bacteria during vancomycin treatment and its ability to regulate the host's blood glucose and inflammation level gave us an insight into the potential beneficiary effect of certain groups of bacteria during antibiotic treatment and their possible usage as a health supplement for the host. The study also provided insights and paving ways for further investigations to understand better the roles of gut microbiota, metabolites, and meta-metabolites on host physiology. In this study, we mainly focused on the changes in the hosts' physiologies as an outcome of altering gut microbiota and understanding the restoration kinetics. However, we did not investigate the comprehensive mechanism by which the abundance of specific groups of gut microbiota modulated the expression of various genes that regulated different physiologies of the host.

Summary:

Gut, in mammals, harbors a large number of diverse microbiota which plays a significant part in regulating the health and homeostasis of the host. An effective way to understand the function of gut microbiota inside the host is to perturb the microbial population. While the consequence of treatment with antibiotics on the gut microbiota might be destructive but can also be utilized as an effective tool to figure out the function of specific gut microbes inside the host. The magnitude of perturbation and time required for the restoration of gut microbiota can be altered with the nature of antibiotics and strains of mice used for the investigation.

We used some commonly and abundantly used antibiotics such as vancomycin, neomycin, and AVNM cocktail to perturb the gut microbiota and understand the altered host response in terms of metabolic, innate immune profile, and behavioral changes in mice. The study was performed in both Th2- (BALB/c) and Th1- (C57BL/6) biased mice models. The restoration patterns of the gut microbiota were also observed within the sixty days following the termination of antibiotic treatment.

Results revealed that each type of antibiotic treatment followed a specific time-dependent perturbation pattern of gut microbiota. These alteration patterns varied significantly between two strains of mice, C57BL/6 and BALB/c, used in the current study. A strong correlation was observed between the dysbiosis pattern of gut microbes with the expression of different immune regulatory genes and the stress level of the host. We also found that during antibiotic treatments, the alteration in the abundance of four major phyla, i.e., Firmicutes, Bacteroidetes, Proteobacteria, and Verrucomicrobia mainly affected the metabolism of glucose, aromatic amino acids, and short-chain fatty acids of the host. The further results revealed that the restoration pattern of gut microbiota varied between two strains of mice and maximum gut microbes

restored efficiently within 15days following the termination of antibiotics treatment. Cecal microbiota transplantation (CMT) restored both the diversity and composition of gut microbiota more efficiently following antibiotic treatment compared to non-CMT recipient mice.

Chapter: 1

General Introduction

&

Review of Literature

1.1Gut microbiota

There are hundreds of trillions of exceptionally different and complex microbial cells present in the mammalian gastrointestinal tract (1–4). Gut microbiota is the assemblage of Bacteria, Archaea, and Eukarya (5). Their number exceeds more than 10^{14} , which in itself is greater than the sum of the existing cells inside the human body and nearly ten times the genome content than the human genome (2,6). These vast numbers of microbes have coexisted with the host over a prolonged period [7,8], with bacteria being the most abundant member of gut microbes (9). The latest study shows that the human gut microbiota consists of more than 35000 bacterial species (10). Meta Hit and Human Microbiome Project have given the most extensive view of human-associated microbes (11,12). These studies showed that 2172 prokaryotic microbes are present inside the human body to account for 12 phyla isolated. 386 of the species identified in humans are strictly anaerobic and are non-culturable (13,14). Hence culture-independent methods like high throughput and cost-effective sequencing methods are becoming popular to understand gut microbiota composition and diversity (15,16). Bacterial 16s rRNA gene sequencing is the most popular one as this gene is the most conserved one present in all bacteria and archaea (17,18). The human gut consists of diverse phyla of bacteria like Firmicutes, Bacteroidetes, Proteobacteria, Verrucomicrobia, Actinobacteria, Tenericutes, Deferribacteres, Fusobacteria, etc. (2,19–21). Among all these phyla, Firmicutes and Bacteroidetes are two significant phyla consisting of nearly 80-90% of the entire gut bacterial population (15). Healthy gut microbiota contains a meager percentage of Proteobacteria (1-2%) (21).

.

The constitution and variety of microbiota fluctuate in various locales of the GI tract. In the stomach, a comparatively less number of bacterial species are present (5). The high acidic environment of the stomach ensures the survival of only a few capable species like *Streptococcus*, *Staphylococcus*, *Lactobacillus*, *Peptostreptococcus*, *Helicobacter pylori*, etc.. (22). In contrast, the distal portion of the small intestine has an alkaline environment supporting the growth of gram-negative bacteria like *Enterobacteriaceae* (22). However, the colon of the GI tract has the highest microbial density. Due to the higher abundance of the bacterial population in the intestine, they constitute nearly 60% of the fecal dry mass content (23). The quantity of various microorganisms like fungi, protists, archaea, and viruses present in the gut is considerably low compared with the bacterial population (24). More than 99% of the total gut bacterial flora is anaerobic. However, the cecum contains a higher number of aerobic bacteria, than the other regions of the GI tract (22).

1.2 Constitution of the gut microbiota in the mammal:

The composition of microbes in different gut parts depends on multiple factors. The factors include food type and variation in the pH at various gut regions (11). Overall, in mammals, the microbes present in the gastrointestinal tract are conserved. Studies reported differences at the species level due to variation in food intake and other factors (25). Recently the use of the mice model in gut microbial research is attaining popularity because of their high similarity of the gut microbiota between humans and mice model [26–28]. Studies reported mice as standard animal models for gut microbiota and gut-associated disease studies like IBD, rheumatoid arthritis, type 2 diabetes (28–30). Mouse, having a larger cecum than the human (31), makes it capable of extracting nutrients from complex indigestible foods efficiently (25). The gut bacteria present in the cecum of mice can ferment food and produce SCFA better than that of humans. However, in

humans, the fermentation process mainly happens in the colon, and the cecum is vestigial (25,32). Due to the omnivorous nature, both mice and humans shared maximum similarity of structure and function of the digestive tract. For both humans and mice, dominating phyla of gut microbiota are Bacteroidetes and Firmicutes (21). Human gut microbiota has abundant genera like *Prevotella*, *Faecalibacterium*, and *Ruminococcus*, while mice gut bacteria contain more *Lactobacillus*, *Alistipes*, and *Turicibacter* genera (25). However, the abundance of some genera like *Clostridium*, *Bacteroides*, and *Blautia* are nearly similar in the guts of humans and mice (25).

Table 1.1: The organization of the gut microbiota at various portions of the gastrointestinal tract of mammals (11).

Parts of gut	pH	Composition of bacteria	References
Esophagus	< 4.0	“Bacteroides, Gemella, Megasphaera, Pseudomonas, Prevotella, Rothiasps., Streptococcus, Veillonella”	(33,34)
Stomach	2	“Streptococcus, Lactobacillus, Prevotella, Enterococcus, Helicobacter pylori.”	(35,36)
Small intestine	5-7	“Bacteroides, Clostridium, Streptococcus, Lactobacillus,g-Proteobacteria, Enterococcus.”	(2,37)

Colon	5-5.7	“Bacteroides,Clostridium, Porphyromonas,Eubacterium, Ruminococcus,Streptococcus, Enterobacterium,Enterococcus, Lactobacillus,Peptostreptococcus, Fusobacteria, Prevotella,”	(38,39)
Cecum	5.7	“Lachnospira,Roseburia, Ruminococcus,Fecalibacterium, Fusobacteria, Butyrivibrio,”	(40)

We discussed below the characteristics of some significant gut microbiota phyla.

Firmicutes: Firmicutes are the important phylum of mammalian gut microbiota. It consists of nearly (30-50%) of healthy gut microbiota (41). It mainly contains all gram-positive bacteria with low G+C groups. They can be cocci or bacillus in shape. Most of the Firmicutes produce endospores which help them to withstand extreme conditions. This phylum mainly contains clostridia, anaerobic, and Bacilli, facultative aerobic bacteria (42). Some of the notable genera of Firmicutes are Bacillus, Staphylococcus, Clostridium, Eubacterium, Acetobacterium, etc. (21,43).

Bacteroidetes: Bacteroidetes is another major phylum of gut microbiota. It consists of nearly (30-50%) of healthy gut microbiota (44). These are primarily gram-negative, non-spore-forming bacteria. They are mainly rod-shaped and can be both aerobic and non-aerobic bacteria. Some major classes of this phylum are Bacteroidia, Flavobacteriia, Sphingobacteriia (44,45).

Proteobacteria: Proteobacteria are the gram-negative group of microbes having an outer layer of the membrane mainly made out of lipopolysaccharides (46). They consist of 1-2% of the total gut microbiota. This phylum includes the pathogenic bacteria explicitly like *Salmonella*, *Escherichia*, *Helicobacter*, *Vibrio*, *Legionellales* (47,48). Different classes of this phylum are Alphaproteobacteria, Betaproteobacteria, gammaproteobacteria, Deltaproteobacteria, Epsilonproteobacteria, Zetaproteobacteria, etc. (46).

Verrucomicrobia: This phylum contains a few known species. In the human gut, *Akkermansiamuciniphila* bacteria belong to this phylum (49,50). This phylum has several conserved signature indels that distinguish it from other phyla (51). The human gut contains only 0.5-2% of bacteria from this phylum.

Actinobacteria: Actinobacteria is another important phylum of the gastrointestinal tract. These are gram-positive bacteria with high G+C contents (52,53). However, they represent a negligible percentage of total gut microbiota but have some crucial roles in the host (52). *Bifidobacteria* is a significant Actinobacteria, a commonly used gut probiotic strain that has many beneficial effects on the host.

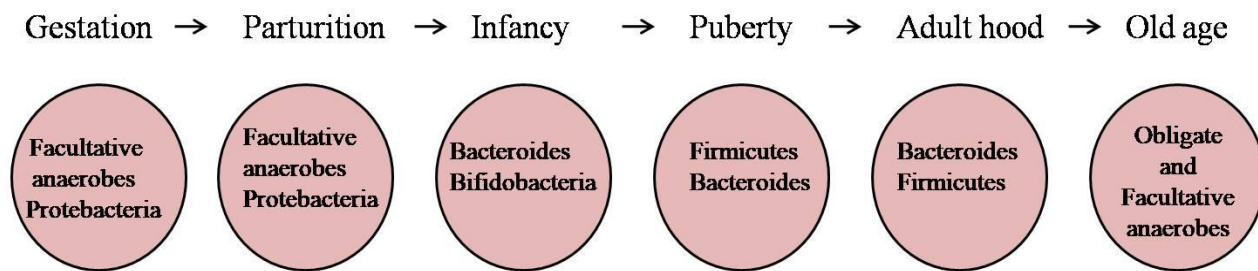
The composition of gut microbiota does not form overnight. It develops with time and is susceptible to diet and other environmental factors.

1.3 Development of gut microbiota:

Contrary to the earlier belief that the growth and occurrence of gut microbiota happen after birth, recent studies indicated that the maternal gut microbes could pass to the embryo through placental passage (54,55). During delivery, the gut microbiota composition varied between C-section and normal delivery mode (56–58). Studies reported that the fecal microbiota of infants

after standard vaginal delivery resembles 72% of the mother's fecal microbiota, while during C-section delivery, it decreased to 41%. The C-section delivery of the infant delays the *Bacteroides* genus colonization (59). In the beginning phases of life, the diversity of gut microbiota is significantly less and it contained mainly Actinobacteria and Proteobacteria phyla (60). With age, the variation in the gut microbiota composition increases throughout the first year of life (61,62). Gradually it resembled the adult microbial profile at 2.5 years of age. Breast milk feeding caused an increase in *Bifidobacterium*, *Streptococcus*, and *Lactobacillus* species in infants' gut (63).

Figure 1.1: Schema showing the development of gut bacteria with age from the gestation period to old age (64,65).

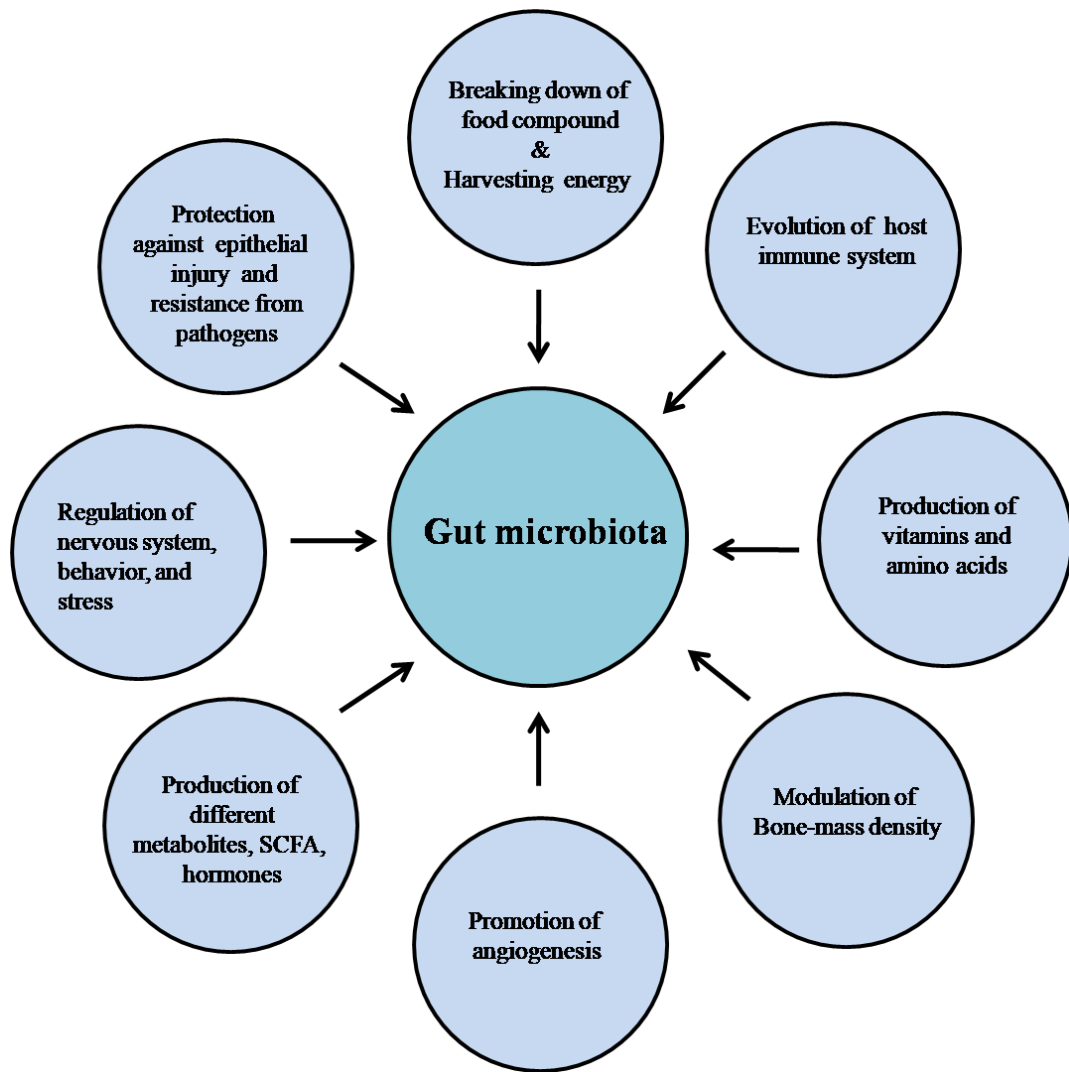


The gut microbial composition at various stages of life has a distinct role inside the host. Most of the significant physiology of the hosts are regulated by certain groups of gut microbiota.

1.4 Functions of gut microbiota in host:

Gut microbiota has several vital roles in regulating different physiology of the host. Other remarkable functions of gut microbiota inside the host are breaking down complex carbohydrate food to a simpler one and harvesting energy, developing the immune system, producing different metabolites, and protecting gut epithelial cells from various pathogens, etc. We have shown a schema of primary functions in Fig 1.2. Gut microbes produce other vitamins like vitamin K and B. The anxiety and stress levels of mice are also dependent on the gut microbial constitution. Gut microbes also regulate the bone-mass density and stimulate the angiogenesis of the host.

Figure 1.2: Major functions of gut microbiota in the host.



One of the critical gut microbial responsibilities is to maintain host immune homeostasis. Gut microbiota does it by controlling interactions of various immune regulatory elements.

1.5 Role of gut microbiota in immune homeostasis:

The immune system is one of the most dynamic processes inside the body, eliminating pathogens without creating autoimmunity. It maintains immune homeostasis by regulating the interactions among various immune regulatory components like tolerogenic dendritic cells (DCs), self-reactive T cells, and T regulatory cells (Tregs) (66). Gut microbiota plays an essential role in the development and maintenance of host immune homeostasis.

1.5.1 Various functions of gut microbes in the evolution of the innate immune system

The early interplay between the immune system of the infant and the microbial cells happens during delivery (67). Such types of associations are crucial to harmonize the host's immune system for an extended period. During breastfeeding, breast milk contains IgA, immune cells, and cytokines that are helpful in the development of infant immune response (68,69). The Gut bacterial migration enhanced significantly during the pregnancy and lactation period (70).

Goblet cells are the leading producer of mucus inside the gut, and this mucosal layer protects the host from pathogens (67,71). This mucosal layer gives food and space for the development of "friendly" microorganisms. The development of "gut-associated lymphoid tissue" (GALT) and the gut flora happens at a similar time (72). The GALT has tolerance towards the gut microbes while it is intolerant to other foreign pathogenic microorganisms (73).

Gut microbiota regulates the immune homeostasis of the host (39,74,75). Antigen processing cells coevolved with the gut microbiota. These cells can shield the body from various germs but tolerate gut microbiota (76,77). In homeostasis, "inflammation anergy" or the non-inflammatory response to own microbial stimuli occurs in the body (75). "Germ-free mice" (GF mice) showed a significantly less number of dendritic cells (DCs) than SPF mice (78,79). Even colonization of

germ-free animals with only one bacterial strain, i.e., *Escherichia coli*, was sufficient to recruit DCs to the host's intestine (80). Studies reported microbes-derived ATP stimulates different dendritic cells to CD70 and CX3CR1 on their surface (75).

Gut microbiota also regulates neutrophils which constitute a significant element of the immune system (70). GF rats are neutropenic, and they showed decreased production of superoxide anion and nitric oxide in the peripheral circulatory neutrophils (75,81,82). Superoxide anion and nitric oxide productions are disturbed with impaired phagocytic activity in germ-free rats. The peptidoglycans of various gut microbes also regulate the immune activity of bone marrow neutrophils through the “cytosolic receptor-nucleotide oligomerization domain 1” (NOD1) (83).

GF mice showed impaired activity of Natural killer cells (NK cells) which suggests the role of gut microbes in modulating the NK cells activity inside the host, which the GF mice lack (75). GF mice lack Reports recommended that GF mice have a deficiency of IL-22 inducingNKp46⁺ cells.

Lamina propria of the GI tract consists of nearly 2-3% of mast cells. GF mice have lower intestinal mast cells and a higher number of systemic mast cells (84). In conventionally raised mice, gut microbiota caused increased translocation of mast cells inside the gut by activating CXCR2 ligands of IECs (85). This process depends on the MyD88 (adaptor of TLR signaling) (86).

The intestinal epithelium cells (IECs) separate commensal microbes from basal sterile tissues of the gut (87). IECs provide mechanical protection to the host from pathogens. In GF mice, alleviation of IEC proliferation rate and reduced expression of antimicrobial genes of IECs was found (75).

1.5.2 Role of gut microbiota in adaptive immune homeostasis:

CD4⁺ T cells are the principal element of the host adaptive immune system (88). Intestinal lamina propria (LP) mainly contains these cells (89). When stimulated, naive CD4⁺ T cells formed different subsets of T cells such as Th1, Th2, Treg cells (75). Different CD4⁺ T cell subtypes produce various types of cytokines. Th1 cells protect intracellular pathogens; however, Th2 cells eradicate the parasite infections from the host's body (75). Th17 is related to autoimmune diseases, while Treg cells are the main component of immune tolerance of the host (90).

In the GF mice, a reduced amount of CD4⁺ T cells and an imbalanced Th1/Th2 immune system mainly manifested the role of gut microbiota in adaptive immune regulation of the host (75). GF mice were biased towards the Th2 immune response. Gut microbiota like *Bacteroides fragilis* has polysaccharide A (PSA), which induces systemic Th1 response in the host (91). Other gut bacteria such as "Segmented Filamentous Bacteria" were the primary activator of LP Th17 cells. Other studies reported Clusters IV and XIVa of Clostridia are the main inducers of host colonic Tregs. PSA of *B. fragilis* halts the Th17 response by signaling on Tregs through TLR2 (92,93). Gut microbiota educates the Tregs to be tolerant of the commensal-derived foreign antigen. Gut microbes like Clostridium species cause elevation of T_{reg} cells by making TGF-β rich environments (94). Control microbiota also regulates IL-1β production in the gut. The microbiota converts the pro-IL-1β to mature active IL1β through MyD88 (95). CD8⁺ T cells of the intestine are primarily present in the intraepithelial compartments. GF mice showed a drastic reduction in the CD8⁺ T cells in the intestine to establish the importance of gut microbiota for regulating the CD8⁺ T cells (75). The constitutions and variations of gut microbiota have a prime function in habituating CD8⁺ T cells to harmonize different peripheral immune systems (96). In the GF

mice, the cytolytic activity of $\gamma\delta$ T cells also decreased significantly compared to conventionally raised mice.

Gut microbiota also regulates the B cells primarily present in the Peyer's patches of the host. These are mostly immunoglobulin- A (IgA) producing plasma cells. GF mice have less abundance of Peyer's patches which is also associated with less production of IgA in the GF mice. Secreted immunoglobulin A (IgA) regulates the compartmentalization of intestinal bacteria. Intestinal dendritic cells produce IgA that is specific for commensals (97).

Reports showed that imbalanced gut microbiota might cause various autoimmune (98)." *Gut microbiota like B. fragilis* has PSA, which is helpful to decrease colitis by inducing anti-inflammatory IL-10 secretion and reduce the production of the colonic IL-17 cytokine in the immunocompromised mice (99). *Bacteroides thetaiotaomicronbacteria* can reduce the inflammation caused by *Salmonella enterica*. It activates the transport of PPAR- γ outside the nucleus of the cells, which regulates the inflammation (75). Gut microbiota-induced SCFAs also decrease the inflammation of the gut (100).

Clostridium group of bacteria from Firmicutes phylum is associated with the production of various SCFAs from soluble fibers and carbohydrate foods of the gut (4,100). Multiple species of gut bacteria from the Instentimonas genus are associated with the formation of butyrate from lysine, while Bacteroidetes caused propionate production using threonine as a substrate (4,101,102). The SCFAs produced by gut microbes alleviated the LPS and inflammation of the host by inducing the synthesis of various anti-inflammatory cytokines (4,103,104). During the dysbiosis of gut microbiota, a higher level of the pathogenic gram-negative bacteria elevated the systemic endotoxin level (4,105). TLR 4 receptors of IECs were activated through LPS which

was associated with the higher pro-inflammatory cytokines level of the host (4,106,107). Conserved microbial-associated molecular patterns (MAMPs) of gut microbes activate different Toll-Like Receptors of gut epithelial cells, which causes the production of various cytokines.

Different pattern recognition receptors of gut microbiota activate the antimicrobial peptide-like RegIII γ in the gut epithelial cells. Lectin, which affects gram-positive bacteria, is also modulated by the gut microbiota in MyD88 dependent manner (70).

Therefore, all these various studies and literature give a subtle outcome that the commensal gut bacteria protects the host from different pathogens by enhancing the inflammatory potential of the host via modulating the innate and adaptive immune responses (39,98).

1.6 Gut microbiota regulates the different metabolism and production of various metabolites of the host.

Gut microbiota regulates different metabolic pathways of the host by both producing and utilizing various metabolites of the body. Specific microbes present in the gut regulate the metabolism of carbohydrates, proteins, and lipids. Specific metabolites like short-chain fatty acids produced by the gut microbiota also modulate the host's inflammatory response. Metabolites produced by gut microbiota play a crucial role in maintaining harmony between the host's immune and metabolic systems.

1.6.1 Function of gut microbiota for the production of different Short-chain fatty acids.

Gut microbiota induces the production of different short-chain fatty acids (SCFAs) like acetate, propionate, and butyrate by digesting complex carbohydrate foods (100,108,109). These SCFAs have some significant roles in maintaining intestinal function by regulating gut integrity, immune response, combating tumors, supporting the electrolyte balance of the host, and providing energy

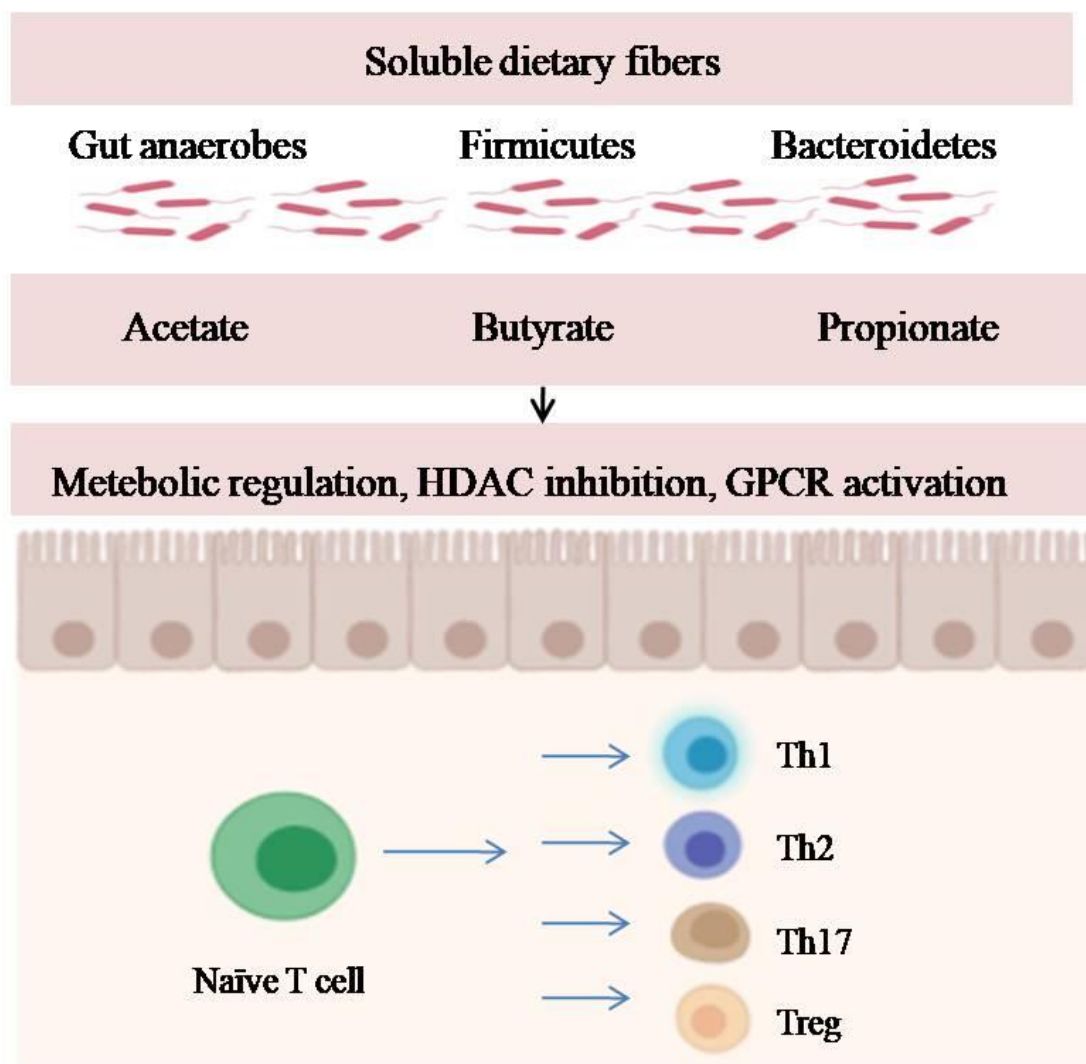
for the host epithelial cells (104,110,111). The gut microbial-induced SCFAs could reduce host inflammatory responses and regulate intestinal G protein-coupled receptors (112). Some studies showed that gut microbiota induces peroxisome proliferator receptor- γ (PPAR- γ) signal, responsible for maintaining host immune homeostasis (113). Clostridia group of gut microbiota mainly produces butyrate. Some antibiotic treatment groups cause a reduction in Clostridia or Firmicutes bacteria resulting in less production of butyrate, which subsequently decreases the transduction of the PPAR- γ signal (114). This decrease in PPAR- γ caused an increased level of nitrate in the colonic lumen of the host (113).

Butyrate is mainly synthesized through Firmicutes phylum, while acetate and propionate are through Bacteroidetes phylum (4,100). Some earlier reports showed that *Akkermansiamuciniphila* also produced acetate and propionate up to some extent in the gut (104). Bacteria from the Actinobacteria phylum (mainly *Bifidobacterium* species) produce acetate and lactate in the gut by fermenting carbohydrates (115). Several species of bacteria belong to the *Ruminococcaceae*, and the *Lachnospiraceae* family of Firmicutes phylum are a significant supporter of the get butyrate level in the host (116,117). A lower concentration of O₂ in the host's colon makes a supportive environment for the development of Bacteroidetes and Clostridia, which mainly produce butyrate (118). The antibiotic-induced dysbiosis caused an increase in aerobic pathogens like *Salmonella typhimurium* and *E.coli* growth in the colon (119,120). Mainly, acetoacetyl CoA and crotonyl CoA produce butyrate in the gut. Various reports showed that different genes related to butyrate-producing pathways are present in the host's gut microbiota (121,122). SCFAs regulate gut barrier function; specifically, butyrate contributes to this field (4,123,124). Butyrate acts as a histone deacetylase (HDAC) inhibitor

and alleviates the NF-κB signaling pathway of the host, which results in decreased inflammation of the host (4,125).

Reports showed that the considerable elevation in the expression of the TNF- α gene caused a significant reduction in the expression of tight junction proteins that eventually led to the impaired gut barrier function of the host (126,127). The expression of Occludin and Claudin genes maintains the firmness of the gut (128). Modulation in gut microbiota composition led to altered inflammation and permeability of the gut (126,129). Reports indicated a significant decrease in the abundance of *Roseburia* in the fecal sample of IBD patients (130).

Figure 1.3: Gut microbiota-produced SCFAs (Acetate, propionate, butyrate) regulating the host's immune system (131).



The dysbiosis of gut microbiota causes an alteration in the production of SCFA and disturbance in the immune homeostasis of the host that creates different metabolic and immune-related diseases inside the host. As gut microbiota regulate the glucose, aminoacid, fatty acid

metabolisms of the host, their dysbiosis leads to various metabolic disorders like diabetes, IBD, obesity, etc.

1.6.2 Function of gut microbiota during different metabolic diseases of the host.

Understanding gut microbiota for regulating different host metabolism and their role in various metabolic diseases is growing rapidly. High-throughput metagenomics and metabolomics studies gave us ideas about the mechanistic regulations with the cause-and-effect relations of different gut microbes during various metabolic disorders of the host. Studies reported an association of gut microbial dysbiosis with type 2 diabetes, malnutrition, arthritis, obesity, cardiometabolic diseases, IBD, non-alcoholic liver disease (132).

Table1.2: Alteration in the gut bacterial population during different metabolic diseases.

Diseases	Increased bacteria	Decreased bacteria	References
Obesity	<i>Dorea longicatena</i>	Bacteridetes to Firmicutes ratio	(132,133)
	<i>Roseburia intestinalis</i>	<i>Akkermansia muciniphila</i>	
	<i>Ruminococcus gnavus</i>	<i>Clostridium histolyticum</i>	
	<i>Ruminococcus torques</i>	<i>Clostridium coccoides</i>	
	<i>Eubacterium ventriosum</i>	<i>Faecalibacterium prausnitzii</i>	
		<i>Methanobrevibacter smithii</i>	
		<i>Bacteroides thetaiotaomicron</i>	
Type 2 diabetes	<i>Clostridium clostridioforme</i>	<i>Akkermansia muciniphila</i>	(134–136)
	<i>Clostridium hathewayi</i>	<i>Clostridia</i> lessp. SS3/4	
	<i>Prevotella copri</i>		

Bacteroides vulgatus

Malnutrition		“Anaerobes to facultative anaerobes ratio	(137–140)
		<i>Bifidobacterium longum</i>	
		<i>Bifidobacterium pseudolongum</i> ”	
Metabolic liver disease	“ <i>Klebsiella pneumoniae</i> <i>Streptococcus anginosus</i> <i>Veillonellaatypical</i> ”	<i>Coprococcus comes</i> <i>Faecalibacteriumprausnitzii</i>	(141–144)
Cardiometabolic diseases	“ <i>Faecalibacteriumprausnitzii</i> <i>Klebsiella</i> spp.	<i>Enterobacter aerogenes</i> <i>Escherichia coli</i>	(145–148)
Rheumatoid arthritis	<i>Prevotella</i>	<i>Bifidobacterium</i> and <i>Bacteroides</i>	(149)
IBD, CD	Proteobacteria Enterobacteriaceae Lachnospiraceae Ruminococcus	Bacteroidetes Lactobacillus Eubacterium <i>Bifidobacterium</i>	(150,151)

1.7 Gut microbiota regulates the production of different hormones

The enterochromaffin (EC) cells of the gastrointestinal tract (GI tract) are the leading producer of serotonin in the host (113). A lower serotonin concentration in GF mice than SPF mice indicated

the influence of gut microbes to regulate host serotonin level (152,153). Microbial metabolites can regulate EC cells through their FFAR2 and FFAR3 receptors (154,155)and olfactory receptors (156,157).

Glucagon-like peptide 1 (GLP-1) is synthesized by breaking down the proglucagon of the ileal and colonic L cells inside the body. Inside the body, it is released with the response to glucose (158)to increase insulin production and decrease glucagon production from the pancreas (159). GLP-1 also affects the satiety and food intake of the host (160). Different gut microbial composition affects the GLP-1 level in the host. For example, *Oscillibacter* and *Lactobacillus-like* bacteria influence GLP-1 production by modulatingDPP-4-like activity (161,162). Some reports showed“bile acid-interceded” stimulation of TGR5 (163), different SCFAs (164), LPS, and indole-like metabolites (165)to modulate host GLP-1 level (152).

The host's colon contains a large number of L-cells that produce Peptide tyrosine-tyrosine (PYY) hormone. The host's food intake and satiety are regulated by the PYY hormone and induce neuropeptide Y (166). SCFA butyrate caused an increase in the PYY expression in the gut (167,168).

During obesity and diabetic conditions, higher endotoxin (LPS) levels of serum caused inflammation with a disturbing concentration of glucose in the host, creating a metabolic endotoxemia condition (4,169,170). The increased gram-negative group of bacteria in the gastrointestinal tract caused the metabolic endotoxemia condition of the host. Supplements of *Akkermansiamuciniphila* of Verrucomicrobia phylum caused modulation of insulin sensitivity and decreased blood glucose levels in diabetic patients (171–173).

1.8 Role of gut microbiota on stress and behavior of host (HPA axis)

Gut microbiota has a significant contribution during the stress response of the host. The stress level of the host also altered with gut microbial modulation showing the bidirectional relationship between gut and brain (174). Reports stated, “gut microbiota, vagus nerve, central nervous system, neuroendocrine and neuroimmune systems with the hypothalamic-pituitary-adrenal axis (HPA axis) are the major component of gut-brain-axis” (175,176). It also includes the sympathetic and parasympathetic arms of the ANS and ENS of the host (177). Stress simulation could activate the hypothalamic-pituitary-adrenal axis (HPA axis) and the sympathetic nervous system of mammals (178). Reports revealed higher plasma concentrations of adrenocorticotropin hormone (ACTH) and corticosterone in GF mice than SPF counterpart in response to 1-hour restraint stress (179). The Vagus nerve connects the brainstem with the gut linings. They collect the information from the gut and transfer it to the brain.

The Vagus nerve sensed the microbial-induced FA, specifically butyrate, which subsequently processed the brain's signal to regulate inflammation and permeability of the gut lining (176). Impaired vagus nerve functions were correlated with dysbiosis of gut microbiota during stress (9). Reports established altered gut microbial constitution caused behavioral modulation of mice in different anxiety and depression measurement tests (129,180). GF mice had less “anxiety-like” behavior compared to SPF mice. GF mice stayed longer duration on the open area of the elevated plus-maze than their SPF counterparts (181). When GF mice were transplanted with *Bifidobacterium infantis* bacteria, it decreased the anxiety feeling of mice (129). However, transplantation of only *Escherichia Coli* bacteria in the gut of GF mice caused a significant increase in the stress of mice (129,182,183). Following transplantation of *Clostridium* species or *E.coli* in GF mice, the free catecholamines levels increased in the gut lumen (184). Oral

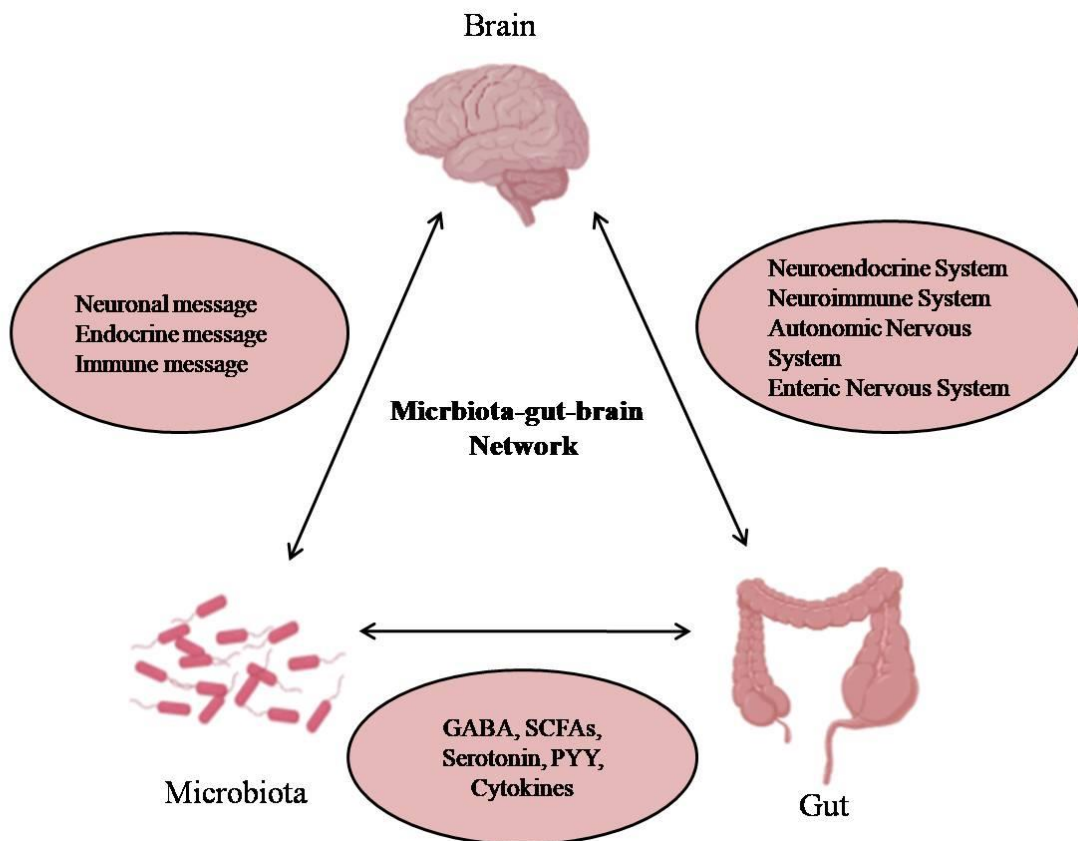
administration of *Campylobacter jejuni* activated the amygdala, prefrontal cortex, and hypothalamus of mice which causes an inflammatory reaction in the host (185). Various species of bacteria from Firmicutes phylum reduced the “anxiety and depression-like” behavior in mice (129,186). Increased levels of *Akkermansiamuciniphila* bacteria inside the gastrointestinal tract could be related to the reduced anxiety behavior of mice (187). Several reports suggested that the higher “Firmicutes to Bacteroidetes ratio (F/B ratio)” in the gut was associated with an excessive level of stress in mice (129,188,189). Earlier reports suggested that mice's anxiety and depression levels increased significantly by introducing a pathogen to the host's gut. The altered constitution of gut microbiota is related to the modulation of “Brain-derived neurotrophic growth factor (BDNF), corticotropin-releasing hormone (CRH), and CRH binding protein (CRHBP)” of the host (129,190–192). In anxiety patients, the level of BDNF is lower, and CRH is higher than normal individuals (129). These probiotics caused a decrease in calcium-dependent potassium channel opening (193). Gut microbes have essential contributions in maintaining the tryptophan and serotonin level of the host (153,194).

Studies revealed that *Lactobacillus Farciminis* treatment altered the HPA axis response in rats during restraint stress (195). The combination of *L. helveticus* and *L. rhamnosus* bacteria decreased the chronic stress in rats (196). Prenatal stress alleviated the *Bifidobacteria* and *Lactobacilli* bacteria number in the gut of rhesus monkeys. Some probiotics, such as *L. Rhamnosus* and *B. Longum*, showed anxiolytic effects on mice.

Various microbes inside the gut use both essential and nonessential amino acids (12). Several reports stated that “during the metabolism of amino acids, gut microbiota produces various metabolites like ammonia, polyamines, NO, biogenic amines (BAs), short-chain fatty acids (SCFAs), hydrogen sulfide (H_2S), and phenolic and indolic compounds in the host” (197–199).

Luminal and mucosal bacteria stay in different niche environments as the former prefer fermentation of short-chain substrates of diet while later digest long-chain material from endogenesis (200,201). Other bacteria like *Eubacterium*, *Lactobacillus*, and *Clostridium* make lumen their niche while *Fusobacterium* and *Helicobacter mucus*. (202).

Figure1.4: The two-way relationship between gut-microbiota and gut-brain axis [203]. Gut microbes communicate with the gut-brain axis through endocrine, immune, neuronal, and hormonal pathways (203).



As mentioned above, the gut microbiota regulates all the significant physiologies of the host; it is crucial to understand the specific microbes - host interactions. Though many microbes present inside the gut, only a few distinct groups are mainly needed to regulate all the significant

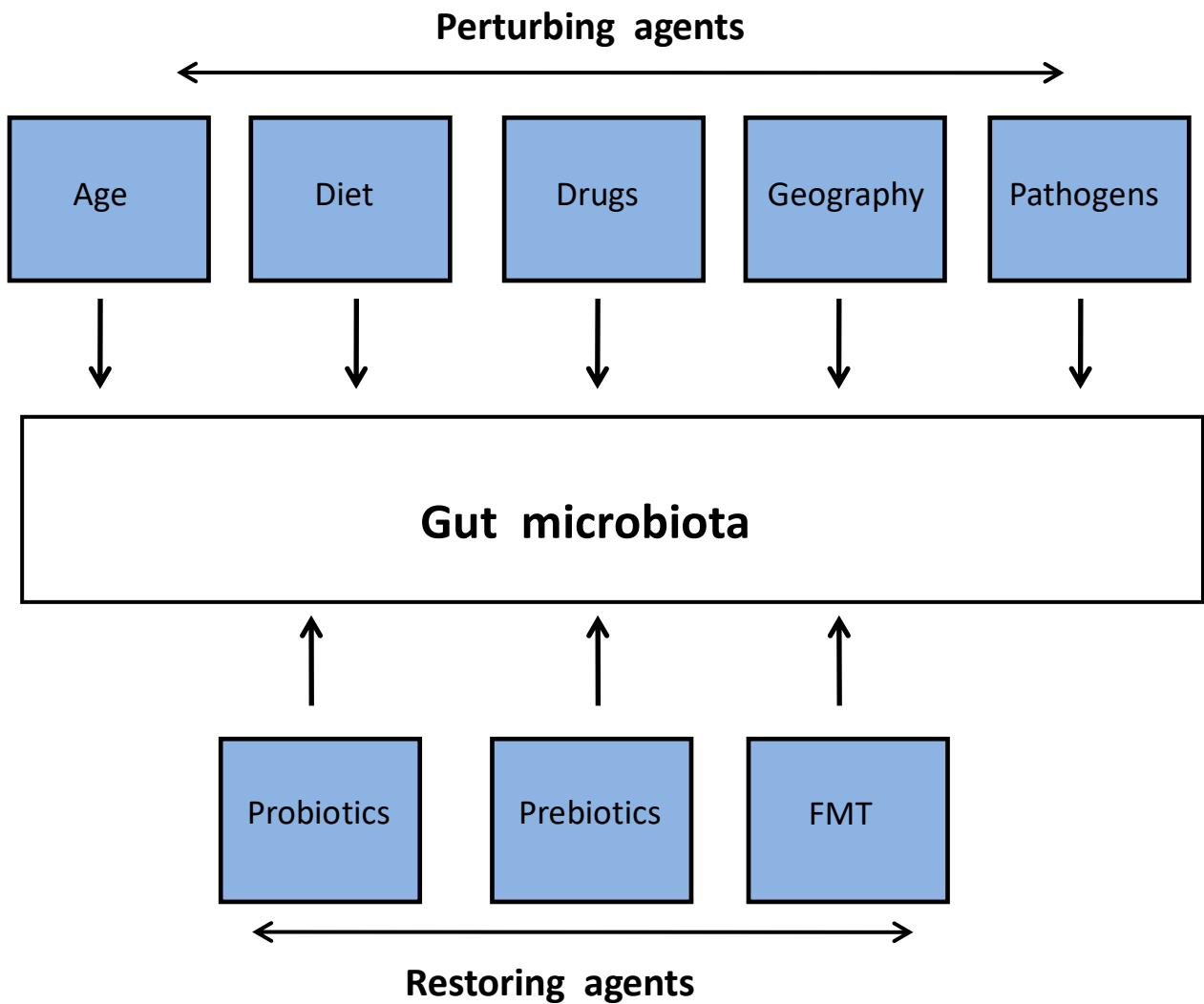
functions in the host body. It is essential to know the microbe-host interactions to identify specific microbial groups that control particular host physiology. Perturbation is the most effective way to understand host-microbiota cross-talk. One can understand the role of specific groups of gut microbes by altering the composition and diversity of gut microbes. The different methods of gut microbial perturbation are discussed below.

1.9 Different ways to perturb the gut microbiota:

Gut microbiota can be altered in different ways like age (61), diet (130), geography (204,205), stress (181), pathogen (206), and treatment with antibiotics (207). The gut microbial alteration pattern can be used as a powerful apparatus to comprehend the function of a specific group of microbes in the host (4,208). During the perturbation of microbes, both composition and diversity change significantly (24).

Adults have a higher diversity of gut microbiota compared to infants (209). Adult microbiomes contain more enzymes of “fermentation and methanogenesis-related process.” Different aminoacid metabolism-related enzymes are present in the adult microbiome; however, during infancy, mainly cystine metabolism-related enzymes are found to be dominant (210,211). Various potent perturbing and restoring agents of gut microbiota are shown in Fig.1.5.

Figure 1.5: Different ways to perturb and restore the gut microbiota.



Different studies showed that a high beef diet caused an increased level of *Bacteroides* and *Clostridia* and decreased *Bifidobacterium adolescentis*. Consumption of whey and pea protein diet caused a rise in the *Bifidobacterium* and *Lactobacillus* bacteria, reducing the pathogenic *Bacteroides fragilis* and *Clostridium perfringens* species (130,212–214). Pea protein also increased anti-inflammatory cytokines level by increasing intestinal SCFA levels in the host (110). However animal-based protein diet caused an elevation of bile-tolerant anaerobes

in the gut (21,215–217). The gut microbiota of Italian kids varied significantly from the children of a rural African village. Italian children have more *Bacteroides* and *Alistipes* as they consume more animal proteins (218). The gut microbiota of malnourished children has more pathogenic bacteria compared to healthy children (219).

Gut microbiome composition also alters with the geographic origin of populations. Some studies showed the different prevalence of *Prevotella*, and the urease gene significantly varied among the populations from different geographical origins (210). Firmicutes phylum is dominated in the fecal sample of European children while Bacteroidetes phylum is dominated in the Boulpon children. African populations have a higher level of biodiversity than the European population (218).

Intact commensal gut microbes make a layer of the microbial barrier to prevent the entry of pathogens and provide colonization resistance (220). Alteration of gut microbiota increased the host's susceptibility significantly towards different pathogens following antibiotic treatment (76).

Clostridium difficile infection rate increases considerably after antibiotic disruption of gut microbiota (221,222). Salmonella-like pathogen infection also increased in the host after antibiotic exposure for a long time (114). The germ-free mice were also more vulnerable to pathogens than SPF mice, showing the significant role of intact gut microbiota (2).

Among different factors that affect the gut microbiota, host genetics is one of the major contributing factors to cause the variation in the gut microbial composition. C57BL/6 and BALB/c are two inbred mice models used commonly in gut microbiota studies.

1.10 Use of BALB/c and C57BL/6 mice as model organisms for the gut microbiota perturbation study.

Host genetics play an essential role in understanding the immune response during infection (223,224). The genetic difference of the host is also associated with the variation in pathogen susceptibility and association of commensal microorganisms (224). Researchers used various inbred strains of mice to understand the importance of host genetics in host-microbiome cross-talk. These inbred mice gave us an idea about the role of genetic components regulating the host behavior, immune response (225). BALB/c and C57BL/6 mice are two inbred strains of mice commonly used to study different microbiome-related immune reactions in the host. It was observed that C57BL/6 and BALB/c mice were two hereditary distinct inbred mice with Th1 and Th2 immune tendencies. The gut microbiota of these two mice strains also varied (223,226–229). C57BL/6 mice were viewed as “more dynamic” and “less anxious,” while on the contrary, the BALB/c mice were “less dynamic” and are “more anxious” during different stress-related behavior studies (225). Gut microbial diversity and IgA levels of these two mice strains also varied significantly. BALB/c mice have more gut microbial diversity and basal IgA levels than C57BL/6 mice (4,226). Some reports revealed that the extent of dysbiosis of gut microbiota following the same dose of antibiotic treatment varied significantly between two strains of mice (4). These two mice strains are excellent models to understand genetic predisposition and other environmental factors contributing to the host's susceptibility towards stress and pathogens (225,230).

As discussed above, various perturbing agents can significantly alter the diversity and constitution of gut microbes. However, following perturbation, it is essential to understand the restoration pattern of gut microbiota. Restoration of gut microbiota depends on various factors

like the extent of perturbation, types of perturbing agents, the period of exposure, etc. Different procedures like applying probiotics, prebiotics, and FMT can be used to accelerate the restoration process of gut microbiota following perturbation.

1.11 Restoration of gut microbiota

Antibiotic treatment can significantly modulate the gut microbial constitution in the host (4). However, by terminating the antibiotic therapy, gut microbiota recovers significantly. (231,232). Reports also showed that incomplete recovery of gut microbiota happened following antibiotic treatment (233,234). Restoration of gut microbiota following antibiotics treatment relies upon various factors, for example, types of antibiotics, the period of antibiotic treatment, age, and genetics of the host. Some reports showed that different probiotics, prebiotics, and other supplements accelerated the restoration process of gut microbiota (232,235).

1.12 Fecal and/or cecal microbiota transplantation

Fecal microbiota transplantation (FMT) is when fecal sample suspension is delivered from a healthy donor to the recipient's intestinal tract to alter the gut microbiota constitution directly and provide a medical advantage to the recipient (236–238). To choose a suitable donor, the FMT procedure needs specific criteria listed as “without any family history of autoimmune, metabolic, and malignant diseases and it should pass the screening test for any possible pathogens” (238). The fecal sample of a healthy donor is obtained in sterile containers and screened for potential pathogens. Then the solution was made by adding fecal samples with water or saline. Then the removal of particulate matter was done through filtration (238,239). “Through a nasogastric tube, nasojejunal tube, esophagogastroduodenoscopy, colonoscopy, or retention enema” were the listed ways for delivering the fecal solution to the recipient (9). FMT is popularly prescribed as a medication for *Clostridium difficile* infection (CDI) (237).

Clostridium difficile infection is complicated to treat through antibiotics. A large section of patients with CDI infection again develop recurrent CDI (rCDI), which causes a high mortality rate among patients. FMT is also used to treat IBD and UC-like medical issues.

The mechanisms by which FMT treats CDI successfully are still not well known. Metagenomic analysis data showed that the variety and richness of gut microbes decreased significantly in CDI patients. In CDI patients, comparatively, a higher level of Proteobacteria and a lower Firmicutes and Bacteroidetes phyla level were observed (240). FMT caused the restoration of the gut microbiota community, specifically Firmicutes and Bacteroidetes, and decreasing the Proteobacteria level to outcompete *C. difficile* (240). FMT caused “the competitive exclusion of the pathogen” by beneficial gut microbes, which creates unfavorable environments for the growth of *C. difficile*. (238) Similarly, the disturbed gut microbiota is a major reason for IBD development, resulting in a higher inflammation level in the host. CD patients have a diminished degree of the *Clostridium* cluster IV and *Faecalibacterium prausnitzii* compared to healthy individuals (146,238,241,242). These microbes have anti-inflammatory properties, and the reduction of their number caused higher inflammation in the gut. FMT caused the restoration of these microbes and alleviated the effect of IBD.

However, it is essential to note that fecal microbiota may not be a comprehensive representation of the gut microbiome (25). It is, therefore, equivalent to find ways to replace fecal microbiota with gut microbiota, if possible. While it is difficult to transplant the intestinal microbiota in humans, but can be done in animal model systems.

In mice, the cecum is one of the largest and most significant parts of the gastrointestinal part and contains the most diverse and dense gut microbiota community. The cecum is the leading region

for fermentation of plant materials, breakdown of polysaccharides, production of vitamin K, vitamin B, and various SCFA. Reabsorb of nutrients also happens in the cecum. The densest and diverse population of microbes in the cecum of rodents makes it a suitable region for microbial study. In the current study, we have used cecal content for microbiome analysis and used cecal material for transplantation study instead of FMT to see the consequences of using a more representative sample.

Table 1.3: Alteration pattern of gut microbiota following different antibiotics treatment.

Antibiotics	Increased gut bacteria	Decreased gut bacteria	References
Vancomycin	Proteobacteria <i>Verrucomicrobia</i> <i>Klebsiella</i> <i>Escherichia/</i> <i>Shigella.</i> Lactobacillus, <i>A. muciniphila</i>	Firmicutes Bacteroidetes Clostridium <i>Ruminococcaceae</i> <i>Lachnospiraceae</i>	(234,244–256)
Neomycin	Bacteroidetes Actinobacteria Proteobacteria	Firmicutes Actinobacteria Proteobacteria	(257–260)
Amoxicillin	<i>Proteobacteria</i> <i>Enterobacteriaceae</i> <i>Enterococcus.</i>	<i>Actinobacteria</i> <i>Firmicutes</i> <i>Lactobacillus</i>	(261–267)

	<i>Prevotellaceae</i>	<i>Bacteroides,</i>	
	<i>Escherichia,</i>	<i>Butyricimonas</i>	
	<i>Parabacteroides,</i>	<i>Eubacterium</i>	
	<i>Enterobacter</i>	<i>Lachnospira</i>	
		<i>Bifidobacterium</i>	
		<i>Ruminococcus, Blautia</i>	
		<i>Roseburia,</i>	
		<i>Prevotella</i>	
Ciprofloxacin	Bacteroidetes	Actinobacteria	(233,268,269)
	Firmicutes	Bacteroidetes	
	Bacteroides	Firmicutes	
	Blautia	Bifidobacterium	
	Eubacterium	Alistipes	
	Roseburia	Faecalibacterium,	
		Oscillospira,	
		Ruminococcus,Dialister	
		Lachnospiraceae	
Metronidazole	<i>Proteobacteria</i>	Firmicutes	(270–278)
	Actinobacteria	Bacteroidetes	
	Verrcomicrobia	Tenericutes	
	<i>Escherichia</i>	Bacteroides	

coli and *Shigella* B.Vulgatus
Bifidobacteria
Enterobacteria

Table 1.4: Altered profile of gut bacteria following different cocktails of antibiotics treatment.

Antibiotics	Increased gut bacteria	Decreased gut bacteria	References
Cocktail			
Ciprofloxacin, vancomycin, metronidazole	<i>Klebsiella</i> <i>Escherichia</i> <i>Shigella</i> , Proteobacteria, <i>Streptococcus</i>	<i>Firmicutes</i> <i>Bacteroidetes</i> , <i>Prevotella</i> , <i>Megamonas</i> , <i>Lachnospiraceae</i> and <i>Bacteroides</i>	(279–281)

2	ampicillin, metronidazole, neomycin, vancomycin	γ -Proteobacteria	Firmicutes, Bacteroidetes, Actinobacteria, Deferribacteres, Tenericutes	(282–285)
3	meropenem, gentamicin, vancomycin	<i>Enterococcus faecalis</i> <i>Fusobacterium nucleatum</i>	<i>Bifidobacterium</i>	(231)
4	Ampicillin, neomycin	Bacteroides, Enterobacter, Lactobacillus Klebsiella,		(286)
5	<u>ciprofloxacin</u> , <u>metronidazole</u>	<i>C. viridae</i> , <u><i>Streptococcus</i></u> , <u><i>Staphylococcus</i></u>	<i>Bifidobacteriaceae</i> , <i>Enterobacteriaceae</i>	(287)
6	ciprofloxacin, clindamycin	<i>Veillonella</i>	E.coli Bacteroides	(288)

Table 1.5: Altered gut microbiota profile during antibiotics therapy and subsequent recovery period.

Antibiotics	Changes in gut microbiota during perturbation	Changes in gut microbiota during the restoration	Restoration ways	Refer ences
Vancomycin,	Firmicutes ↓	Firmicutes ↑	FMT	(236)
metronidazole	Bacteroidetes ↓ Proteobacteria ↑	Bacteroidetes ↑ Verrucomicrobia ↑ Proteobacteria ↓	6 months	
Amoxicillin	<i>Lachnospiraceae</i> ↓ <i>Coriobacteriaceae</i> ↓ <i>Clostridiales</i> ↓ <i>Enterobacteriaceae</i> ↑ <i>Bacteroidaceae</i> ↑	Total recovery of gut microbiota after 1 week <i>Enterobacteriaceae</i> ↓ <i>Bacteroidaceae</i> ↓ <i>Clostridiales</i> ↓	Probiotics	(232)
Ampicillin	Proteobacteria ↑	<i>Lachnospiraceae</i> ↑	Probiotics	(235)
Streptomycin	<i>Enterobacteriaceae</i> ↑	Firmicutes ↑	Two weeks	
Clindamycin	Firmicutes ↓ <i>Xanthomonas</i> ↑	Proteobacteria ↓ <i>Xanthomonas</i> ↓		

Vancomycin	Bacteroidetes ↓ <i>Klebsiella</i> ↑ <i>Escherichia/Shigella</i> ↓	Incomplete recovery of gut microbiota	22-week post- antibiotic treatment	(234)
amoxicillin-clavulanic acid	Proteobacteria ↑ Actinobacteria ↓ Firmicutes ↓	Proteobacteria ↓	7 days FMT	(264)
ampicillin	<i>E. coli</i> ↑	Proteobacteria ↓	28 days	(289)
gentamicin	<i>Enterococcus</i> ↑	Firmicutes ↑		
erythromycin	<i>Veillonella</i> ↑ <i>Bifidobacterium</i> ↓ <i>Bacteroides</i> ↓ <i>Ruminococcus</i> ↓	Bacteroidetes ↑ Actinobacteria ↑		
ciprofloxacin and vancomycin-imipenem	<i>Alistipes</i> ↓ <i>Streptococcus</i> ↓ <i>Lactobacillus</i> ↓ <i>Clostridium</i> ↓ <i>Turicibacter</i> ↓ <i>Ruminococcaceae</i> ↓ <i>Prevotellaceae</i> ↓ <i>Bacteroides</i> , ↑	<i>Bacteroides</i> ↑ <i>Enterorhabdus</i> ↑ and <i>Enterococcus</i> ↑ Incomplete recovery of gut microbiota	9 days after antibiotic treatment	(290)

Vancomycin	Bacteroidales ↓	Verrucomicrobiales ↑	11 days	(291)
Neomycin	Clostridiales ↓			
Bacitracin				
Meropenem				
Tigecycline	<i>Proteobacteria</i> ↑	<i>Porphyromonadaceae</i> ↑		(221)
	<i>Bacteroidetes</i> ↓	<i>Bacteroidales</i> ↑	5 weeks	
		<i>Enterobacteriaceae</i> ↓		
		<i>Verrucomicrobiaceae</i> ↓		
streptomycin	<i>Turicibacter</i> ↑	<i>Firmicutes</i> ↑	7 days	(292)
and bacitracin	<i>Staphylococcus</i> ↑	<i>Bacteroidetes</i> ↑		
		Incomplete recovery as still high E.coli		
Vancomycin	<i>Klebsiella</i> ↑	<i>Bacteroides</i> ↑	FMT	(293)
	<i>Escherichia</i> ↑		8 Weeks	
	<i>Shigella</i> ↑			
Cefoperazone	<i>Bacteroides</i> ↓	<i>Bacteroides</i> ↑		(294)
	<i>Lactobacillus</i> ↓			

Cefoperazone	<i>Proteobacteria</i> ↑	<i>Proteobacteria</i> ↓	28 Days	(295)
and	<i>Bacteroidetes</i> ↓	<i>Bacteroidetes</i> ↑		
clindamycin	<i>Firmicutes</i> ↓	<i>Firmicutes</i> ↑		
	<i>Deferribacteres</i> ↓			
meropenem,	<i>Enterococcus faecalis</i> ↑	All the phyla recovered	1.5 months	(231)
gentamicin,	<i>Fusobacterium nucleatum</i> ↑	Except for nine species		
vancomycin	<i>Enterobacteria</i> ↑			
(1.5 months)	<i>Bifidobacterium</i> ↓			

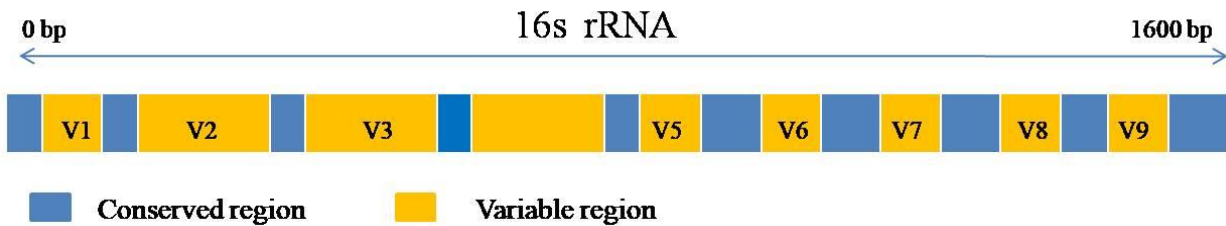
1.13 Different methods to study gut microbiota:

Within a short period, as a result of significant development in technology, bacterial gene sequencing methods emerged considerably and quickly from Sanger to next-generation sequencing methods. Recent technological progress in sequencing methods led to several microbiome studies that promoted culture- and cloning-independent techniques (296). The advantages, disadvantages, and error rates of the different sequencing techniques are varied from each other (11). A massive volume of genomic data can be produced in a short time. Both “16S rRNA-based sequencing of bacterial gene and bioinformatics analysis” are two primary ways to study gut microbiota (11).

The 16S small subunit ribosomal gene is an exclusive housekeeping gene in prokaryotes to identify microbial communities within samples (296).

A total of 9 variable regions are present in a 16s rRNA gene (V1-V9) (297,298). These variable regions are beneficial to distinguish different species (299,300). These regions were amplified through PCR using universal primers during sequencing. The V4 region of the 16S rRNA gene has been used widely in the MetaHIT consortium (296).

Figure 1.6: Schematic diagram of the 16s rRNA gene.



V3, V4, V6, and V8 are the most used reasons for recognizing different bacterial (11). However, the higher sensitivity of the whole-genome metagenomic sequencing method has made it the most effective one to understand the composition of gut microbiota and host-microbiome interaction (301–303).

There are several next-generation sequencing techniques available. Each method has some advantages and disadvantages (11). The accuracy and cost of these techniques also vary from each other.⁴⁵⁴ Pyrosequencing needs a lesser amount of sample, but it is quite expensive, and the possibility of homopolymer errors exists (11). The shotgun sequencing process executes in a short period with a high cost for assembly procedure. Illumina sequencing is a relatively cost-effective, rapid process with high precision. Pacific Bio Sequencing has a higher accuracy rate

(99.9%) and quick processing but high-priced (304). The sequencing method using Ion semiconductor is fast but has multiple errors. However, SOLID or sequencing through the ligation method is comparatively cheap but slow (304).

Chapter: 2

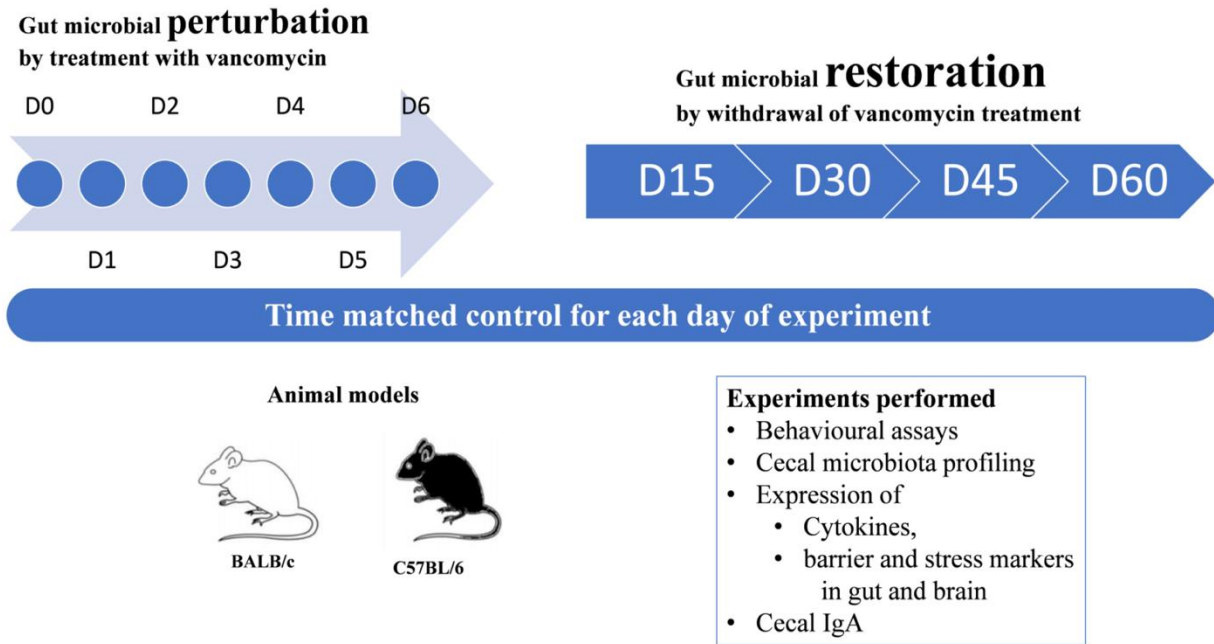
Materials and Methods

2.1 Animals Used in the study: We housed all mice used in the present study in a polysulfone cage using corncob as bedding material. In the current study, we used two immune-biased mice strains, Th1- (C57BL/6) and Th2- (BALB/c). Overall, the mice used for the analysis were adult mice of 6-8 weeks age-old. However, for the cecal microbiota transplantation study, older mice aged 23 weeks and younger mice of 3 weeks were used (305). Food and drinking water were given *ad libitum*. A pathogen-free hygienic environment with a 12 h light-dark cycle (lights on from 7:00 am – 7:00 pm), temperature $24 \pm 3^{\circ}\text{C}$, and humidity 40-70% maintained for animals. These animals were co-housed. We used the animals according to the instructions of CPCSEA — “Committee for Control and Supervision of Experiments on Animals, Govt. of India”. The animal ethics committee under this Committee had sanctioned all the protocols used for this study (129).

2.2 Vancomycin treatment: Vancomycin (Cat#11465492) was orally gavaged at a dose of 50 mg per kg of bodyweight of both strains of immune-biased mice (Fig. 2.1) (305). 0.5 ml of vancomycin was gavaged two times per day at an interval of 12 h for six successive days. The dosage was selected as per previous reports and FDA guidelines (306,307).

2.3 Restoration procedure: We observed mice for sixty days to restore gut microbiota following the termination of vancomycin treatment (129). We termed the 60 days as the restoration phase. Mice were given a regular diet (standard chow and water) (129). Mice were euthanized, and various samples were collected at an interval of every 15 days of restoration, i.e., on the 15th, 30th, 45th, and 60th day. However, we performed the behavioral study by using separate groups of mice.

Figure 2.1: A schema of the experimental protocol for perturbation and restoration of gut microbiota is shown below.



2.4 Sample collection: We split mice into two groups: Control (untreated) and Treatment (groups treated with vancomycin). Mice belong to the treatment group were orally gavaged with vancomycin twice daily for 6 consecutive days. For each treated group, there was a corresponding time-matched control group. Each group consisted of six mice. Mice belonged to the treated, and time-matched control groups were euthanized every day 6 (total of 6-time points) following treatment with vancomycin and four-time points of restoration (on 15th, 30th, 45th, and 60th day). Mice were euthanized using the cervical dislocation method as per protocol approved by the Institutional Animal Ethics Committee. Different samples such as colon, brain, blood, and cecal tissues were collected from mice for various experiments (194) (129).

2.5 Cecal Sample plating: Cecal sample was collected from both strains of mice on day four following treatment with vancomycin. 50 mg of each sample was homogenized in 1 ml of deionized MilliQ water and plated at a dilution of 10^4 fold on **Salmonella-Shigella** specific media and EMB (Eosin methylene blue agar plate) agar plate (308).

2.6 Genomic DNA extraction: We used cecal samples to isolate genomic DNA using the phenol-chloroform method. Cecal samples of weight 150-200 mg were homogenized in 1ml of 1X PBS. 10mins centrifugation of the homogenized cecal sample was performed at 6,700 g (309). The precipitate was lysed by homogenizing it in 1 ml of lysis buffer (containing Tris-HCl 0.1 mol l^{-1} , EDTA 20 mmol l^{-1} , NaCl 100 mmol l^{-1} , 4% SDS (at pH 8) and 45 mins of subsequent heating at a temperature of 80° C . Lipid and protein were removed from the supernatant using an equal volume of phenol-chloroform, this process was repeated until the aqueous phase became colorless. DNA was precipitated overnight at -20° C with three volumes of absolute chilled ethanol. Finally, we washed it with 500 μl of 70% chilled ethanol. We extracted genomic DNA in nuclease-free water. We used NanoDrop 2000 to quantify the extracted gDNA.

2.7 16S-rRNA sequencing (V3-V4 Metagenomics) of gut microbiota:

16S rRNA gene (V3-V4 regions) of the microbiota present inside the cecal sample was amplified. For this amplification, V3F (Forward primer): 5'-CCTACGGGNBGCASCAG-3' and V4R (Reverse primer): 5'-GACTACNVGGTATCTAATCC-3' primer pair was used. In the Illumina Miseq platform, amplicons are sequenced using paired-end (250bpX2) with a sequencing depth of 500823.1 ± 117098 reads (mean \pm SD). Base compositions, quality, and GC content of the FASTQ sequence were checked. More than 90% of the sequences had Phred quality scores above 30 and GC content was nearly 40-60%. Conserved regions from the paired-

end reads were removed. V3-V4 regions were set up through the FLASH program where unwanted sequences were deleted and final V3-V4 regions were assembled (310). Pre-processed reads from all the samples were pooled and clustered into Operational Taxonomic Units (OTUs) through the de novo clustering method based on their sequence similarity using the UCLUST program. QIIME was used for the OTU generation and taxonomic mapping (311). For individual OTU, a representative sequence was established and PyNAST program was used for the alignment against the Greengenes core set sequences (312,313). Representative sequences were aligned against the chimeric data sets. To eliminate the hybrid sequences and for the taxonomic classification, we used RDP classifier against the SILVA database (129).

2.8 RNA extraction: We used RNeasy mini kit for the extraction of RNA from the gut tissue (Cat# 74104, Qiagen India), and RNA later was used to store the extra sample for future use (129). During the extraction process, nearly 20-23 mg of gut tissue was churned using liquid nitrogen and 700 μ l of RLT buffer was added and homogenized well. An equal volume of 70% ethanol was added and mixed well. The solution was centrifuged at 8000 \times g for 5 min at room temp. The clear solution containing lysate was passed through the RNeasy mini column (Qiagen, Germany), which leads to the binding of RNA to the column. The column was washed using 700 μ l RW1 buffer and next with 500 μ l of RPE buffer. 30 μ l of nuclease-free water was finally used to elute the RNA. We used “NanoDrop 2000 (Thermo Fisher Scientific, USA)” to check the quality of extracted RNA.

For RNA extraction from brain tissue, 100 mg of brain tissue was homogenized in 2 ml of TRIzol reagent. Centrifugation was done at 12000 \times g at 4°C for 10 min. The fat monolayer was carefully avoided while pipetting the rest of the sample in a clean 1.5 ml MCT and 400 μ L of chloroform was added to the sample. Centrifugation was again performed at 12000 \times g for 30

min at 4°C. In a new MCT, the RNA phase was shifted and 1.5 volume of 100% Ethanol was mixed to it. Then the sample was loaded to a spin column. “HiPurA Total RNA Miniprep Purification Kit” was used for the extraction of RNA (129).

2.9 cDNA preparation from extracted RNA: cDNA was synthesized by using the Affinity Script One-Step RT-PCR Kit (Cat# 600559, Agilent, Santa Clara, US) using extracted RNA. RNA was mixed with a random 9mer primer, Taq polymerase, and NT buffer, the mixture was kept at 45°C for 30 min for the synthesis of cDNA and temperature increased to 92°C for deactivating the enzyme.

2.10 Real-time PCR (qRT-PCR): 96 well plates with 25 ng of cDNA as template, 1 μM of each of forward (_F) and reverse (_R) primers for various genes, SYBR green master mix (Cat#A6002, Promega, Madison USA), and nuclease-free water were used for the **qRT-PCR experiment**. QuantStudio 7 Real-Time PCR (Applied Biosystems, USA) was used for the qRT-PCR study (129). All values were normalized with the cycle threshold (Ct) value of GAPDH (internal control) and fold change of the desired gene was calculated with respect to control using the protocol described before (229,314).

2.11 Cytokine Analysis at the protein level

Alteration in the cytokine level was checked in the colon tissue of vancomycin treated mice where tissues were collected on the specific time points such as on day zero (untreated control), day three, and day six of vancomycin treatment. These tissues were churned by using lysis buffer containing tris-hydrochloric acid, sodium chloride, triton X-100 in distilled water, and 1X protease inhibitor cocktail (PIC) (Cat#ML051, Himedia, India) (315). The churned tissue was centrifuged at 20,000 g for 20 min (228). ELISA (“BD Biosciences, San Diego, CA, USA”) was performed in the supernatant of the tissue by using the manufacturer’s protocol for TNF- α

(Cat#560478) and IL-10 (Cat#555252) expression. Bradford assay was done to normalize the concentration of protein. We used the Bradford assay for the normalization of protein concentration. Quantification was done by taking the absorbance through Multiskan Go (Thermo Fisher Scientific, Columbus, OH, USA).

2.12 Serum collection: Mice were anesthetized and whole blood was collected by cardiac puncture. Serum was extracted from the blood by centrifuging it at 1,700 g for 15 min at 4 °C (228) (316). If required, serum was stored at -80 °C until further use.

2.13 Measurement of Cecal index: Cecal weight and body weight of each mouse was recorded (129). The cecal index was measured by taking the ratio of the cecal content weight to the bodyweight of the respective mouse (317).

2.14 Gut permeability test by FITC dextran: At some selected time points of perturbation and restoration period, mice were water starved overnight (129). The next day FITC-dextran (Cat#F7250, Sigma-Aldrich, Missouri, US), at a concentration of 100 mg/ml, was dissolved in PBS and orally gavaged to water-starved mice. After 4 h, mice were anesthetized by isoflurane inhalation and blood was collected by cardiac puncture. FITC concentration was estimated by taking absorbance through a Spectrofluorometer (“excitation wavelength of 485 nm and emission of 528 nm at 20 nm bandwidth”) (129). The procedure was performed by following the previously described protocol (318).

2.15 Cecal Microbiota Transplantation (CMT): Cecal sample was collected from sixth-day vancomycin treated mice and diluted with PBS (1gm per 10 ml) to make stock. All the vancomycin-treated groups of mice on the third day were orally gavaged with 400 µl of the stock cecal solution (316).

2.16 Oral Glucose tolerance test (OGTT): OGTT was performed in both BALB/c and C57BL/6 mice on the selected days of vancomycin treatment like day zero, three, and six (4,316,319). Following 6h of starvation of mice from each treatment group, fasting blood glucose level (considered as control glucose level at zero min) was measured by a glucometer by tail vein bleeding. Mice, fasted for 6h, were orally gavaged with glucose at a dose of 1 mg g^{-1} bodyweight of the mouse. Glucose levels in the blood were estimated at four-time points, i.e. 15-, 30-, 60- and 90-mins following glucose gavaging through blood glucose monitoring system or glucometer (“ACCU-CHEK Active, Roche Diabetes Care GmbH, Mannheim, Germany”) (320).

In the CMT group of mice also we have measured the glucose level through a similar procedure as mentioned above. OGTT was performed in the third-day vancomycin-treated group of mice after receiving CMT (4).

2.17 Sample preparation and NMR data acquisition for metabolomics study

Serum was isolated from the blood of antibiotic-treated and control groups of mice as described before. Proteins in the serum were removed by passing it through a pre-rinsed (7 times washed) Amicon Ultra-2ml 3000 MWCO (Merck Millipore, USA) column. Centrifugation was done at 4°C at 12,000g. A total of 700 μL solution for NMR analysis was prepared by mixing serum samples with D_2O and NMR buffer (50 mM Na_2HPO_4 , 1 mM 2,2-Dimethyl-2-silapentane-5-sulfonate sodium salt (DSS-d₆) - as chemical shift indicator). It was loaded into Wilmad® 5 mm NMR tubes (Sigma Aldrich, USA). The NMR was executed at 298K on a Bruker 9.4 T (400 MHz) AVANCE-III Nanobay liquid-state NMR spectrometer fitted with a 5 mm broadband (BBO) probe (305) (4). To assure full water saturation, the pre-saturation technique was used with a mild relaxation delay of 5 seconds. Through a real-time ‘gs’ mode for every sample, offset

optimization was carried out. The acquired spectra were registered and processed using Topspin 2.1 (4).

2.18 Metabolomic Analysis of NMR data

ChenomX (Canada) was used for the analysis of NMR data. We used the Bayesian approach to calculate the concentration of various metabolites in the serum (4). The phase and baseline of the raw spectrum were corrected and concentrations of metabolites were obtained through a profiler using Metaboanalyst (10,312,321–324). Each sample spectrum with 128 scans was collected into 32768 time-domain data points and a spectral width of 8012Hz. Metabolite signals from NMR spectra were identified (targeted) and quantified using Chenomx NMR Suite7.6 (ChenomxInc., Edmonton, Canada). The spectra from the FID files were automatically phased and the baseline corrected and referenced to the DSS peak at 0 ppm through the Chenomx processor. The profiler was used to assign and fit the metabolites peak from the Chenomx library and SCFAs such as acetate, butyrate, and propionate were quantified from the spectral intensities according to Chenomx guidelines.

2.20 Endotoxin detection assay from serum: Limulus Amebocyte Lysate (LAL) test was used for the detection of lipopolysaccharides located in the outer membrane of Gram-negative bacteria. For this test, mice were sacrificed on days zero, three, and six following treatment of mice with vancomycin, and blood was collected by cardiac puncture in an endotoxin-free vial. “Toxin sensor chromogenic LAL endotoxin assay kit from GeneScript (Cat# L00350 Piscataway, NJ, USA)” was used for detecting endotoxin levels in the serum of mice using the manufacturer’s protocol (325).

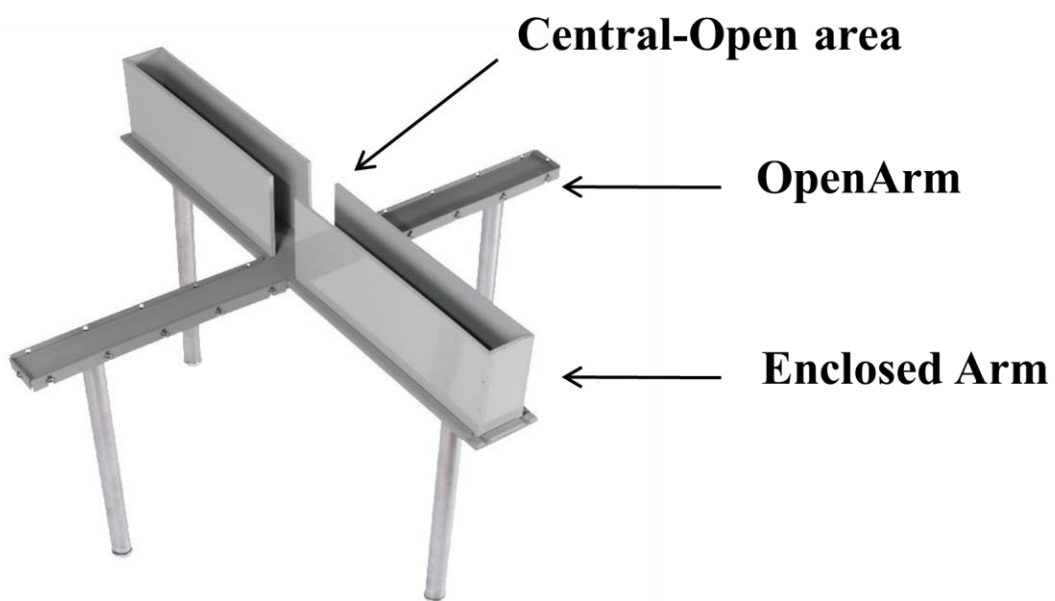
2.21 Acetate detection assay in serum: The concentration of acetate was estimated in the serum of both strains of mice on day zero (untreated control) and day six following vancomycin

treatment through acetate colorimetric assay kit (EOAC-100, San Francisco, USA) (4). Both control and treated mice were anesthetized and blood was collected through cardiac puncture. Blood was kept on ice for 30 min followed by centrifugation at 1,700 g for 15 min at 4°C. After the centrifugation, the supernatant was collected. For each sample, 10 µl of serum was utilized to measure the acetate level through a substrate-enzyme coupled colorimetric reaction at an absorbance of 570 nm.

2.22 Hormonal assay: Concentrations of different hormones like Leptin (Cat# ELM-Leptin), and Insulin (Cat# ELM-Insulin) were measured in the serum samples whereas the concentration of PYY (Cat# EIAM-PYY) was measured in the colon tissue of mice through Raybiotech mouse hormonal assay kit (Norcross, Georgia, USA).

2.23 Elevated plus maze test: Elevated plus maze is commonly used for assessing anxiety levels in rodents - specifically in mice (326). The instrument was made of wood, painted dark, and placed 80 cm above the ground of the room (129). It is fitted with a central platform and four crossed arms, each 50 cm long and 10 cm wide. The walls of the open and closed arms of the instruments were extending 30 cm above the maze floor (326). Each mouse of the untreated and antibiotic-treated groups was positioned at the center of the maze facing one of the open arms during the testing sessions, and every animal was allowed to explore the maze for a total of 5 mins. The time spent in the closed and open arms of the instrument was separately calculated (129). A computerized video tracking system “Smart 3.0, Panlab SMART video tracking system, Harvard Apparatus” was used for the recording of the movement of mice on the instrument. In this test, seven mice were utilized (n=7) (129).

Figure 2.2: An image of the elevated plus-maze instrument



2.24 Forced swim test (FST): Forced swimming test is one of the valid ways of testing despair and depression created by stress in the mice model (327). A cylindrical tank (30 cm height and 20 cm diameter) was made and it was filled up to 19 cm with tap water at $24\pm1^{\circ}\text{C}$ temperature. Each mouse was subjected to a 6 min of swimming session with the last five minutes considered

for the data analysis. During this period, immobility was recorded by using a video camera. When it became static in the water without attempting to flee, the mouse was considered to be immobile and the time spent by the mice in this condition was known as the immobile time. Those motions that were crucial for keeping its head above the surface of the water were not taken as an immobile pose. The sample size for this test was seven mice (n=7) (129).

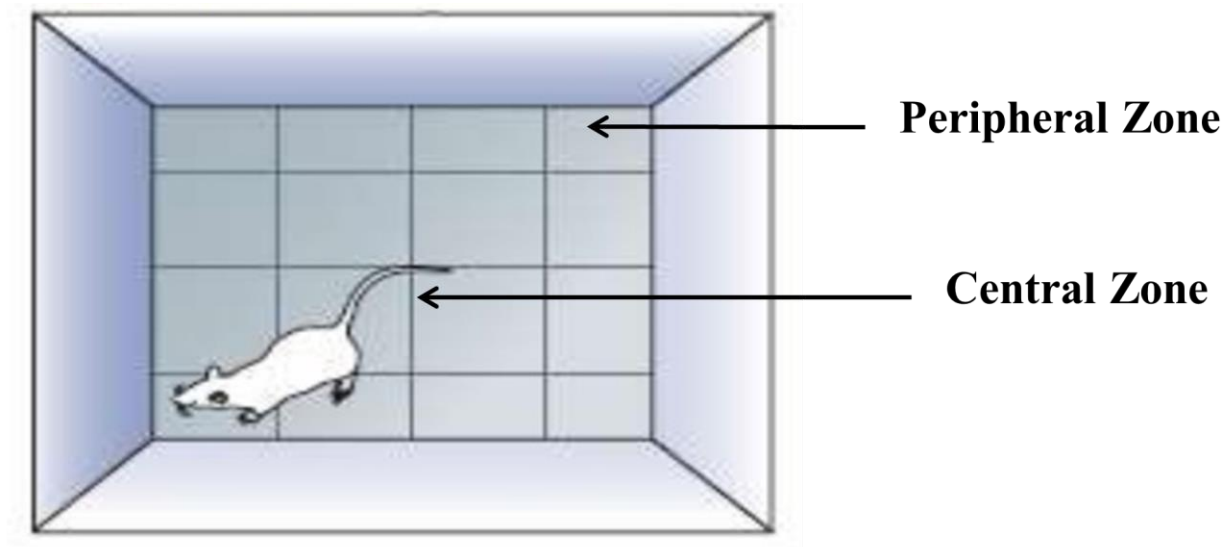
Figure 2.3: An image of the forced swim test



2.25 Open field (OF) test: Open field test is commonly used to measure anxiety and locomotor activities in small rodents (328). The instrument is a square box comprised of wood and bright light from the roof brightens the dark part of it (129). Each animal was placed in the middle of the box for five mins. Its locomotor activity was measured by using a computerized video

tracking system “Smart 3.0, Panlab SMART video tracking system, Harvard Apparatus”. The software also calculated the cumulative time spent by the mice in the instrument and the time spent at the periphery and center of the instrument separately (129). The open field was divided by virtual lines into a total of 16 equal squares, out of which 12 squares formed the peripheral zone, and the remaining 4 squares made the central zone of the box. The sample size for this test was seven mice (n=7)

Figure 2.4: An image of the open field test instrument.



2.26 Animals Used in the CMT study: All mice used in the present study were co-housed in polysulfone cage, and corncob was used as bedding material. Young male BALB/c mice of age 3 weeks and older mice of age 23 weeks were used for this study. Food and water were provided

ad libitum. Animals were co-housed in a pathogen-free environment with a 12h light-dark cycle at temperature $24 \pm 3^\circ$ with nearly 55% of humidity. All protocols were approved by the Institute Animal Ethics Committee constituted by CPCSEA (Reg. No.- 1643/GO/a/12/CPCSEA).

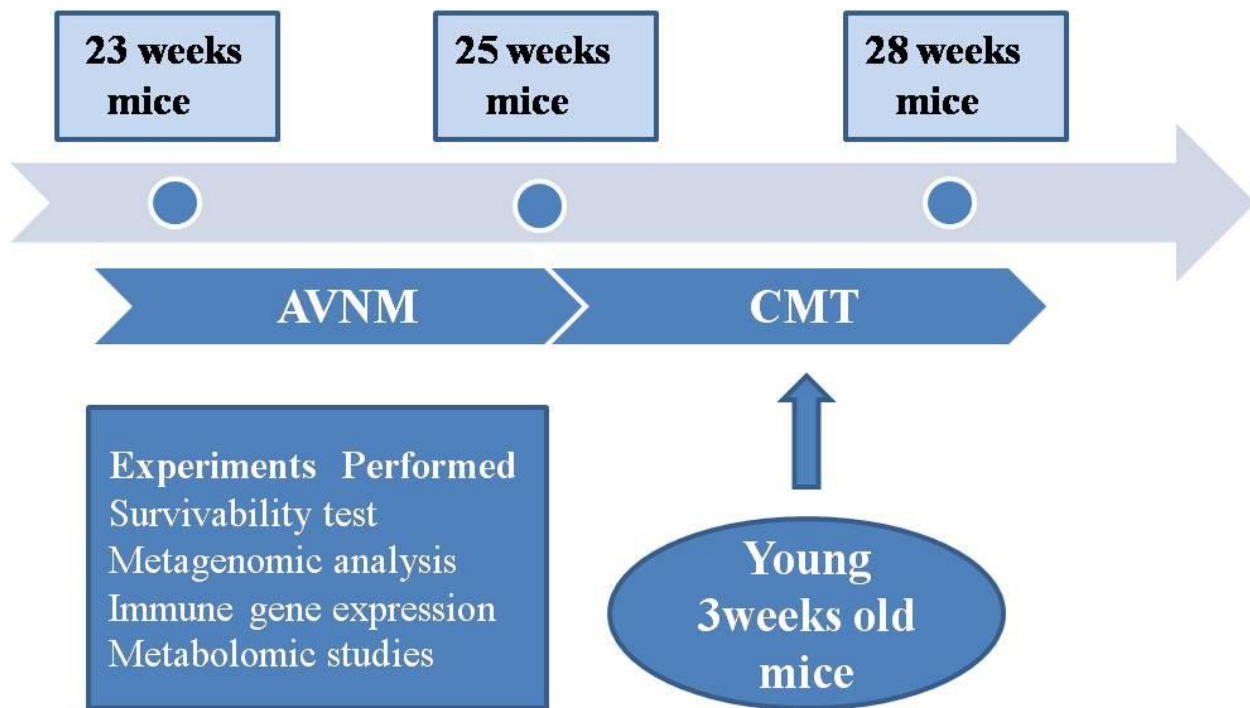
2.27 *Salmonella Typhimurium* (ST) culture and dose standardization:

ST stock solution was obtained from ATCC 14028 of Himedia. *Salmonella* was cultured on the nutrient broth. The dosage of *Salmonella* challenge was determined by a dose titration with three doses such as 10^7 CFU/mouse, 10^8 CFU/mouse, and 10^9 CFU/mouse of ST. 23 weeks of older mice (n=6) were orally gavaged with these doses and were kept under observation for 15 days. The decisive selected dose for further studies was 10^8 CFU/mouse of ST based on the survival data as described in the result section.

2.28 Cecal microbiota transplantation (CMT): Cecal microbiota transplantation was done followed by an antibiotic treatment with AVNM. AVNM cocktail (MP Biomedicals, Illkirch, France) was made by mixing four antibiotics i.e., ampicillin (1gm/lit), vancomycin (500mg/lit), neomycin (1gm/lit), and metronidazole (1gm/lit) in the drinking water. This cocktail of antibiotics was changed at a gap of every two days and a freshly prepared AVNM mixture was added to the drinking water bottle of mice. The dosages of AVNM treatment were selected as per previous reports (329,330). The antibiotic treatment was done in 23 weeks old mice for two weeks. The procedure for CMT was developed for the current study based on a previous report by Bastard et al. (261). The younger mice (3 weeks) which were specific pathogen-free, healthy (not having any gastrointestinal disorder or other diseases), and without being exposed to any antibiotics for the last three months were selected as donor mice for the CMT procedure. Fresh cecal matter from younger donor mice was collected in a sterilized container and reconstituted in 1X PBS with a dose of 1g/10ml. The reconstituted cecal matter was mixed evenly by vigorous

vortexing. Then the cecal solution was filtered to remove any particulate matter. After AVNM treatment, the cecal microbiota transplantation was performed for the next three weeks in older mice. The older mice were orally gavaged with the cecal matter (200 µl) of younger mice once per week for up to three weeks.

Figure 2.5: Timeline of the experimental procedure for Cecal microbiota transplantation from younger to older mice and other host physiology-related studies.



2.29 Grouping and Sample collection of mice: Mice were separated into four different groups, i.e., untreated control mice (both young 3 weeks and old 23 weeks aged mice), antibiotic-treated mice (AVNM), antibiotic-treated mice followed by cecal microbiota transplantation (AVNM+CMT) restoration, antibiotic-treated mice followed by restoration without cecal microbiota transplantation (AVNM-CMT). Mice from each group were euthanized by cervical dislocation. Samples like blood, cecum, colon were collected from all groups of mice (n=3). The liver and spleen were collected only from mice after salmonella infection (n=3). Tissue samples, which were not used immediately, were stored in RNA later for RNA analysis until further usage (229,314,315).

2.30 Treatment with other antibiotics: C57BL/6 mice were divided into three groups: i) vancomycin ii) neomycin iii) AVNM treated group. Antibiotics were treated for seven consecutive days. Vancomycin-treated group of mice was gavaged orally with vancomycin at a dose of 50 mg per kg of body weight, twice daily at a gap of 12h. Similarly, neomycin-treated mice were also gavaged orally with neomycin at a dose of 50mg per kg of body weight twice daily. The dosages were selected as per previous reports and FDA guidelines (306,307,331,332).

In AVNM treated group, the AVNM cocktail (MP Biomedicals, Illkirch, France) was made by mixing four antibiotics, i.e., ampicillin (1gm/lit), vancomycin (500mg/lit), neomycin (1gm/lit), and metronidazole (1gm/lit) in the drinking water. This cocktail of antibiotics was changed at a gap of every two days (at 48hrs interval), and a freshly prepared AVNM mixture was added to the drinking water bottle of mice. The dosages of AVNM treatment were selected as per previous reports (282,329,330). The AVNM mixture is a broad-spectrum antibiotic cocktail that inhibits both Gram-positive and Gram-negative bacteria of the gut. Ampicillin is one of the β -lactam antibiotics which acts against both Gram-positive and Gram-negative

bacteria. Vancomycin is one of the glycopeptide antibiotics which mainly acts against Gram-positive bacteria of the intestine. Neomycin is an aminoglycoside antibiotic with bactericidal activity against Gram-negative bacteria and metronidazole primarily works against anaerobes (330).

2.31 Statistical Analysis:

All the graphs were plotted using GraphPad Prism version 7.0. Both unpaired parametric ‘t’-test (to compare any 2 data sets) and one-way ANOVA (to compare more than two datasets) were performed for statistical analysis of data as described in the text (305). We calculated the significance across multiple treatments using two-way ANOVA (Bonferroni test).

Chapter: 3

Results and Discussion

Chapter 3.1: Perturbation of gut microbiota through Vancomycin and its effect on the physiology of Th1- and Th2-biased mice.

3.1.1 Introduction:

Perturbation of gut microbiota can be used as an effective tool to understand its role in the host; abundance and diversity of gut microbiota vary with different factors like age (61), diet (130), geography (204,205), stress (181), pathogen (206), and antibiotics (207). However, among all these factors, antibiotic can be used as one of the most potent agents to study the role of gut microbiota, as the effect of antibiotics is not only limited to targeted pathogens but also the vast number of commensal microbes present in the gastrointestinal tract of the host (333). In fact, in the long term, various commonly used antibiotics can change the composition, diversity, and richness of commensal gut microbiota resulting in the alteration of different metabolism of the host (269,334) and thus, lead to various metabolic diseases like diabetes, obesity, and IBD (335,336).

Among various antibiotics, Vancomycin is majorly prescribed orally against the infection of two multi-drug resistant strains, i.e., *Clostridium difficile* and *Staphylococcus aureus* (337–339). Despite the effectiveness of Vancomycin in IBD, CD patients, it can cause effective alteration in the gut microbiota composition by elevating pathogens and alleviating health commensal microbes (234).

However, the dose and time-dependent effects of Vancomycin on gut microbiota are still unknown. The microbiota present in the gastrointestinal tract is crucial for evolving a mature immune system of the host (70). Studies revealed that the gut microbiota impacted the host's immune system through the interactions of their molecular patterns (lipopolysaccharide,

peptidoglycan) with toll-like receptors (TLR4, TLR2) present in the epithelial cell of the gut. These interactions produce various cytokines and chemokines for immune regulation (340).

Microbiota present in the gut controls major nutrients like carbohydrates, amino acids, fatty acids, and vitamins. Some short-chain fatty acids such as "acetate, propionate, and butyrate" are produced by certain groups of gut microbes also regulate the inflammatory response and metabolism of the host by binding to free fatty acid receptors (FFAR2/3) present in intestinal epithelial cells, immune cells, adipocytes (104). Intestinal epithelium acts as a barrier to the entry of different pathogens, inflammatory molecules, and toxins into the mucosal tissue (341). The commensal microbes present on intestinal epithelial cells maintain their integrity by controlling the expression of various tight junctions by occludin, claudins, etc. (342).

In this chapter, we mainly focused on the effect of the clinical doses of vancomycin treatment on the diversity and composition of gut microbiota in mice. A time-dependent variation pattern of gut microbiota was found during vancomycin treatment. We compared the perturbation of gut microbiota and its associated changes in host physiology between Th1- and Th2- biased mice. We reported in this chapter primarily the correlation between the gut microbial metagenomic alteration pattern and various host immune and metabolic changes. We found some strong associations between the prevalence of certain gut microbes' expression and the expression of different immune regulatory and tight junction protein genes in the gut.

3.1.2 Results:

Selection of antibiotics:

Plating data of fecal samples of different antibiotic-treated mice (Fig.3.1.1 A. and B.) showed changes in colony count from the first day to the seventh day of treatment. The clinical dose of

the vancomycin-treated group showed the most significant changes in colony count compared to other antibiotic-treated groups (neomycin, amoxicillin, ciprofloxacin). So, we chose to use Vancomycin as the perturbing agent among other antibiotics for our further study. A sudden increase in certain bacterial colonies was observed on the NB agar plate after the second day or fourth dose of vancomycin treatment. The bacterial colony count on a plate from the second day to the fourth day was one log higher in BALB/c, and two logs higher in C57BL/6 mice of Vancomycin treated group than other antibiotics treated and control groups of mice. After the fifth day of treatment, the bacterial population started decreasing on the plate.

Figure 3.1.1: Kinetic perturbation of gut microbiota following different antibiotics treatment in Th1- and Th2- biased mice.

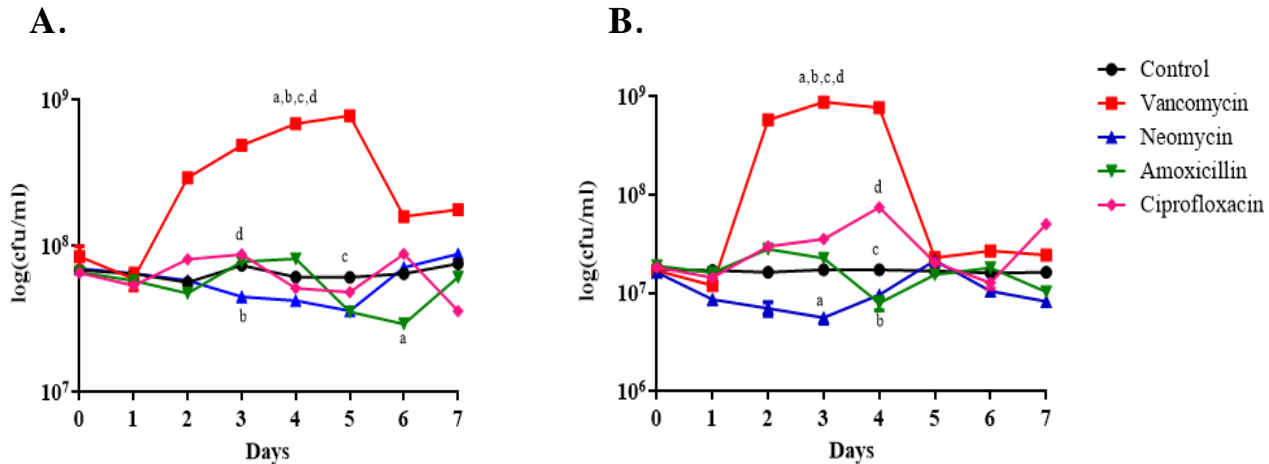


Fig.3.1.1 showing the kinetics of the Colony Forming Unit of the fecal sample in the NB agar plate following different antibiotics treatment in A. BALB/ c, B. C57BL/6 mice.

Vancomycin treatment alters the abundance and diversity of gut microbiota

Perturbation of gut microbiota following treatment with Vancomycin was reported in both human and mouse models (234,246,343,344). From the earlier reports, we acknowledged the importance and aspects of the effects of Vancomycin in understanding the role of gut microbiota. However, the impact of the host's immune profiles and genetic background on the gut microbiota was not addressed earlier. The mammalian host immune responses could be broadly differentiated in either Th1 or pro-inflammatory and Th2 or tolerogenic. We tested the effect of Vancomycin on two immunologically different mice strains.

We used 16S rRNA (metagenomic) based sequencing protocol to understand the kinetics of altered microbiota profile in the cecum following treatment with Vancomycin. Metagenomic analysis of the cecal content revealed that the microbial compositions changed significantly in both BALB/c and C57BL/6 mice following treatment with Vancomycin (Figure 3.1.2). The results of untreated mice shown in Figure 3.1.2A and Figure 3.1.2C, mainly revealed that in both BALB/c and C57BL/6 mice, the gut microbiota overtly belongs to the Firmicutes and Bacteroidetes phyla. The abundance of the phyla, Firmicutes and Bacteroidetes, was reduced while the abundance of Proteobacteria phylum was increased significantly by the second day following treatment with Vancomycin. The Proteobacteria level reached maximum by day five (93% of total abundance) in BALB/c mice and by day four (81% of total abundance) in C57BL/6 following treatment with Vancomycin (Figure 3.1.2B and Figure 3.1.2D).

On the contrary, Firmicutes level plummeted from 70-80% (untreated control group) to below 10% (the fourth day following treatment with Vancomycin), and Bacteroidetes level reduced from 25-30 % (untreated group) to 1% (the fourth day following treatment with

Vancomycin) in both BALB/c and C57BL/6 mice (Figure 3.1.2B and Figure 3.1.2 D). After day four of treatment with Vancomycin, BALB/c and C57BL/6 mice showed a significantly different gut microbiota profile with the appearance of phylum, Verrucomicrobia. A sudden increase in Verrucomicrobia phylum, from day five onwards, in C57BL/6 and from day six onwards, in BALB/c mice following vancomycin treatment replaced the previously predominant Proteobacteria phylum. Verrucomicrobia phylum was found to be more (72%) in C57BL/6 mice on the sixth day of vancomycin treatment compared to BALB/c mice (30%). This result was significant to understand the differential response exhibited in two different strains of mice (C57BL/6 and BALB/c) used in this study following treatment with Vancomycin. We showed changed phyla of gut microbiota following vancomycin treatment in Fig. 3.1.2.

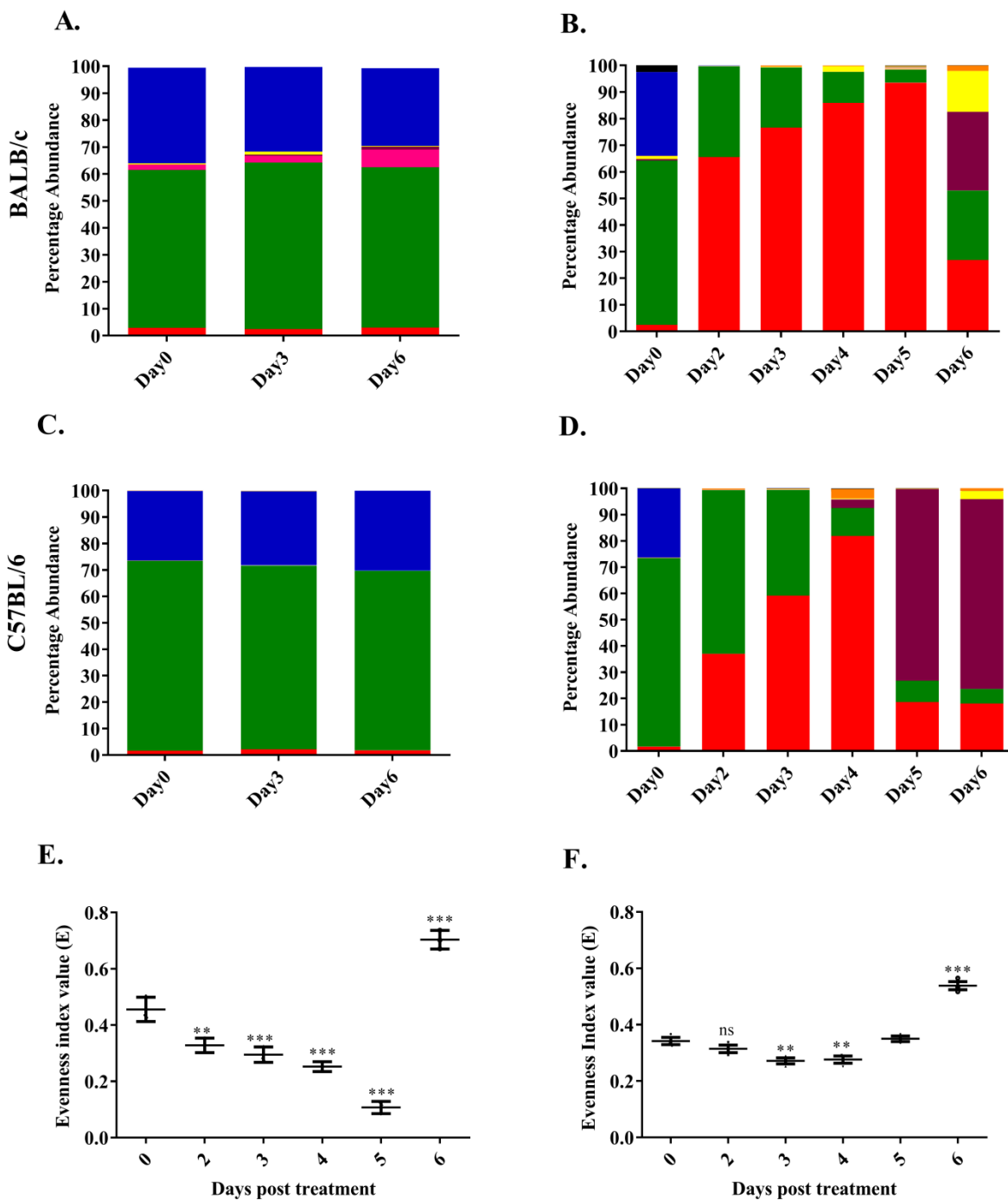


Figure3.1.2: Phylum level changes in the gut microbiota. Alteration kinetics of various phyla of gut microbiota are shown, control A. BALB/c and C. C57BL/6 and Vancomycin treated B. BALB/c and D. C57BL/6 mice. The data shown are the average of three biological replicates. To avoid clutter, the standard deviation (SD) calculated using 2-way ANOVA is not shown. However, SD was less than 10% on average. Kinetics of changes in phylum-level Equitability index (E) of the gut microbiota following treatment with Vancomycin in E. BALB/c and F. C57BL/6 mice. Statistical significance of diversity in panels E. And F. was calculated by two-way ANOVA. ('***' corresponds to $P \leq 0.001$, '**' corresponds to $P \leq 0.01$, '*' corresponds to $P \leq 0.05$ level of significance). Error bars are one standard deviation of the mean value and determined from the average values of biological replicates.

Besides, we further determined the alpha diversity of gut microbiota by using the Shannon methodology. Shannon equitability index (the evenness in the distribution of various microbial taxa) was calculated. Shannon equitability index was found to be decreased up to the fifth day in BALB/c (Figure 3.1.2E) and up to the fourth day in C57BL/6 mice (Figure 3.1.2F) following vancomycin treatment. However, it was increased in the latter days of vancomycin treatments, like on day six for BALB/c and day five for C57BL/6 mice. Cecal index and cecal liquid content were considerably higher in vancomycin-treated mice than control mice (Table. 3.1.1).

Table 3.1.1: Measurement of the cecal index and cecal liquid content at different time points in BALB/c and C57BL/6 mice.

Mice	Conditions	Day	Cecal index (±SD)	P-value	Cecal liquid content in µl (±SD)	P-value
BALB/c	Control	zero	0.01 (±0.001)		6.1 (±1.4)	
	Vancomycin treated	three	0.02 (±0.005)	0.0014	200 (± 26)	0.0005
	Vancomycin treated	Six	0.02 (±0.002)	< 0.0001	211 (± 20)	0.0006
C57BL/6	Control	zero	0.008 (±0.002)		7.3 (± 1.9)	
	Vancomycin treated	three	0.03 (±0.003)	< 0.0001	245 (± 40)	0.004
	Vancomycin treated	Six	0.03 (±0.002)	< 0.0001	232 (± 34)	0.0028

Means of the cecal index and cecal liquid content of different groups with their respective standard deviations (±SD) were represented. Statistical significance between each of the treated groups and their respective control groups was calculated by using a t-test and p-values were shown.

At the genus level, the gut microbiota of untreated time-matched control of either type of mice majorly composed of Blautia, and Intestinimonas genera of the Firmicutes phylum as well

as *Bacteroides*, and *Alistipes* genera of Bacteroidetes phylum (Figure 3.1.3A and Figure 3.1.3C). However, on the fourth day of vancomycin treatment, *Escherichia-Shigella* and *Desulfovibrio* were the most predominant genera of both BALB/c and C57BL/6 mice (Figure 3.1.3B and Figure 3.1.3D). These results were further validated by plating day four cecal homogenate in specific media- EMB agar (*E.coli*) and Salmonella-Shigella agar plate (*Shigella sp.*). Plating data of cecal samples from day four following vancomycin treatment showed overgrown colonies compared to untreated mice on the specific media (Figures 3.1.3E and 3.1.3F). This trend, however, changed as the treatment with Vancomycin continued beyond day four. On day six following vancomycin treatment, the genus level data showed a predominance of *Akkermansia muciniphila* in both strains of mice. However, *A. muciniphila* level was significantly higher, in C57BL/6 (80%) than BALB/c (30%) mice. We performed 16S based qPCR using *A. muciniphila* species-specific primers to confirm the metagenomic data (Table 3.1.2). Through qPCR, we found that nearly 21- and 24833-fold higher abundance of *A. muciniphila* in Vancomycin treated BALB/c and C57BL/6 mice, respectively, on day six post-vancomycin treatment compared to the time-matched untreated control mice. While on day three following vancomycin treatment, the abundance of *A. muciniphila* was so low that the threshold cycle value (C_t) could not be determined for either BALB/c or C57BL/6 mice.

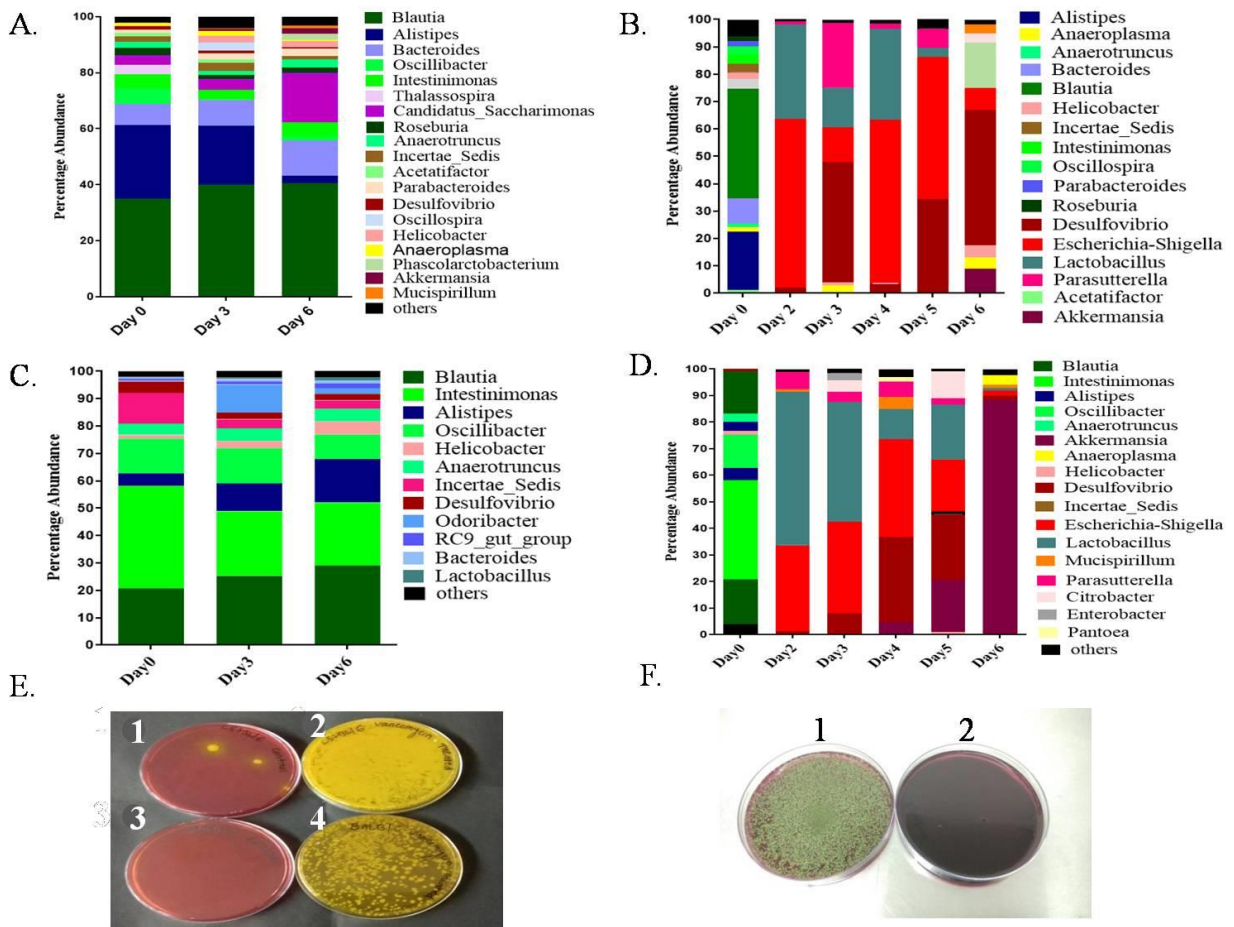


Figure 3.1.3: Metagenomic analysis of genus-level variation of gut microbiota in Vancomycin treated and its respective control group of mice. Alteration kinetics of gut microbiota at the genus level, in control A. BALB/c, and C. C57BL/6 and in Vancomycin treated B. BALB/c, and D. C57BL/6 mice are shown. The data shown are the average of three biological replicates, and the standard deviation was less than 10% on average. The percentage abundance of different genera for various treatment conditions is shown on the 'Y'-axis. The days elapsed post-treatment, or time-matched control is shown on the 'X'-axis. Evidence of E. Shigella colony growth on day four on Salmonella-Shigella specific media agar plate [1. control C57BL/6, 2. vancomycin treated C57BL/6, 3. control BALB/c, and 4. vancomycin treated BALB/c] and F. Growth of *E.*

coli. colonies on day four on EMB (Eosin methylene blue agar plate), [1. vancomycin treated C57BL/6 and 2. Control C57BL/6].

Table 3.1.2: 16S qPCR detection of *A. muciniphila* bacteria abundance in fecal samples of treated and control mice.

Mice	Conditions	Day	Ct	Value (±SD)	P-value from qPCR	Remarks	OTU number	P-value
BALB/c								
	Control	zero	27.4 (±0.6)			Low	300 (±86)	
						abundance		
	Vancomycin treated	three	Could not be determined			Diminished	3 (±1)	
	Vancomycin treated	six	23 (±0.7)	0.0012		Increased by 21 fold from day zero	12531 (±2892)	0.0019
C57BL/6								
	Control	zero	29 (±0.9)			Low	10 (±4)	
						abundance		
	Vancomycin treated	three	Could not be determined			Diminished	5 (±2)	

Vancomycin treated	six	14.4 (± 0.5)	< 0.0001	Increased by 217482 24833 fold (± 10926) from day zero	< 0.0001
--------------------	-----	--------------------	----------	--------------------------------------------------------------------	----------

Ct value of cecal DNA using *A. muciniphila* specific primer in qPCR for untreated, Day three, and Day six following vancomycin treatment in BALB/c and C57BL/6 mice. Means of Ct value and OTU numbers with their respective standard deviations ($\pm SD$) were shown. Statistical significance between each of the treated groups and their respective control groups was calculated using a t-test.

The above results indicated that both the mice strains showed an initial increase in Proteobacteria abundance following treatment with Vancomycin in a time-dependent manner, followed by an increase in abundance of Verrucomicrobia Phylum by day six. The differential abundance of *A. Muciniphila* on day six showed a significant increase in C57BL/6 over BALB/c following treatment with Vancomycin.

The inflammatory response in the colon changed during vancomycin-mediated microbiota perturbation in a time-dependent manner.

We checked the effect of the vancomycin-mediated microbial perturbation on the mRNA expression of various pro- (TNF- α , IL-6, IL-1A, IL-17) and anti-inflammatory (TGF- β and IL-10) genes in both mice strains. The mRNA level expression data from colonic tissue revealed the time-dependent increase of pro-inflammatory cytokines till day four of treatment in both mice

strains (Figures 3.1.4A and 3.1.4B). A decrease in the expression of the pro-inflammatory cytokines was associated with a reduction of Proteobacteria abundance after day four of vancomycin treatment (Figures 3.1.4C and 3.1.4D). Next, we also observed a marked increase of TLR4 expression, upstream regulator of the inflammatory response (345) on the third day, and it decreased by the sixth day of treatment in both mice strains (Figures 3.1.4E and 3.1.4F). However, we found a significant increase in the expression of TLR2 on day five and day six following vancomycin treatment in C57BL/6 mice compared to BALB/c mice. The rise of TLR2 gene expression was correlated with the higher abundance of *A. muciniphila* during day five and day six following vancomycin treatment in C57BL/6 mice.

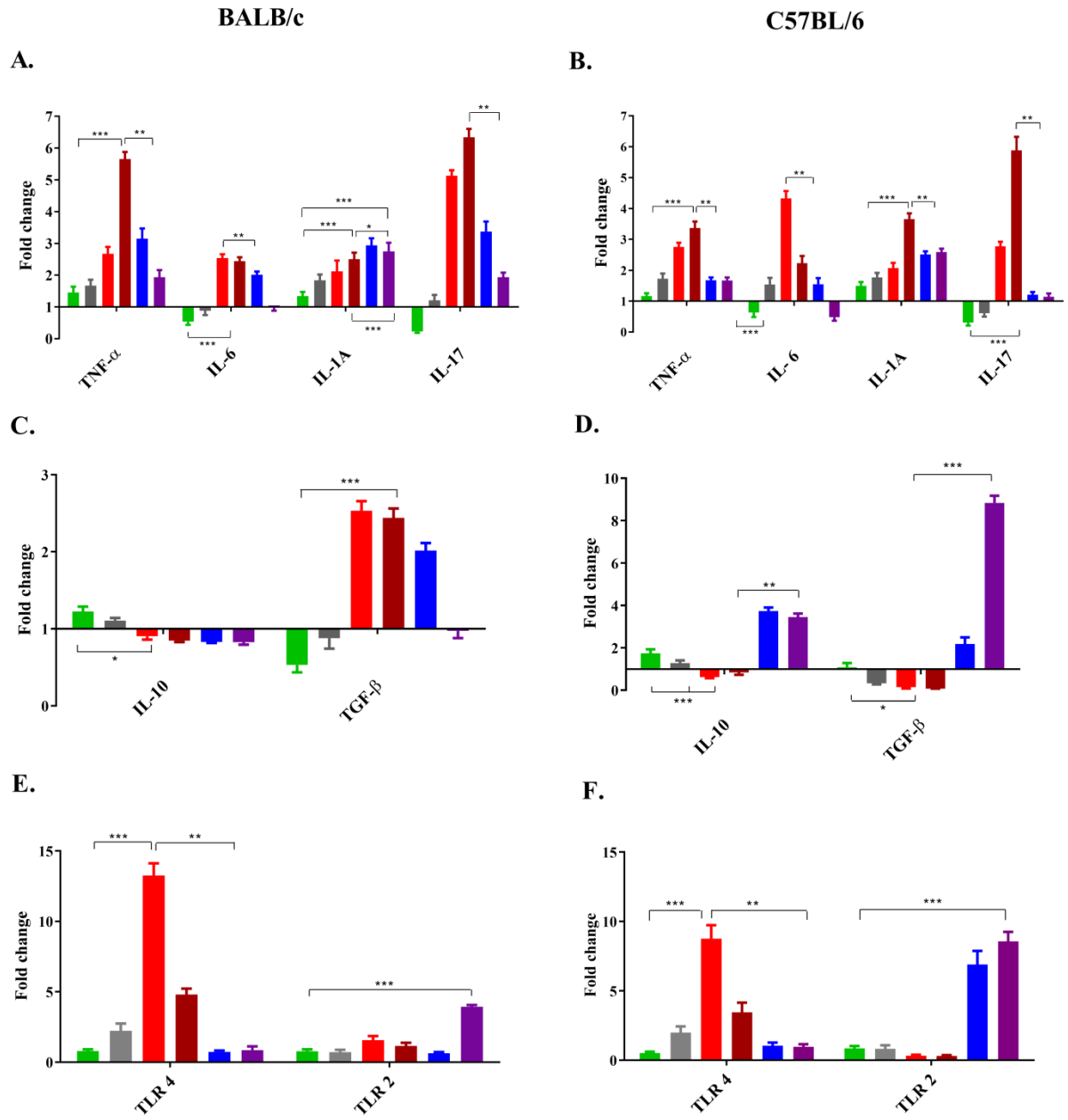
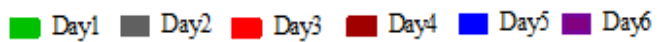


Figure 3.1.4: Transcriptional gene expression profile of different immune genes grouped like pro-inflammatory in [A. BALB/c and B. C57BL/6], anti-inflammatory in [C. BALB/c and D. C57BL/6] and Toll-like receptors TLR4 and TLR2 in [E. BALB/c, and F. C57BL/6 mice]. Two-

way ANOVA calculated statistical significance. ('***' corresponds to $P \leq 0.001$, '**' corresponds to $P \leq 0.01$, '*' corresponds to $P \leq 0.05$ level of significance). Error bars are one standard deviation of the mean value and determined from the average values of three biological replicates.

Validation of qRT-PCR results was done at the protein level expression by ELISA (Figures 3.1.5A and 3.1.5C). ELISA results revealed that on the third day following vancomycin treatment, the TNF- α level was significantly more in both BALB/c and C57BL/6 mice concerning the third day-matched untreated (control) groups of mice. Similarly, IL-10 cytokine level was more in BALB/c and C57BL/6 on day six following treatment with Vancomycin compared to the day sixth time-matched untreated mice (Figures 3.1.5A and 3.1.5C).

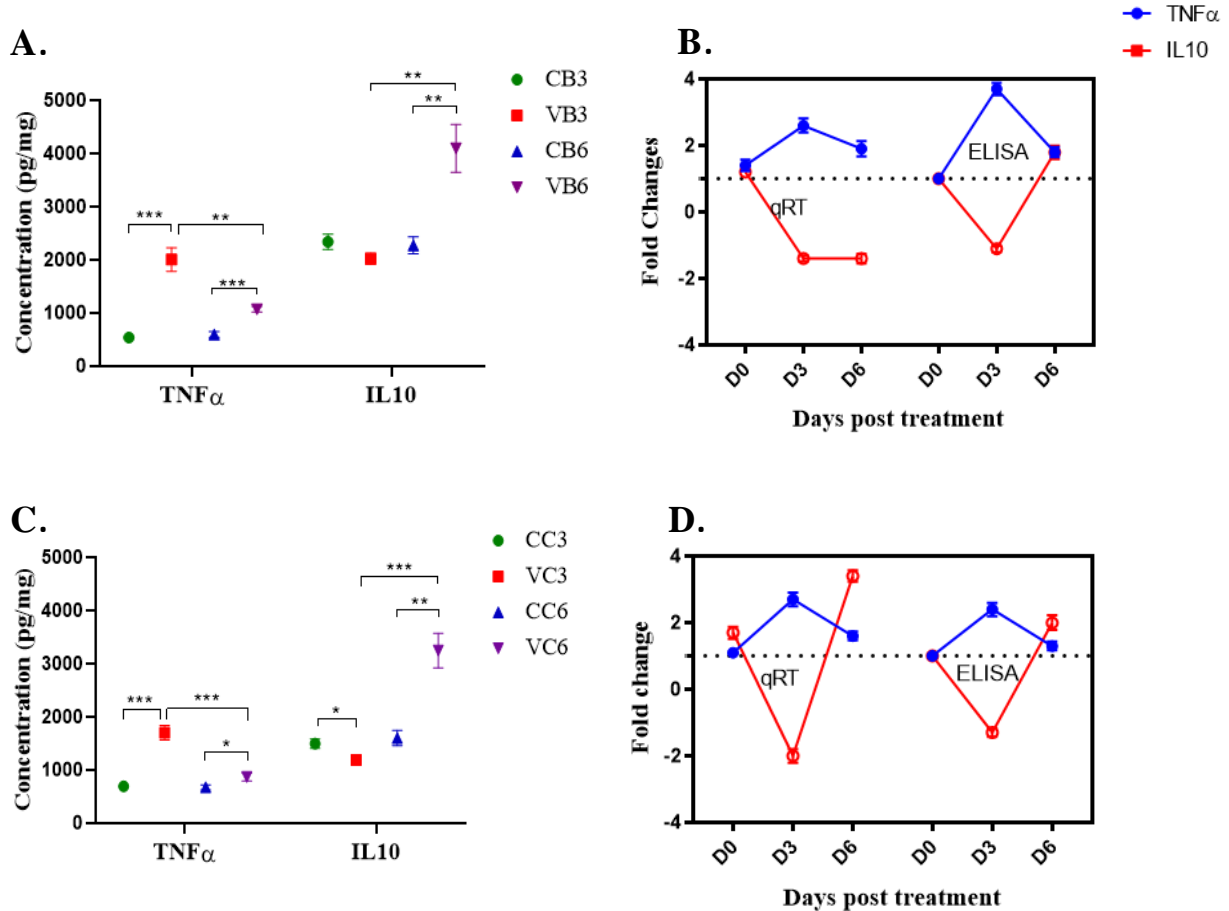


Figure 3.1.5: Protein level gene expression and comparative analysis of qRT PCR and ELISA data for TNF- α and IL-10. Mean values ($n=3$) of protein level concentration (in pg mg^{-1}) with a standard deviation of TNF- α (blue) and IL-10 (red) expression on days zero, three, and six for control and Vancomycin treated A. BALB/c, and C. C57BL/6 are shown. Statistical significance was calculated by two-way ANOVA ('****' corresponds to $P \leq 0.001$, '**' corresponds to $P \leq 0.01$, '*' corresponds to $P \leq 0.05$ level of significance). Fold change values of expression of TNF- α (blue) and IL-10 (red) to compare the values obtained from qRT-PCR, and ELISA studies

are shown for B. BALB/c and D. C57BL/6. Error bars of the data are already established in the preceding figures.

In summary, our data suggested that the pro-inflammatory response in colonic tissue was linked with increased Proteobacteria abundance during vancomycin-mediated microbial disruption. The emergence of Verrucomicrobia phyla from day five onwards may lead to a transition from pro-inflammatory to anti-inflammatory response irrespective of the initial immune bias of the mice. However, on the sixth day following vancomycin treatment, the decrease of the pro-inflammatory cytokine and an increase of anti-inflammatory cytokine expression were more significant in C57BL/6 BALB/c mice. This result can be correlated with the significant difference in the abundance of Verrucomicrobia phylum between BALB/c and C57BL/6 mice on the sixth day following vancomycin treatment.

Effect of vancomycin treatment on gut barrier integrity:

Vancomycin treatment caused a considerable disturbance in the gut barrier integrity and increased the permeability of the gut. FITC-dextran based gut permeability assay showed a higher level of gut permeability in vancomycin-treated mice than control mice. Serum FITC-dextran level was significantly higher in day three treated mice than the day zero control groups of mice. Important to note that the level decreased to normal (day zero control) on the sixth day of treatment in both mice strains (Figure 3.1.6C). These results prompted us to evaluate the gene expression of different colonic tight junction proteins (occludin and claudin 1) that maintain the gut's barrier function (Chelakkot, Ghim& Ryu, 2018). Results revealed that the expression of the claudin 1 gene decreased continuously from day one to day six following treatment with Vancomycin in BALB/c and C57BL/6 mice (Figures 3.1.6A and 3.1.6B). In the occludin gene,

for the BALB/C mice, its expression decreased from day zero to day six, while for C57BL/6 mice, it reduced from day zero to day four. In C57BL/6 mice, we observed a slight increase in occludin gene expression on days five and six compared to day three following vancomycin treatment.

Till day three following vancomycin treatment, both FITC dextran data and expression of tight junction genes showed almost similar results, i.e., decreased gut barrier integrity. While on day six following vancomycin treatment, FITC-dextran studies suggested restoration of the gut barrier for both BALB/c and C57BL/6 mice, but the expression of claudin 1 and occludin genes was still low. We need more profound studies to understand this difference on day six of vancomycin treatment.

In agreement with increased gut permeability, we intended to see whether it also induced the transfer of gut microbial products like endotoxin to the blood due to barrier disruption. Endotoxin concentration on day three following vancomycin treatment was higher than the untreated group of mice. However, it decreased on day six following vancomycin treatment (Figure 3.1.6D). On day six, BALB/c mice had slightly higher endotoxin levels in serum compared to C57BL/6 mice. From the above findings, it is clear that the disruption of gut barrier integrity is strongly associated with the Proteobacteria level. In contrast, restoration is associated with Verrucomicrobia abundance in both mice strains.

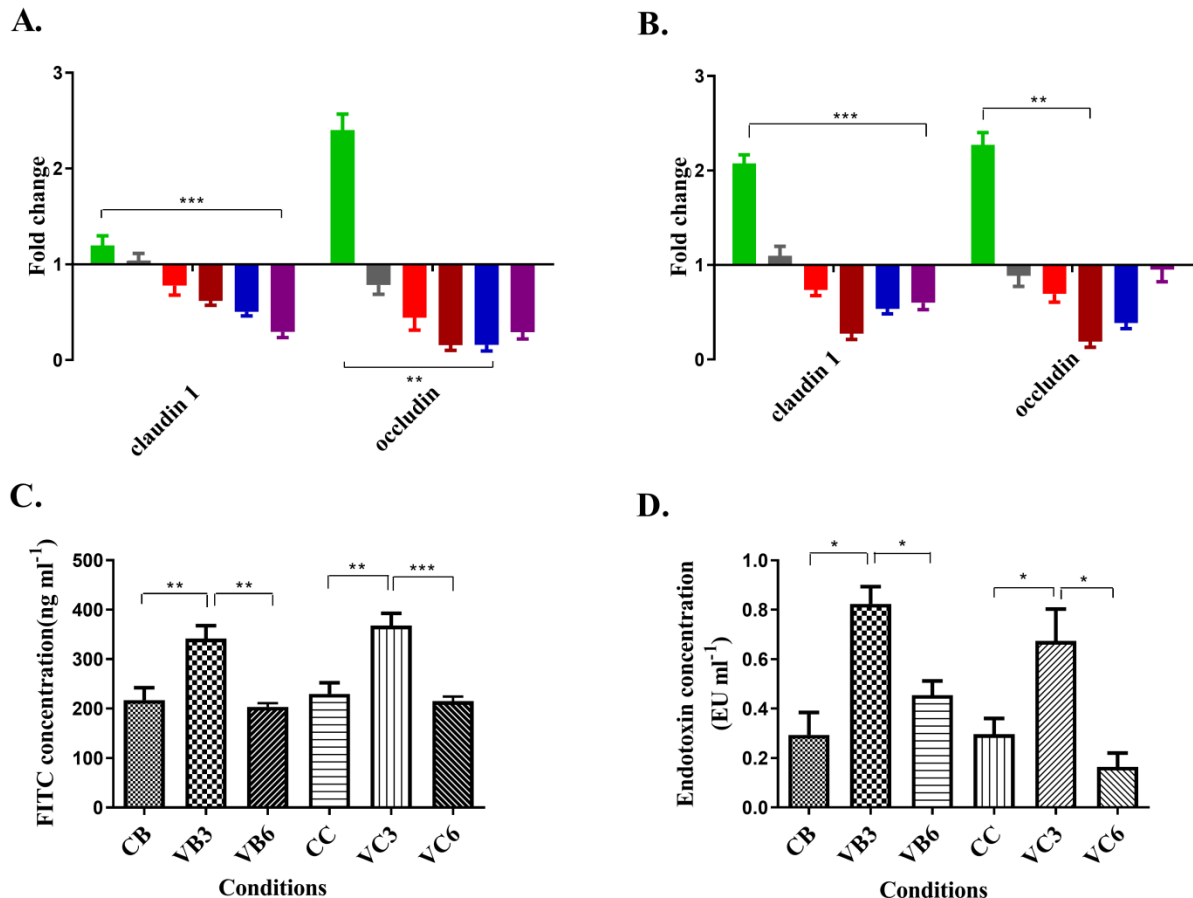
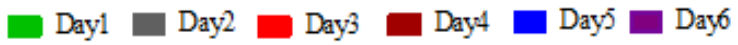


Figure 3.1.6: Measurement of intestinal integrity of BALB/c and C57BL/6 mice following treatment with Vancomycin. Transcriptional expression levels of tight junction genes, such as Claudin 1 and Occludin, in gut tissue by qRT-PCR, are shown in Vancomycin treated and untreated (control) groups A.BALB/c and B.C57BL/6 mice. C. Gut permeability data by measuring FITC dextran concentration in serum. D. Endotoxin concentration in the serum for both strains of mice are shown, where CB, VB3, and VB6 implies untreated (control), day three

and day six post vancomycin treated BALB/c and CC, VC3 and VC6 denote untreated (control), day three) and day six post vancomycin treated for C57BL/6 mice. Two-way ANOVA calculated comparisons among the groups. In the figure for panels' A.', 'B.', 'C.' and 'D.', '***' corresponds to $P \leq 0.001$, '**' corresponds to $P \leq 0.01$, '*' corresponds to $P \leq 0.05$ level of significance.

Differential level of Verrucomicrobia in the gut regulated blood glucose level following treatment with Vancomycin

Antibiotic-mediated gut microbiota perturbation can affect different host metabolic functions. One such measurement involves the regulation of blood glucose homeostasis (108,346,347). The current report revealed a high abundance of Verrucomicrobia phylum on the sixth day of vancomycin treatment. Since previous studies reported that *Akkermansia muciniphila* sp. from Verrucomicrobia phylum positively regulated glucose metabolism (172,348), we intended to check if Vancomycin induced time-dependent changes in microbiota profile regulated the glucose level in blood. We performed an "oral glucose tolerance test (OGTT)" from zero to 90 min in both strains of mice at different time points post vancomycin treatment. The glucose tolerance test revealed that glucose metabolism was different in the control and vancomycin-treated mice (Figures 3.1.7A and 3.1.7B). Important to note that the results from OGTT studies of the control animals for both BALB/c and C57BL/6 remain unchanged on days zero, three, and six (data not shown). On the day third following vancomycin treatment, fasting blood glucose (0^{th} min) levels in the Th2- and Th1-biased mice (BALB/c $194.6 \pm 6.3 \text{ mg dl}^{-1}$ and C57BL/6 $186 \pm 6 \text{ mg dl}^{-1}$) were significantly higher than their respective zero-day untreated (BALB/c $115 \pm 3 \text{ mg dl}^{-1}$ and C57BL/6 $126 \pm 4 \text{ mg dl}^{-1}$) mice. On day six

following vancomycin treatment, glucose levels dropped (BALB/c 148.6 ± 7 mg dl⁻¹ and C57BL/6 103 ± 5 mg dl⁻¹). The reduction of blood glucose level on day six following vancomycin treatment was more prominent in C57BL/6 than BALB/c mice (Figures 3.1.7A and 3.1.7B). The metabolism rate of glucose in the blood of the sixth-day Vancomycin treated mice was faster than the third-day treated mice. This rate was higher in Vancomycin-treated C57BL/6 mice compared to BALB/c mice. Next, we hypothesized that the differential level of Verrucomicrobia of C57BL/6 and BALB/c mice might affect the blood glucose level. To prove the causal role of Verrucomicrobia, we transplanted the cecal microbiota from sixth-day Vancomycin treated mice (higher Verrucomicrobia) to third-day Vancomycin treated mice. We observed a significant drop in blood glucose level in the third-day Vancomycin-treated C57BL/6 mice after CMT. However, the blood glucose level remained unchanged even after CMT in the third-day vancomycin-treated BALB/c mice (Figures 3.1.7A and 3.1.7B). Together, these data suggested that high Verrucomicrobia level, on the sixth day of Vancomycin treated C57BL/6 mice, helped to bring back the blood glucose level efficiently. In the case of BALB/c mice, the lower abundance of Verrucomicrobia phylum on the day sixth of vancomycin treatment was not sufficient to lower the blood glucose level

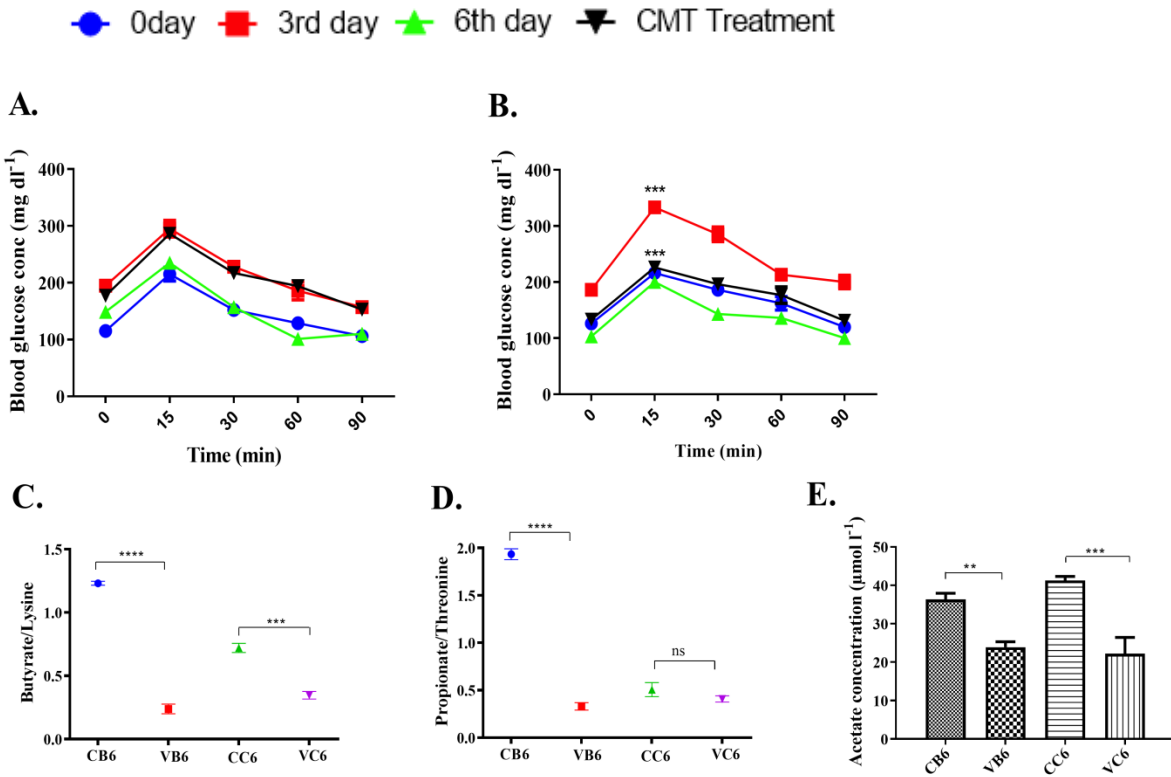


Figure3.1.7: Glucose and SCFA level in the serum of mice. Kinetics of fasting blood sugar in A. BALB/c B. C57BL/6 mice following treatment with Vancomycin on days zero, three, and six and following treatment with CMT from day six vancomycin treated mice transferred to Vancomycin treated day three group of mice. The ratio of abundance, from chemometric¹H-NMR studies for major short-chain fatty acids, of C. butyrate production over lysine and D. propionate production over threonine in untreated control BALB/c (CB) and C57BL/6 (CC) and Vancomycin treated BALB/c (VB), and C57BL/6 (VC) are compared for Day zero and Day six following treatment with Vancomycin. Also, E. acetate concentration in the serum by using acetate detection kit on day six in Vancomycin treated groups of mice (VB6, VC6) along with

the time-matched control mice (CB6, CC6) of BALB/c and C57BL/6, respectively. In the figure, '****' corresponds to $P \leq 0.0001$, '***' corresponds to $P \leq 0.001$, '**' corresponds to $P \leq 0.01$, level of significance).

Metabolites level in serum changed following vancomycin treatment

Antibiotic treatment can drastically reduce the Short-chain fatty acids (SCFAs) level, which are crucial regulators and indicators of several major physiologies of the host, such as supplying fuel to intestinal epithelial cells, maintaining gut barrier integrity, and enhance anti-inflammatory cytokine production (100,108). We measured the amount of SCFAs in the host serum using NMR-based metabolomics (Table. 3.1.3). It is known that gut microbes could produce metabolites like acetate, propionate, and butyrate that belong to SCFAs by metabolizing dietary fibers [100]. Butyrate supplies energy to colonocytes and helps in maintaining intestinal homeostasis via anti-inflammatory actions (349).

The current results revealed that the abundance of butyrate/lysine (Figure 7C) in serum was reduced significantly for both mice strains (VB6 and VC6). In contrast, the ratio of propionate to threonine in serum decreased significantly only in BALB/c (VB6) but not in C57BL/6 (VC6) on day six following treatment with Vancomycin (Figure 3.1.7D). The differential response of the ratio was measured concerning time-matched untreated control mice of the same strain. On day six, a significant decrease in the conversion of substrates into SCFAs was found, like butyrate from lysine in both strains of mice and propionate from threonine in only BALB/c mice following treatment with Vancomycin. Results also indicated the higher accumulation of the substrate like lysine in the blood of both BALB/c and C57BL/6 mice on day six following vancomycin treatment. However, the high-level accumulation of threonine was

only found in the vancomycin-treated BALB/c mice. We also measured the abundance of acetate in the serum of both BALB/c and C57BL/6 mice using an acetate detection kit (Figure 7E). Its concentration was considerably less on the sixth day of Vancomycin treated group of mice than the control group for both strains. It is commonly known that Firmicutes and acetate produce butyrate and propionate are produced by Bacteroidetes by metabolizing dietary fiber, whereas *A.muciniphila* bacteria of the Verrucomicrobia phylum also produce propionate (100). Hence, these results indicated that the serum SCFA level decreased due to a significant reduction of Firmicutes and Bacteroidetes phyla in the gut of vancomycin-treated mice. However, on day six of vancomycin treatment, in C57BL/6 mice, no significant decrease was observed in the production of propionate from threonine due to the higher abundance of *A.muciniphila* compared to BALB/c mice.

Table 3.1.3: The abundance of various SCFAs and associated metabolites in untreated (control) and Vancomycin treated BALB/c and C57BL/6.

Conditions	CB	VB6	P-value	CC	VC6	P-value
Acetate	157.5 (± 4.9)	54.3 (± 5.7)	< 0.0001	94.6 (± 3.5)	70 (± 0.6)	0.0003
Butyrate	223.2 (± 18.3)	65.9 (± 17.1)	0.0004	130.8 (± 6.3)	76.6 (± 12.2)	0.0024
Lysine	179 (± 8.5)	275.6 (± 9.1)	0.0002	199.6 (± 2.6)	219.8 (± 7.8)	0.0131

Propionate	223.2 (± 5.9)	119.8	0.0001	132.6	91.8	0.0058
		(± 10.6)		(± 3.7)	(± 12.6)	
Threonine	115.7 (± 7.6)	293.9 (± 7.1)	< 0.0001	248 (± 19.8)	278.4	0.0716
					(± 8.7)	

Results for day six of control BALB/C (CB6) and C57BL/6 (CC6) with Vancomycin treated BALB/C (VB6), and C57BL/6 (VC6) mice are shown. Means of different metabolite concentrations (μmoll^{-1}) and their respective standard deviations ($\pm\text{SD}$) were established. Statistical significance between each of the treated groups and their respective control groups was calculated by using the t-test, and p-values were shown.

.

Effect of vancomycin treatment on metabolic hormones

We estimated the concentration of some metabolic hormones such as insulin, PYY, and leptin in the serum of the mice as the gut microbiota of the host regulated these hormones. Results revealed that the insulin level decreased significantly on day six compared to day three following vancomycin treatment in C57BL/6 mice, but not in the BALB/c mice (Figure 3.1.8A). Hence, vancomycin treatment on day six showed a reduced amount of serum insulin concomitant with the blood glucose level in C57BL/6 mice. However, on day three following vancomycin

treatment, insulin levels were significantly higher than their respective day zero untreated group of mice for both strains. We did not find any significant changes in serum leptin concentration during vancomycin treatment in both BALB/c and C57BL/6 mice concerning their respective untreated controls (Figure 3.1.8B). Further results revealed that the concentration of PYY hormone in the gut decreased in both BALB/c and C57BL/6 mice from day zero to day six following vancomycin treatment (Figure 3.1.8C). The current report reveals that Vancomycin-mediated gut microbiota perturbation may regulate blood glucose and insulin level differently for C57BL/6 and BALB/c mice in a time-dependent manner.

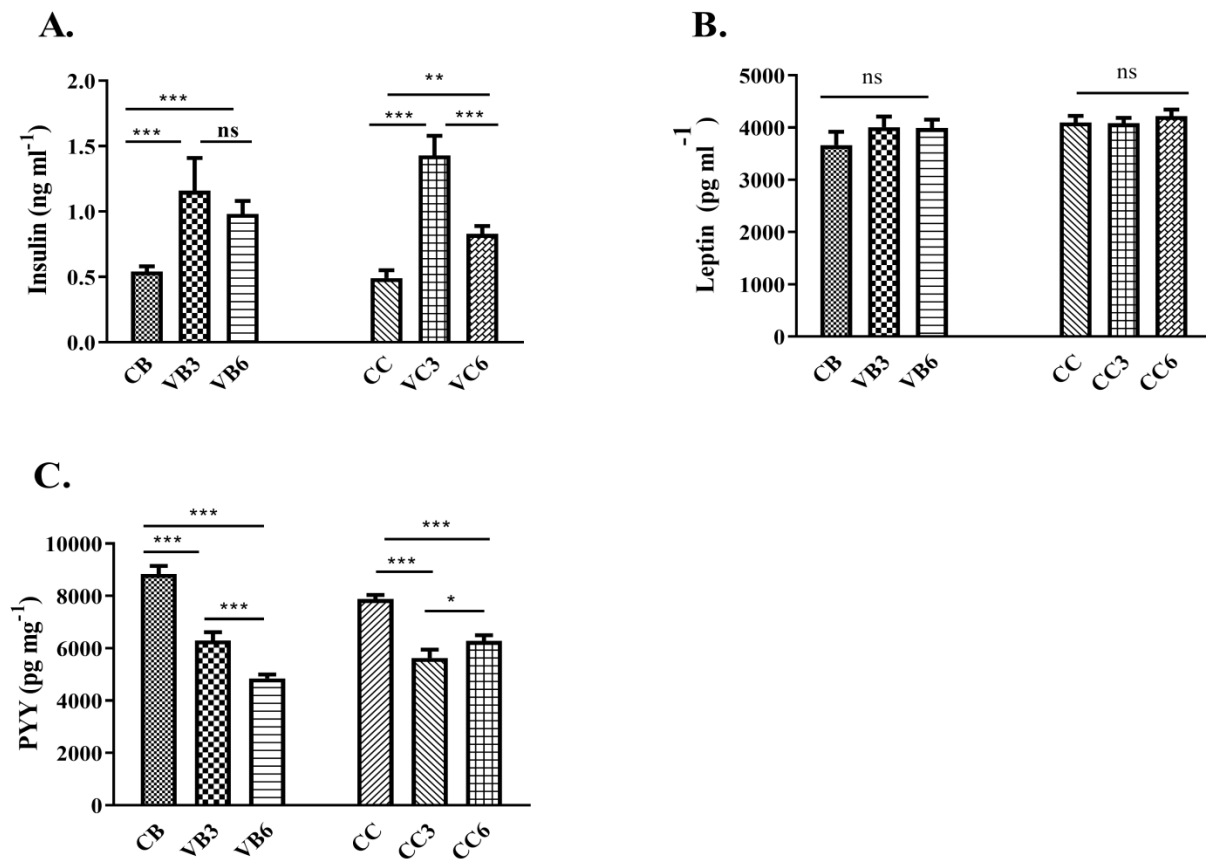


Figure 3.1.8: Alteration in the concentration of select hormones during vancomycin treatment.

The concentration of A. Insulin (ng ml^{-1}), B. Leptin (pg ml^{-1}), and C. PYY (pg mg^{-1}) in the serum

of control BALB/c (CB) or C57BL/6 (CC) and Vancomycin treated mice on the third day (VB3, VC3) and sixth day (VB6, VC6) of BALB/c and C57BL/6 mice respectively. Comparisons among the groups were calculated with two-way ANOVA. In the figure, '***' corresponds to $P \leq 0.001$, '**' corresponds to $P \leq 0.01$, '*' corresponds to $P \leq 0.05$ level of significance). Error bars shown are one standard deviation from the mean value of four replicates ($n=4$).

Table 3.1.4: Sequences of forward (_F) and reverse (_R) primers for PCR studies to confirm the presence and expression level of various genes used in this study.

Genes specific for	Sequences of the primers used
<i>A. muciniphila</i> _F	5'-CAGCACGTGAAGGTGGGGAC-3'
<i>A. muciniphila</i> _R	5'- CCTTGCGGTTGGCTTCAGAT-3'
IL-10_F	5'-AGGCAGTGGAGCAGGTGAAGAGTG-3'
IL-10_R	5'-GCTCTCAAGTGTGGCCAGCCTTAG-3'
TNF- α _F	5'-CCACGTCGTAGCAAACCACCAAAG-3'
TNF- α _R	5'- TGCCCCGGACTCCGCAAAGTCTAAG-3'
CLDN 1_F	5'-TGCCCCAGTGGAAAGATTACT-3'
CLDN 1_R	5'-CTTGCAGAACCGCAGGACAT-3'

TLR 4_F	5'- CGCTGCCACCAGTTACAGAT-3'
TLR 4_R	5'-AGGAACTACCTCTATGCAGGGAT-3'
OCLN_F	5'- GTTGAACGTGGATTGGCAG -3'
OCLN_R	5'- AAGATAAGCGAACCTTGGCG -3'
IL-6_F	5'-AGACAAAGCCAGAGTCCTTCAGAG-3'
IL-6_R	5'-CCACAGTGAGGAATGTCCACAAAC-3'
TLR 2_F	5'-GCCCGTAGATGAAGTCAGCTCACCC-3'
TLR 2_R	5'-CGGGCATCTACTTCAGTCGAGTGG-3'
IL-17_F	5'-TCCAGAAGGCCCTCAGACTA-3'
IL-17_R	5'-ACACCCACCAGCATCTTCTCA-3'
TGF-β_F	5'-CCCAGCATCTGCAAAGCT-3'
TGF-β_R	5'-GTCAATGTACAGCTGCCGCA-3'
IL-1A_F	5'-ATCAGTACCTCACGGCTGCT-3'
IL-1A_R	5'-TGGGTATCTCAGGCATCTCC-3'

3.1.3 Discussion

Metagenomic data of the cecal sample showed that Vancomycin altered the gut microbiota most extensively by decreasing the phylum like Firmicutes and Bacteroidetes and increasing

pathogenic Proteobacteria level. Both the NGS and plating data (NB, EMB, and salmonella-shigella specific agar plate) showed similar types of results —increase in the Proteobacteria phylum at the initial days of vancomycin treatment while the increase in the Verrucomicrobia phylum in the last two days of the treatment. On day three of the vancomycin treatment, the plating of the cecal sample on the EMB agar and salmonella-shigella plate showed overgrown colonies were mostly E.coli and Shigella. This data was correlated with the metagenomic data of the cecal sample at the genus level. The Verrucomicrobia phylum that increased on the last two days of the vancomycin treatment mainly contains the Akkermansia genus, an obligately anaerobic and nonculturable microbe (350). So, the fifth and sixth days of vancomycin treatment showed decreased colony count on the plate.

During vancomycin treatment, the Proteobacteria phylum started increasing drastically up to the fourth day, and it replaced all other phyla like Firmicutes, Bacteroidetes, Actinobacteria, Tenericutes, Verrucomicrobiaetc. This increase in only one phylum (Proteobacteria) caused a decrease in diversity and equitability of other gut microbiota; therefore, equitability was least on the fourth day of C57BL/6 and fifth day of BALB/c mice. On the above days of treatment (up to the fourth day of vancomycin treatment), except Proteobacteria, other phylum levels were significantly less, and the proportion of Proteobacteria was above 90% among the other major groups of gut microbes. But after the fifth day of treatment, different types of microbes like Firmicutes, Tenericutes, Verrucomicrobia groups started increasing in the gut, which caused an increase in the diversity and equitability in BALB/C mice. The highest equitability was found on the sixth day of treatment.

In the Proteobacteria phylum, Escherichia and Shigella genera increased during vancomycin treatment. These genera belong to gram-negative bacteria containing LPS, which increased the

endotoxin level in the blood. These bacteria activated the TLR4 receptor present in the gut epithelial cell, which increased the expression of pro-inflammatory cytokines. A combinational effect of the increase in Proteobacteria and a decrease in Firmicutes caused the gut's elevation. Firmicutes, specifically the Clostridium group present in the gut, produced various short-chain fatty acids from complex carbohydrate foods (170). Instentimonas bacteria (Firmicutes phylum) produced butyrate from lysine [101], and Bacteroidetes produced propionate from threonine in the gut (101,102). The production of these SCFA in the gut suppressed the LPS and pro-inflammatory cytokines like TNF- α , IL-6 level, and enhanced the release of the anti-inflammatory cytokine-like IL10 (103,104). In the current study, vancomycin treatment caused a decrease in Firmicutes and Bacteroidetes in the gut, which resulted in less SCFA production and increases inflammation.

Overexpression of Inflammatory cytokine-like TNF α was associated with higher gut permeability by suppressing the expression of tight junction proteins like occludin and claudin 1 (126,127). In this study, lower expression of tight junction protein in vancomycin-treated mice caused an increase in gut permeability. Increased level of Verrucomicrobia phylum in the gut showed many health-related benefits in the host (171,172). During obesity and diabetic conditions, metabolic endotoxemia was observed where endotoxin (LPS) levels increased in the blood, which caused inflammation and impaired glucose metabolism in the host (169,170). In the current study, on day six of the vancomycin treatment, the increased level of Verrucomicrobia caused a significant decrease in the inflammation of the mice with enhanced glucose metabolism. The increase in Proteobacteria phylum during vancomycin treatment elevated the endotoxin level of blood. The elevated endotoxin resulted in impaired glucose metabolism and insulin resistance (highest level of both insulin and glucose in third-day

Vancomycin treated mice) in mice up to the fourth day of vancomycin treatment. On the sixth day of vancomycin treatment, in C57BL/6, the replacement of Proteobacteria by Verrucomicrobia caused significant improvement in glucose metabolism in mice; fasting glucose and insulin level in blood came to normal. This effect was more prevalent in C57BL/6 mice than BALB/c. After successful transfer of the cecal sample from the sixth day of Vancomycin treated C57BL/6 mice (*A. muciniphila* level is above 70%) to the third day of Vancomycin treated mice, blood glucose level decreased significantly on the third-day mice, which showed the influential role of *Akkermansiamuciniphila* in controlling the blood glucose level. On the sixth day of vancomycin treatment, *A.muciniphila* level was significantly higher in C57BL/6 mice than BALB/c, which might cause a more prominent effect in decreasing glucose and insulin level in C57BL/6 mice.

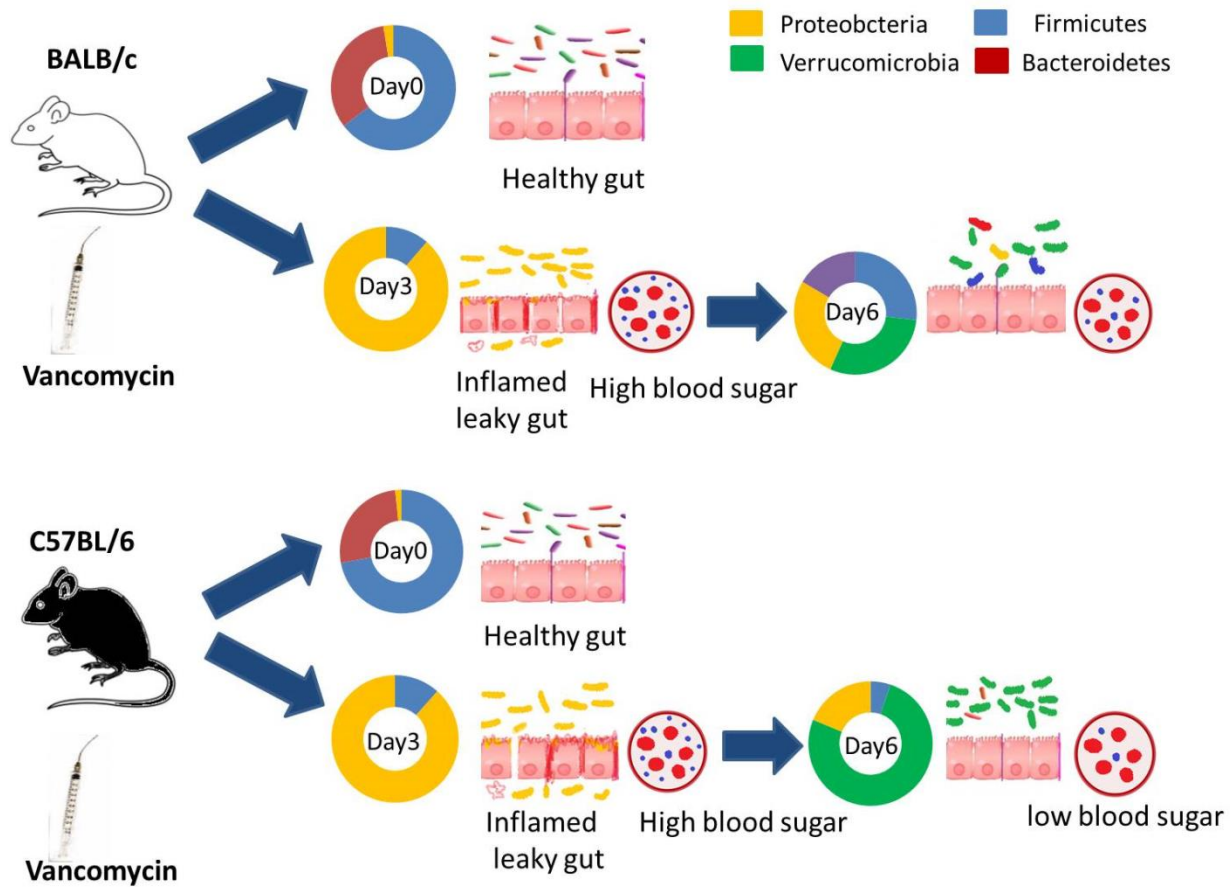
SCFA stimulated PYY hormone production by activating Gq coupled receptor FFA2 of endocrine cells present in the gut (168). After vancomycin treatment, the SCFA level decreased, which caused a reduction in PYY production.

The clinical dose of vancomycin treatment perturbed the gut microbiota of mice in a very distinct way - by depleting the healthy microbes and increasing the infectious microbes in the initial days of treatment, which disrupted the equilibrium of various physiological processes (immunological and metabolic) of the body. However, at the later stages of treatment, the body tried to restore the balance in various physiological processes by increasing certain types of healthy microbes like Verrucomicrobia. Generally, the Verrucomicrobia phylum that appeared in massive number at the later stages of vancomycin treatment was present at a significantly less number in the control group, but their functional role was similar to a significant group of healthy microbes of the gut; they helped to restore the equilibrium by alleviating the adverse effect of Proteobacteria.

We found that initial doses of Vancomycin caused depletion in Firmicutes and Bacteroides phylum with a drastic increase in Proteobacteria phylum in the gut, which caused an increase in gut inflammation, gut permeability, and cecal index with a decrease in glucose metabolism, and perturbed SCFA metabolism of the host. However, at later stages of vancomycin treatment, one phylum of healthy microbes started increasing at a significant level, i.e., Verrucomicrobia (Akkermansia genus), the restoration of the gut environment by decreasing inflammation and increasing glucose metabolism.

The graphical abstract of the current chapter is shown in Figure 3.1.9.

Figure3.1.9: Graphical representation of vancomycin-induced perturbation of gut microbiota and its effect on BALB/c and C57BL/6 mice (Chapter 3.1).



Chapter 3.2: Restoration kinetics of gut microbiota following the cessation of vancomycin treatment and its consequence on the physiology of Th1- and Th2- biased mice.

3.2.1 Introduction:

We established that vancomycin treatment altered the gut microbiota composition significantly in a time-dependent manner in the preceding chapter. Therefore, it was necessary to understand the restoration kinetics of gut microbiota following the cessation of vancomycin therapy. As our previous results revealed, perturbation patterns of gut microbiota varied between two strains of mice (BALB/c and C57BL/6). In the current chapter, we compared the restoration kinetics of gut microbiota between two strains of mice. This chapter mainly focuses on the effects of host genetics on the restoration pattern of gut microbiota. The alliance between the gut microbiota composition and behavioral changes in mice was also studied thoroughly during the perturbation and restoration period.

Sometimes, overuse and abuse of antibiotics caused many permanent alterations in the gut microbiota composition (334–336), while some earlier studies also showed that, after the termination of antibiotic therapy, the gut microbiota recovers significantly (231,232). The correlation between particular gut microbiota perturbation with a specific dose and duration of antibiotic exposure is still poorly characterized. Moreover, following the termination of antibiotic treatment, the restoration kinetics of these microbes and their effect on the host still need to be understood. This study mainly focused on the perturbation and restoration kinetics of gut microbes after antibiotic treatment and its impact on the host behavior and immune system. After six days of vancomycin treatment, mice were left for restoration studies for the next 60

days. In this restoration period, the alteration profile of gut microbiota and various host physiologies were studied.

Various reports showed that altered gut microbiota or the introduction of a pathogen to the gut causes various behavioral changes like anxiety and depression in mice (174,185,351). Germ-free mice (GF mice) without any gut microbiota from birth and specific pathogen-free mice (SPF mice) having commensal gut microbes show different behavior in stress, which shows the significant role of gut microbiota in regulating the behavior of the host. So, here we studied the changes in behavior (both anxiety and depression) of both BALB/c and C57BL/6 SPF mice by perturbing their gut microbes through antibiotics. "Elevated plus maze (EPM), Open field (OF), and Force swimming test (FST)" are some widely used techniques to study behavioral changes like anxiety and depression in mice (182,352–354). Brain-derived neurotrophic growth factor (BDNF) level changes with the stress created by the variation of gut microbiota of mice (190). BDNF exerts an antidepressant effect in the hippocampus (355) of the host. Therefore, in this study, we analyzed the BDNF level in the brain after perturbation and restoration of gut microbiota.

Furthermore, it was also reported that a higher level of corticotropin-releasing hormone (CRH) in the hypothalamus was related to the chronic depressive state of the host (191). CRH binding protein (CRHBP) has an anxiolytic effect as it binds and inhibits CRH activity in the brain (192). In this study, CRH and CRH binding protein (CRHBP) levels were tested at mRNA level in the brain during antibiotic perturbation and restoration.

Antibiotic perturbation of gut microbiota disrupts the host-microbes interactions that alter the host's immune response, like the stimulation of TLR and cytokine production (356).

This chapter measured some necessary pro-and anti-inflammatory cytokine levels in the gut after perturbation and restoration of gut microbiota.

Gut microbiota has a significant role in maintaining a protective intestinal barrier against the entry of pathogenic bacteria by maintaining the expression of tight junction proteins (357). Different tight junction proteins support the integrity of the blood-brain barrier (BBB) of the host; however, the expression of these tight junction proteins can be modulated by various SCFA and metabolites produced by gut microbes (180). In the current chapter, we checked the expression of occludin and claudin genes in mice's gut and brain tissue after perturbation and restoration of gut microbiota.

3.2.2 Results:

Constitution of gut microbiota during vancomycin treatment and restoration period in BALB/c and C57BL/6 mice.

Earlier reports showed that the treatment with vancomycin could cause significant alteration of the gut microbiome (250,346). In the current study, we mainly focus on comparing alteration patterns of gut microbiota profile during perturbation and restoration period following vancomycin treatment in BALB/c and C57BL/6 mice. Cecal metagenomic data revealed a considerable a) decrease in the abundance of significant phyla like Firmicutes and Bacteroidetes and b) increase in the abundance of Proteobacteria up to the 4th day of vancomycin treatment in both BALB/c and C57BL/6 mice (Table 3.2.1). On the 4th day, following treatment with vancomycin, the abundance of Proteobacteria phylum was the highest (above 80% in both BALB/c and C57BL/6 mice). At a later stage of vancomycin treatment (after the 4th day), the abundance of Verrucomicrobia phylum increased significantly in C57BL/6 mice compared to

BALB/c mice (Table 3.2.1 and Fig. 3.2.1). On the 6th day following vancomycin treatment, Verrucomicrobia abundance was nearly 30% in BALB/c mice and 71% in C57BL/6 mice (Fig. 3.2.1).

We stopped vancomycin treatment after the 6th day and left the mice to recover (termed as restoration phase). We selected some critical time points to study the recovery pattern of gut microbiota, such as the 15th, 30th, and 60th day following the termination of vancomycin treatment. The cecal 16s rRNA sequencing data revealed a notable elevation in Firmicutes and Bacteroidetes phyla while a considerable decrease in Proteobacteria and Verrucomicrobia phyla in both BALB/c and C57BL/6 mice (Table 3.2.1 and Fig. 3.2.1). BALB/c mice had a greater capacity for the restoration of the gut microbiota compared to C57BL/6 mice. Between both strains of mice, the restoration of the gut microbial constitution in BALB/c mice happened more rapidly. It became similar to its respective untreated group of mice at a more incredible speed compared to C57BL/6 mice after the cessation of vancomycin treatment (Fig. 3.2.1). Some specific time points were selected to display the major transformation of the gut microbial constitution during the perturbation and restoration period (Fig. 3.2.1). On the 15th day of restoration, C57BL/6 mice had comparatively high abundance (20%) of Proteobacteria, and low (12%) abundance of Bacteroidetes phylum (Fig. 3.2.1I) were observed compared to its respective time-matched control group of mice (Fig. 3.2.1F). While BALB/c mice had 10% Proteobacteria and no significant difference in Bacteroidetes phyla (Fig. 3.2.1D) was found compared to its untreated control mice (Fig. 3.2.1A).

On the 60th day of restoration, in BALB/c mice, maximum gut microbiota from all the major phyla was restored and looked almost similar to the microbiota of untreated control mice (Fig. 3.2.1). However, there was an incomplete restoration of some major phyla that happened in the

case of C57BL/6 mice like the abundance of Bacteroidetes phylum was found to be comparatively lower and Proteobacteria phylum higher than their respective control group of mice. The restoration was more effective in BALB/c mice (Figs. 3.2.1A and 3.2.1E) than C57BL/6 mice (Figs. 3.2.1F and 3.2.1J).

The gut microbial diversity reduced significantly following vancomycin treatment in both BALB/c and C57BL/6 mice. Shannon diversity index (H) at the phylum level was found to be the lowest on the 4th day following vancomycin treatment in both BALB/c and C57BL/6 mice. During the restoration period, the H value increased to be like the untreated mice (Fig. 3.2.1).

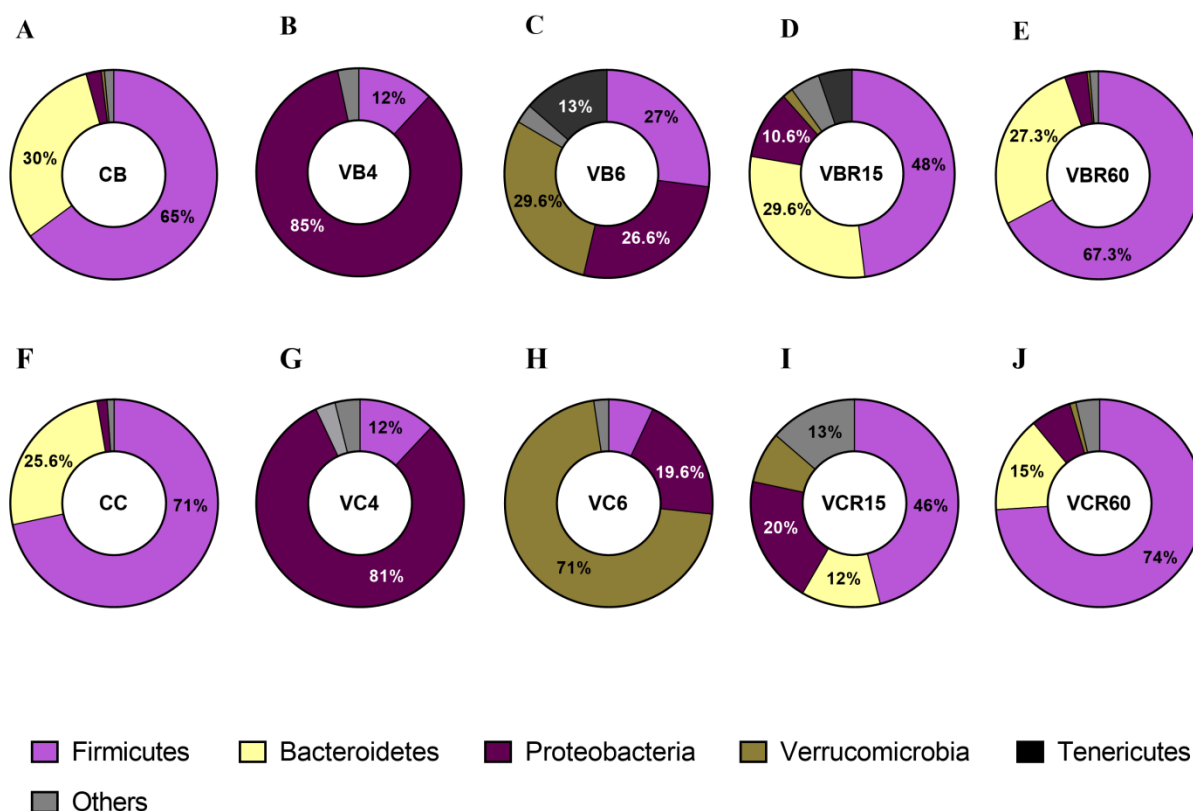


Figure 3.2.1: Composition of gut microbiota at phylum level during perturbation and restoration period. Donut chart showing the relative changes in significant gut phyla microbiota at essential time points of the experiment: 0th day (untreated mice), 4th and 6th day of perturbation by vancomycin, 15th and 60th day of restoration in both BALB/c and C57BL/6 mice.

The gut microbial composition of BALB/c mice was shown in the top row on day A. 0th (untreated control) (CB), B. 4th (VB4), C. 6th (VB6) day following treatment with vancomycin, or D. 15th (VBR15), and E. 60th (VBR60) day following the withdrawal of vancomycin treatment. The bottom row showed the composition of gut microbiota of C57BL/6 mice on day F. 0th (CC), G. 4th (VC4), and H. 6th (VC6) day following treatment with vancomycin, or I. 15th (VCR15), and J. 60th (VCR60) day following the withdrawal of vancomycin treatment. Each phylum was denoted with a unique color code and represented at the lower part of the figure.

Table 3.2.1: Percent abundance of major phyla of gut microbiota during vancomycin perturbation and restoration.

Phylum	Perturbation Days	Restoration Days
Mice	0 2 3 4 5 6	15 30 60

BALB/c	F	65± (3)	35±	23±	11±	5.1± (2)	26.9±	48.9±	62± (3)	67.5±
			(4)	(5)	(2)		(2)	(5)		(4)
B	30± (3)	Nil	Nil	Nil	Nil	Nil		29.4±	28± (4)	27.5±
								(5)		(4)
P	2.4±	65±	76±	85±	91.3±	26.6±		9.6± (3)	3.1± (1)	3.6±
	(1.2)	(5)	(5)	(3)	(2)	(5)				(2.2)
V	0.5±	Nil	Nil	Nil	Nil	29.4 ±	Nil	Nil	Nil	
	(0.3)					(3)				
C57BL/6	F	71± (4)	62±	41±	11±	8.3± (4)	5.6± (2)	46.2±	74± (4)	73.5±
		(4)	(5)	(2)				(6)		(6)
B	27.4±	Nil	Nil	Nil	Nil	Nil		12.3±	14± (2)	15± (4)
	(3)							(2)		
P	1.6± (1)	37±	60±	82±	18.5±	19± (3)		21.8±	8± (3)	6.1± (2)
	(3)	(4)	(5)	(2)				(4)		
V	Nil	Nil	Nil	3±	72.3±	72.4±		Nil	Nil	5.3±
				(0.1)	(6)	(3)				(0.4)

Time-dependent percent changes in the abundance of major gut microbial phyla: Firmicutes phylum (F), Bacteroidetes (B), Proteobacteria (P), and Verrucomicrobia phylum (V) in BALB/c

and C57BL/6 mice. We presented the means of percent abundance of gut microbiota with their respective standard deviations (\pm SD).

We have also checked the genus level alteration pattern of gut microbiota during the perturbation and restoration period following vancomycin treatment (Table. 3.2.2). Results revealed that the control untreated group of mice mainly contained Blautia, Intestinimonas genera of Firmicutes phylum and Alistipes, Bacteroides genera of Bacteroidetesphylum. Whereas up to day four of vancomycin treatment caused an increase in Escherichia – Shigella pathogenic Proteobacteria and later continued vancomycin doses on day five and six caused an increase in *Akkermansia muciniphilla* genus of Verrucomicrobia phylum (Table. 3.2.2).

Table 3.2.2: Percent abundance of major phyla of gut microbiota during vancomycin perturbation and restoration.

Mice	Genus	Perturbation Days			Restoration Days				
		0	2	3	4	5	6	15	30
BALB/ c	Blautia	45± (5)	Nil	Nil	Nil	16± (2)	43± (4)	41± (5)	47± (4)

Intestinim onas	15± (3.5)	Nil	Nil	Nil	Nil	9± (1.7)	4.5± (0.4)	3± (1.2)	3.3± (1)
Alistipes	9± (2.3)	Nil	Nil	Nil	Nil	Nil	14± (2)	26± (4)	21± (2)
Bacteroides	21± (3)	Nil	Nil	Nil	Nil	Nil	16± (3)	16	18.2
Akkermansi a	Nil	Nil	Nil	Nil	Nil	25.4	Nil	Nil	Nil
Escherichia -Shigella	Nil (6)	61± (1)	12± (7)	60± (6)	52± (3)	24± (2)	8.9± (0.05)	1.9± (0.04)	0.5± (0.04)
Lactobacill us	0.7± (0.1)	34± (3)	14± (2)	8± (2) (0.5)	3± (0.5)	Nil	1± (0.2)	Nil	Nil
Desulfovibri o	Nil (0.6)	2± (5)	43± (3)	30± (4)	25± (4)	21	1± (0.05)	2± (1) (0.2)	0.8± (0.2)

.

C57BL	Blautia	20± /6	Nil	Nil	Nil	Nil	Nil	17± (4)	35± (5)	32± (4)
	Intenstinim onas	37± (5) 5± (2)	Nil	Nil	Nil	Nil	Nil	35± (6)	30± (7)	34± (6)
	Alistipes	Nil	Nil	Nil	Nil	Nil	Nil	4± (0.8)	5± (0.4)	5
	Bacteroides	23± (4.2)	Nil	Nil	Nil	Nil	Nil	9± (1.7)	10± (3)	12± (4)
	Akkermansi a	0.9± (0.1)	Nil	Nil	4± (1)	28± (6)	88± (7)	12.6	Nil	1± (0.3)
	Escherichia -Shigella	Nil (4)	32± (4)	34± (4)	36± (3)	19± (4)	1± (0.2)	12± (2)	8± (1.3)	3± (1.1)
	Lactobacill us	0.8± (0.1)	57± (5)	44± (6)	11± (2)	20± (3)	Nil	Nil	Nil	Nil
	Desulfovibri o	1± (0.2)	1± (0.3)	7± (1.6)	32± (5)	24± (3)	1± (0.4)	9± (2) (1.8)	8± (2.1)	8±

Time-dependent alteration of gut microbial abundance at the genus level, in the BALB/c mice and C57BL/6 mice. Means of percent abundance of gut microbiota with their respective standard deviations (\pm SD) were represented.

Gut microbiota alteration caused a higher level of anxiety behavior in mice.

Gut microbiota has significant effects on the behavior of mice (358). Alteration in the composition of gut microbes can lead to the modulation in the behavior of mice. At the time of vancomycin treatment, both strains of mice spent a long time in the closed compared to the open arms of the EPM instrument (Figs. 3.2.2A and 3.2.2B) compared to its respective untreated group of mice. The behavior in EPM showed a higher level of anxiety in mice, and it increased continuously from the 0th day to the 6th day following treatment with vancomycin in BALB/C mice. In C57BL/6 mice, anxiety level increased from 0th day to 4th day following vancomycin treatment, but after the 4th day, the anxiety level decreased. On the 6th day, following vancomycin treatment, C57BL/6 mice spent less time in the closed arm than its 4th day. In both strains of mice, the stress behavior of mice reduced significantly during the restoration phase; mice stayed comparatively short span in the closed arms of the EPM instrument during the restoration phase compared to the perturbation period. BALB/c and C57BL/6 mice, on the 15th day of restoration, BALB/c mice displayed a lesser extent of anxiety-like behavior compared to the C57BL/6 mice. However, on the 60th day of restoration, stress levels decreased significantly in both strains of vancomycin-treated mice, and their behavior was found to be almost indistinguishable from their respective control group of mice (Figs. 3.2.2A, and 3.2.2B).

In the open field (OF) test, vancomycin-treated mice displayed a comparatively higher level of anxiety behavior than control mice. The results from the OF test showed that during vancomycin

treatment, mice spent less time in the center than control mice (Figs. 3.2.2C and 3.2.2D). Up to the 4th day following vancomycin treatment, both BALB/c and C57BL/6 mice showed an increase in anxiety-like behavior (less time spent in the center). However, from the 4th day to the 6th following vancomycin treatment, C57BL/6 mice showed significantly less anxiety-like behavior (more time spent in the center) compared to BALB/c mice.

However, both strains of mice stayed longer duration in the center of the OF instrument during the restoration period compared to their perturbation period that showed comparatively lower stress level of mice during the restoration period. While for BALB/c mice, there was no significant difference in the center time, C57BL/6 mice showed a substantial difference between 15th-day restoration and time-matched control. On the 60th day of restoration, both vancomycin-treated BALB/c and C57BL/6 mice behave nearly like their respective control group of mice (Figs. 3.2.2C and 3.2.2D).

During the Forced swimming test (FST), mice spent more time in an immobile state during vancomycin treatment than the untreated group of mice. The control group of mice were more dynamic and tried to escape from the water, while the vancomycin-treated group of mice showed the opposite behavior. This behavior showed an elevated level of depression in vancomycin-treated mice (Figs. 3.2.2E and 3.2.2F). This depressive behavior was highest on the 4th day following vancomycin treatment in both BALB/c and C57BL/6 strains. However, on the 6th day of vancomycin treatment, C57BL/6 mice displayed a considerably lower level of depressive behavior than BALB/c mice. During the restoration period, on the 15th day, both strains of mice showed a significantly lower level of depressive behavior than the perturbation period, which can be comparable with the control group of mice.

Overall, the vancomycin-induced gut microbial perturbation in mice caused induction of the stress-related behavior in the open field, elevated plus maze, and forced swim tests. However, with the recovery of gut microbiota during the restoration period, the stress behavior of mice was also alleviated.

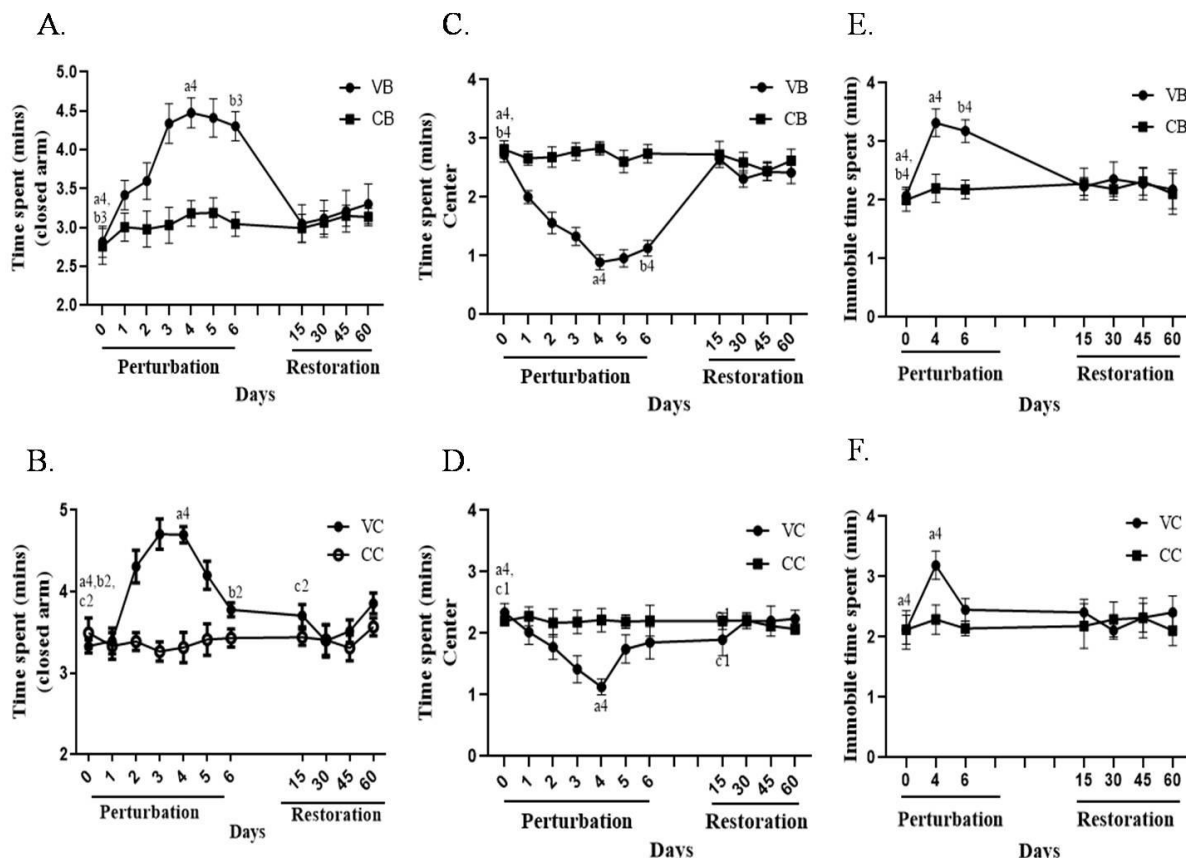


Figure 3.2.2: Behavioral studies following treatment with vancomycin. Detection of anxiety level in BALB/c and C57BL/6 mice through Elevated Plus Maze (EPM) test, open-field (OFT), and forced swimming test (FST). Elevated plus-maze data are showing time spent in the closed arms (in minutes) for vancomycin treated A. BALB/c (VB) and untreated control mice (CB), or B. C57BL/6 (VC) and untreated control mice (CC) during various time points of gut microbiota

perturbation (following treatment with vancomycin) and restoration (withdrawal of vancomycin treatment).

Open Field Test data are showing time spent in the center (in minutes) for vancomycin-treated C. BALB/c (VB) and untreated control mice (CB), or D. C57BL/6 (VC) and untreated control mice (CC) during various time points of gut microbiota perturbation and restoration.

Forced swimming test data are showing Immobility time spent (in minutes) for vancomycin-treated E. BALB/c (VB) and untreated control mice (CB), or F. C57BL/6 (VC) and untreated control mice (CC) during various time points of gut microbiota perturbation and restoration.

(Statistical significance changes were calculated by comparing values of the treated groups at various time points with their respective untreated groups through two-way ANOVA and t-test. 'a' showed Comparison between 0thday and 4th day of perturbation; 'b' showed the comparison between 0thday and 6th day of perturbation; 'c' showed the comparison between 0th day and 15th day of restoration. c1 corresponds to P≤0.05; b2,c2 corresponds to P≤0.01; b3 corresponds to P≤0.001; a4,c4 corresponds to P≤0.0001. Error bars shown are a standard deviation from the mean value of seven replicates (n=7).

BDNF and CRH levels in the mice brain altered during vancomycin treatment and restoration period

Changes in behavior are an indication of changes in brain function. As described before, there are a few signature molecules, "brain-derived neurotrophic factor (BDNF) and corticotropin-releasing hormone (CRH)," whose expression levels speak volumes (359). BDNF is necessary for the maintenance of neuronal circuit formation and its level of expression in the brain is associated with depression and anxiety of the host. Gut microbiota has a significant role in

regulating BDNF expression (354,360). We studied mRNA level expression of BDNF from the brain's hippocampus in both antibiotic perturbed and restored mice. It was found that the BDNF level decreased in both vancomycin-treated BALB/c and C57BL/6 mice (Fig. 3.2.3A.). Up to the 4th day following vancomycin treatment, both BALB/c and C57BL/6 mice showed a decrease in BDNF expression. C57BL/6 mice had a comparatively lower BDNF expression in the brain than BALB/c mice on day six of vancomycin treatment. However, within 15 days of the restoration period, the BDNF level was found to be significantly elevated in the brain of both strains of mice.

Like BDNF, gut microbiota also modulates CRH in the brain's hypothalamus and regulates stress response in the host (361). Vancomycin-treated mice showed elevated expression of CRH and alleviated expression of CRHBP in the hypothalamus region of the brain than the untreated group of mice (Figs. 3.2.3B. and 3.2.3C.). However, during the restoration phase, the expression of CRH and CRHBP became comparable with the control group of mice. On the 15th day of restoration, BALB/c mice showed higher similarity in the expression of BDNF, CRH, and CRHBP with their control groups, while C57BL/6 mice showed less similarity with their control group.

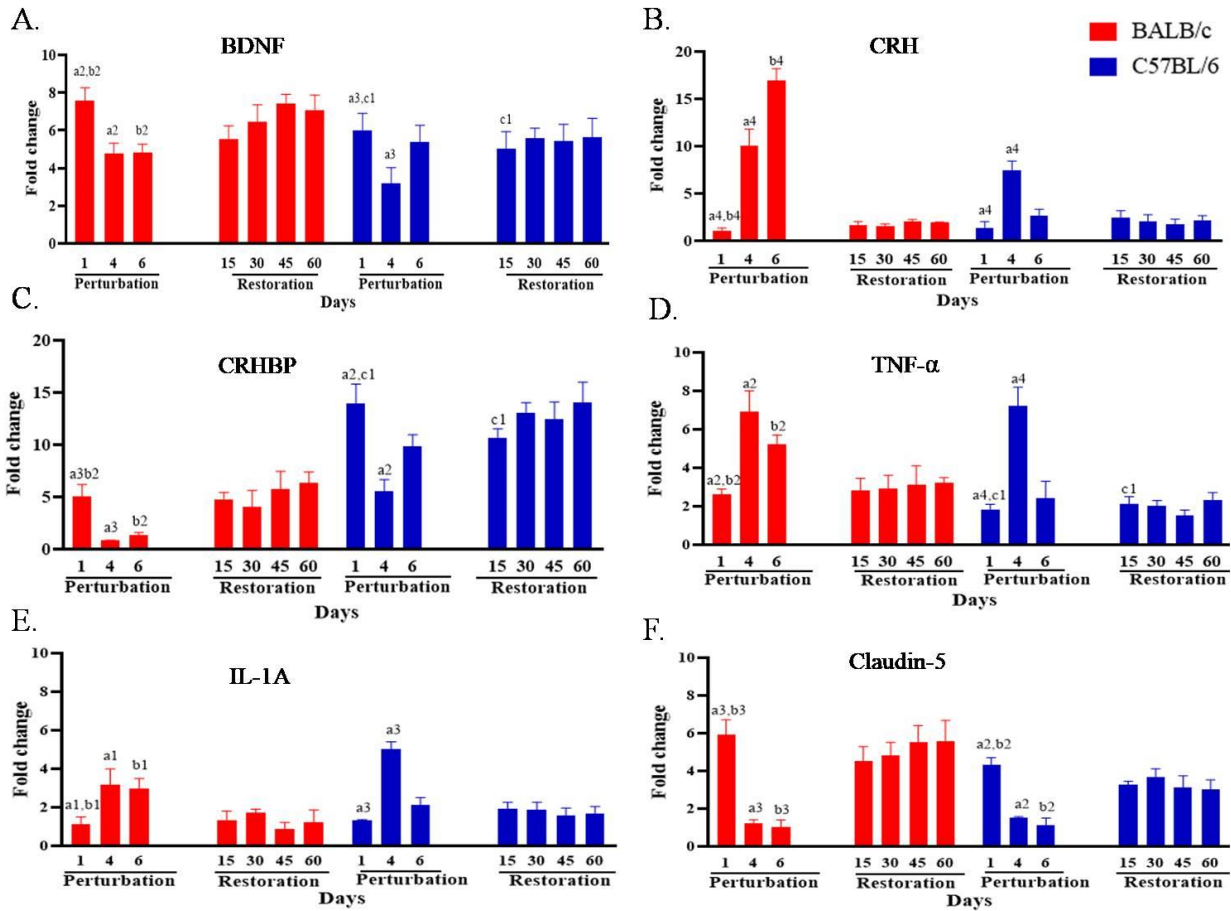


Figure 3.2.3: Transcriptional profile of different genes in the brain of mice.

Kinetics of expression (by qRT-PCR) of various stress-related and inflammatory genes in the brain of the mice during vancomycin perturbation and restoration period. A. BDNF, B. CRH, C. CRHBP gene expression at mRNA level in BALB/c and C57BL/6 mice. Immune genes D. TNF- α , E. IL-1A and tight junction genes F. Claudin 5 expression at mRNA level in the brain of BALB/c and C57BL/6 mice.

(Statistical significance changes were calculated by comparing values of the treated groups at various time points with their respective untreated groups through two-way ANOVA and t-test. 'a' showed Comparison between 0thday and 4th day of perturbation; 'b' showed the comparison

between 0thday and 6th day of perturbation; 'c' showed the comparison between 0thday and 15th day of restoration.a1, b1 and c1 corresponds to P≤0.05; a2,b2 corresponds to P≤0.01; a3,b3 corresponds to P≤0.001; a4,b4 corresponds to P≤0.0001. Error bars shown are a standard deviation from the mean value of six replicates.

The inflammatory response changed in the gut and brain with antibiotic treatment.

Gut microbiota regulates the brain's immune response and inflammatory state and its perturbation can cause cytokine-induced depression in the host (358,362). In the current study, we checked the expression of select cytokines like TNF- α , IL-1A, and IL-10 genes at mRNA level in mice brain by qRT PCR. During vancomycin treatment, it was found that the levels of both TNF- α and IL-1A increased significantly in the brain of BALB/c and C57BL/6 mice (Figs. 3.2.3D and 3.2.3E). Their expression was highest on the 4th day following vancomycin treatment. We couldn't find any significant differences in the IL-10 gene expression in the brain of vancomycin-treated mice (data not shown to avoid clutter).

Tight junction protein expression in the brain maintains the integrity of the blood-brain barrier (BBB). BBB of germ-free mice is more permeable than their specific pathogen-free (SPF) counterparts (180), which showed the significance of gut microbiota in maintaining healthy BBB. In this study, we checked the expression of Claudin 5 at the mRNA level in the brain of both BALB/c and C57BL/6 mice following antibiotic treatment. A significant reduction was observed in the expression of Claudin 5 gene at the mRNA level in the vancomycin-treated mice brain compared to its time-matched untreated group of mice during the perturbation period (Figs. 3.2.3F). On the 15th day of restoration, we observed an increase in Claudin 5 expression in the brain and became similar to the control group of mice.

During the perturbation and restoration phase of gut microbiota, we observed the altered expression pattern of various immune-related genes and tight junction protein genes in the gut. We found a significant increase in pro-inflammatory cytokines gene expressions like TNF- α and IL-1A (Figs. 3.2.4A and 3.2.4B) and a decrease in anti-inflammatory cytokine-like IL-10 (Fig. 3.2.4C) in the gut following vancomycin perturbation. On the 4th day following vancomycin treatment, expression levels of TNF- α and IL-1A were the highest, and expression of IL-10 was the lowest in both BALB/c and C57BL/6 mice to its time-matched control value. Within 15 days of restoration, all the cytokines in the gut became similar to their respective control mice in both BALB/c and C57BL/6 mice.

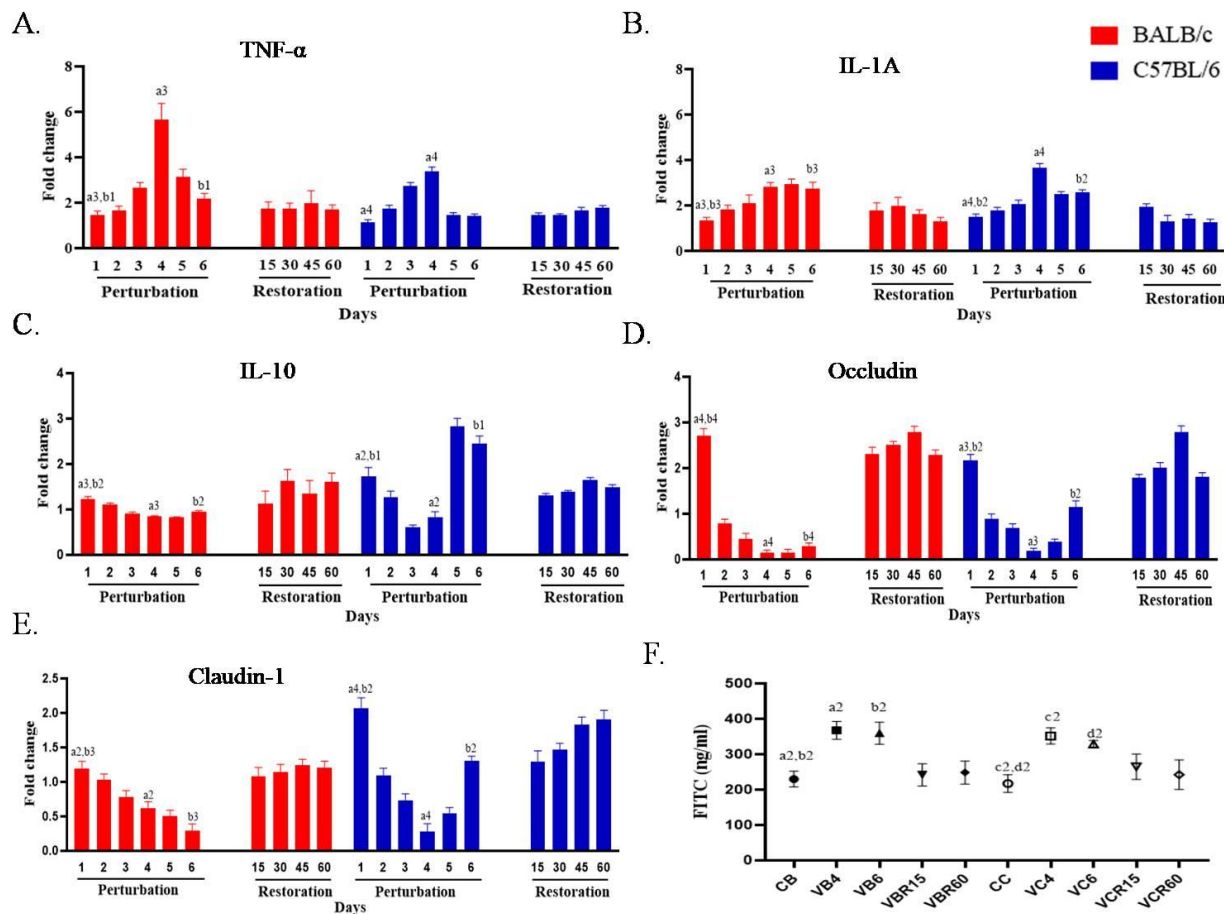


Figure 3.2.4: Transcriptional profile (by qRT-PCR) of various immune genes and tight junction genes in mice's colonic tissue during vancomycin perturbation and restoration period.

Kinetics of expression of various immune genes at mRNA level in the colon of vancomycin treated BALB/c (VB) and C57BL/6 (VC) mice, A. TNF- α , B. IL-1A C. IL-10, and tight junction genes D. Occludin and E. Claudin 1. F. FITC dextran concentration in serum at various time points of perturbation and restoration period.

(Statistical significance changes were calculated by comparing values of the treated groups at various time points with their respective untreated groups through two-way ANOVA and t-test. 'a' showed Comparison between 0th day and 4th day of perturbation; 'b' showed the comparison between 0thday and 6th day of perturbation; 'c' showed the comparison between 0thday and 15th day of restoration.b1 and c1 correspond to $P \leq 0.05$; a2,b2,c2,d2 corresponds to $P \leq 0.01$; a3,b3 corresponds to $P \leq 0.001$; a4,b4 corresponds to $P \leq 0.0001$. Error bars shown are a standard deviation from the mean value of six replicates.

Antibiotic treatment increased gut permeability by modulating the expression of tight junction protein.

The tight junction proteins like Occludin and Claudin regulate the integrity of the gut (128). Alteration of gut microbiota could compromise the expression of tight junction proteins and might lead to inflammation (126). In the current study, we found a lower expression of Occludin (Fig. 3.2.4D) and Claudin 1 (Fig. 3.2.4E) at mRNA level in colonic tissue during vancomycin treatment in both BALB/C and C57BL/6 mice, which might be a reason for the increased permeability of the gut. During the restoration process, their expression increased and became similar to the control mice within 15 days of the restoration period. For further confirmation of

gut permeability, FITC conjugated dextran was gavaged to the 4th-day mice following vancomycin treatment and 60th-day mice of restoration group following cessation of antibiotic treatment. FITC dextran concentration was found to be significantly higher on the 4th day following vancomycin treatment in both Th1- and Th2- biased mice (367±25 ng/ml in BALB/c and 350±23 ng/ml in C57BL/6) (Fig. 3.2.4F). During the restoration period, FITC concentration in the serum came to the normal level.

Table 3.2.3: Measurement of the cecal index at different time points of perturbation and restoration periods in BALB/c and C57BL/6 mice.

Conditions	Days	BALB/c	C57BL/6
Perturbation	0	0.01±0.001	0.008±0.002
	4	0.029±0.005	0.032±0.003
	6	0.027±0.002	0.033±0.002
Restoration	15	0.013±0.002	0.013±0.003
	30	0.012±0.001	0.010±0.002
	45	0.009±0.001	0.0095±0.002
	60	0.008±0.001	0.010±0.003

Means of the cecal index with their respective standard deviations (±SD) at various time points

were represented.

Gut microbiota abundance and composition regulate the cecal size of mice. The cecum is known to be a better representation than the fecal sample for understanding intestinal microbiota profile and cecum size changes during dysbiosis of gut microbiota (330,363). Enlargement of cecum size was observed in vancomycin-treated mice than the untreated group of mice. The cecal index was calculated and found to be increased continuously during the perturbation period in both BALB/c and C57BL/6 mice (Table 3.2.3.). During the restoration process, the cecum size decreased and came to the normal level within 15 days following cessation of vancomycin treatment.

IgA level varied with the strains of mice and antibiotic treatment. IgA concentration from the cecal sample of BALB/c and C57BL/6 mice showed a significant difference. Basal IgA level was higher in the control of BALB/c mice compared to control C57BL/6 mice (Fig. 3.2.5). It was also observed that during vancomycin treatment, the IgA level significantly decreased in the cecal sample of both strains of mice; however, it again increased during the restoration period.

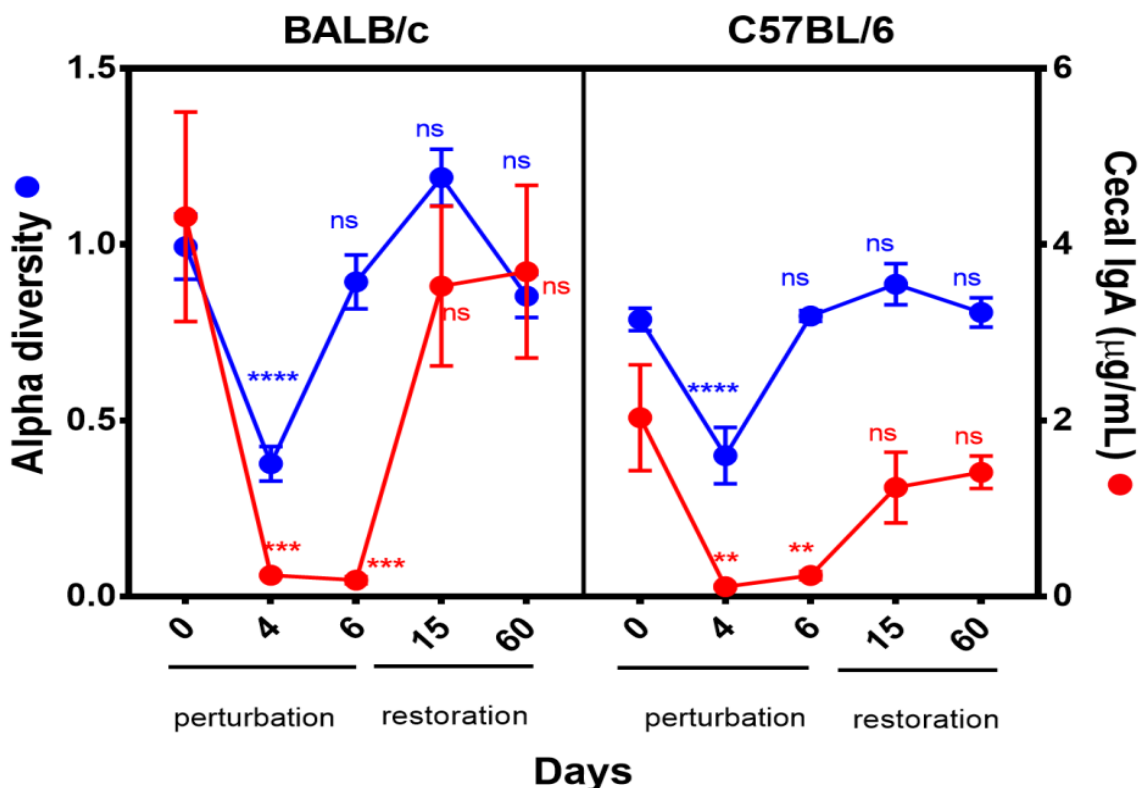


Figure 3.2.5: The alteration patterns of Shannon diversity index of gut microbiota and IgA level were compared during vancomycin treatment and subsequent restoration period of BALB/c and C57BL/6 mice.

The Shannon diversity index of gut microbiota decreased during the perturbation period and increased during the restoration period. We found a positive correlation between IgA level and diversity of gut microbiota was found; with the increase or decrease of cecal IgA level, diversity of gut microbiota also increased or decreased respectively.

Table 3.2.4: Comparison of Firmicutes to Bacteroidetes ratio (F/B) at different time points of BALB/c and C57BL/6 mice.

Perturbation Days	F/B ratio of BALB/c	F/B ratio of C57BL/6
0	2.12±0.23	2.73±0.44
2	1628±101	20717±912
3	9773.5±628	1134.06±121
4	5002.8±700	5754.77±506
5	3099.15±9.8	1630.37±33
6	2106.38±2810	580.63±78
Restoration Days		
15	1.63±0.78	2.32±0.67
30	2.17±0.19	4.92±1.2
60	2.68±0.41	4.78± 0.81

Firmicutes to Bacteroidetes (F/B) ratio increased significantly during the perturbation period and it was highest on the day third and four following vancomycin treatment in BALB/c and C57BL/6 mice respectively. However, during the restoration period, the ratio decreased and became similar to the untreated group of mice.

Table 3.2.5: Sequences of forward (_F) and reverse (_R) primers for qRT-PCR studies to confirm the presence and expression level of various genes used in this study.

Gene-specific for

Sequences of the primers used

TNF- α _F	5'-CCACGTCGTAGCAAACCACCAAAG-3'
TNF- α _R	5'- TGCCCCGGACTCCGCAAAGTCTAAG-3'
IL-10_F	5'-AGGCAGTGGAGCAGGTGAAGAGTG-3'
IL-10_R	5'-GCTCTCAAGTGTGCCAGCCTTAG-3'
IL-1A_F	5'-ATCAGTACCTCACGGCTGCT-3'
IL-1A_R	5'-TGGGTATCTCAGGCATCTCC-3'
Claudin 1_F	5'-TGCCCCAGTGGAAGATTACT-3'
Claudin 1_R	5'-CTTGCGAACGCGAGGACAT-3'
Occludin_F	5'- GTTGAACTGTGGATTGGCAG -3'
Occludin_R	5'- AAGATAAGCGAACCTTGGCG -3'
Claudin 5_F	5'- TTA AGG CAC GGG TAG CAC TCA CG -3'
Claudin 5_R	5'-TTA GAC ATA GTT CTT CTT GTC GTA ATC G-3'
BDNF_F	5'-TCATACTTCGGTTGCATGAAGG-3'
BDNF_R	5'-ACACCTGGGTAGGCCAAGTT-3'
CRH_F	5'-ACCAAGGGAGGAGAAGAGAG-3'
CRH_R	5'-TGCAAGAAATTCAAGGGCTG-3'

CRHBP_F 5'-AAGGGAGAGAGCCGCTA-3'

CRHBP_R 5'-TTTCCATTGCTGCCAT-3'

3.2.3 Discussion

Both perturbation and restoration patterns of the gut microbiota varied between BALB/c and C57BL/6 mice. Reports showed that following antibiotic treatment, the incomplete recovery of the gut microbiota happened (231,333). Gut microbiota recovery pattern depends on various factors like types and duration of antibiotics used in the study or the genetics of the host. The current study showed that maximum gut microbiota was restored within 15 days following the cessation of antibiotics treatment. BALB/c mice had a more efficient restoration capacity of gut microbiota than C57BL/6 mice within the same period.

It was reported that alteration in the composition and diversity of gut microbes caused changes in the behavior of mice in EPM, FST, and OF tests (180). It was observed that colonizing the gastrointestinal tract of germ-free mice with pathogenic bacteria like *Escherichia coli* increased the stress level of mice while *Bifidobacterium infantis* alleviated the stress or anxiety-like behavior (182,183). Earlier reports further suggested that different bacteria of Firmicutes phylum helped in reducing anxiety and depression-like behavior in mice (186). *Akkermansiamuciniphila* bacteria caused a reduction in anxiety behavior in mice (187). The higher ratio of Firmicutes to Bacteroidetes (F/B ratio) inside the gut caused elevation of stress and anxiety-like behavior in the host (188,189). In the current study, we observed a correlation between relative patterns of changes in gut microbiota and the behavior of mice. During vancomycin treatment, up to the 4th day, an increase in pathogenic bacteria like *Escherichia*

coli and a decrease in beneficial bacteria were linked to higher anxiety and depressive behavior in both Th1- and Th2- biased mice in EPM, OFT, and FST. After the 4th day, Verrucomicrobia phylum replaced the Proteobacteria phylum in C57BL/6 mice associated with lower anxiety and depressive behavior in C5BL/6 compared to BALB/c mice. On day four following vancomycin treatment, the dominance of a single phylum (Proteobacteria) caused a decrease in the diversity of gut microbes. During the perturbation period, the higher F/B ratio might be related to the increased level of stress or anxiety in the mice compared to the restoration period.

An earlier report showed a higher BDNF level and lower CRH levels in anxiety patients than normal individuals (359). Dysbiosis of gut microbiota caused changes in BDNF and CRH levels in the host (364,365). The current study showed decreased BDNF and increased CRH level during vancomycin treatment that explained the elevated stress behavior in EPM, FST, and OF test of mice during that period. Increased pathogenic Proteobacteria and decreased beneficial microbes during vancomycin treatment were associated with stress in mice, modulating BDNF, CRH, and CRHBP levels in the brain. The expression pattern of these stress-related genes is proposed to be due to the alteration pattern of gut microbes, hence mice's behavior. Increased Proteobacteria level on the 4th day and Verrucomicrobia level on the 6th day following vancomycin treatment showed two opposite effects on the expression of stress-related genes.

Proteobacteria phylum contains mostly gram-negative pathogenic bacteria to contribute LPS to bind to the gut's TLR receptor and activate the expression of pro-inflammatory cytokines (106). Firmicutes, specifically the Clostridium group present in the gut, produce short-chain fatty acid [170], and these SCFA in the gut suppresses the LPS and pro-inflammatory cytokines and enhances the secretion of the anti-inflammatory cytokines (103,104). The current study showed during the perturbation period, the higher Proteobacteria and lower Firmicutes level inside the

gut resulted in increased gut inflammation and permeability. However, most of the alterations in the host physiology during the perturbation period came to the average level during the restoration phase with the efficient restoration of gut microbiota.

Chapter 3.3:Comparative study of different antibiotics treatment on gut microbiota and immune system of the host.

3.3.1 Introduction:

Our previous studies observed the perturbation pattern of gut microbiota following vancomycin treatment and its effect on the host. However, different antibiotic treatments can alter the gut microbiota composition in distinct ways. Therefore, in this chapter, we reported the effects of select antibiotics like neomycin, AVNM cocktail on the gut microbiota and host physiology. Various antibiotics can perturb the huge number of diverse microbes of the gut to understand the role of specific microbes in maintaining various host physiology (366–369). Each antibiotic has a unique mode of action and acts against some specific group of microbes. Therefore, every antibiotic can alter the composition and abundance of gut microbiota in a distinct way than others. (207,269,333,344). As gut microbiota regulates various host physiologies, we can understand the cross-talk between host and specific groups of microbes by altering the composition of gut microbiota through different antibiotics. Gut microbiota produces various short-chain fatty acids that regulate the inflammatory response of the host (100). SCFAs in the gut suppress the LPS and pro-inflammatory cytokines like TNF- α , IL-6 level and increased the production of anti-inflammatory cytokines like IL-10 (103,104). During the dysbiosis of gut microbiota, the increase in the pathogenic Gram-negative group of bacteria caused an increase in the blood endotoxin level through their LPS which enhanced various pro-inflammatory cytokines by activating different Toll-Like Receptors (TLR4) of the gut epithelial cells (105–107,169,170).

The correlation between the antibiotic-induced alterations of specific groups of microbes with the immune and metabolic response of the host was not evident in the literature. Therefore, treatment with single and different combinations of antibiotics can give us certain ideas about the

extent of perturbation of specific gut bacteria and their effect on the host immune and metabolic response.

In this study, we compared the efficiency of perturbation of mouse gut microbiota by antibiotics like vancomycin or neomycin or a cocktail of antibiotics containing ampicillin, vancomycin, neomycin, and metronidazole or known as AVNM in short. Vancomycin is a broad-spectrum antibiotic to treat MRSA or drug-resistant *Clostridium difficile* induced colitis (306,337). Neomycin is an aminoglycoside antibiotic that arrests the growth of intestinal bacteria (332). AVNM, the mixture of four different antibiotics, is well established as a gut microbiota depleting agent in mice (330). The role of gnotobiotic or germ-free mice models is well documented and important model system in microbiome study, but because of the non-availability or inaccessibility of this model to a wide variety of scientific community, the AVNM treated mouse model serves as a good alternative. Because of the different structures and functions of the antibiotics used, the treatment with each type of antibiotic caused a different kind of gut microbial modulation.

Moreover, the alteration of gut microbes due to different antibiotics treatment caused the host's differential immune and metabolic response. Expression of various pro- and anti-inflammatory immune genes and the production of specific SCFAs were strongly correlated with the abundance of particular phyla of gut microbes. The cecal size of mice also got differentially affected following treatment with different antibiotics.

3.3.2 Results:

Antibiotic treatment alters the abundance and diversity of gut microbiota.

Earlier reports showed the differential effects of treatment with several antibiotics causing dysbiosis of gut microbiota (333). A comparative analysis of select antibiotics to understand the changes in the gut microbiota composition is warranted to correlate with innate mucosal immunity and systemic metabolites.

The current results revealed that the gut microbiota of untreated C57BL/6 mice majorly contained Firmicutes and Bacteroidetes phyla with a very meager amount of Proteobacteria phylum (Fig. 3.3.1A).

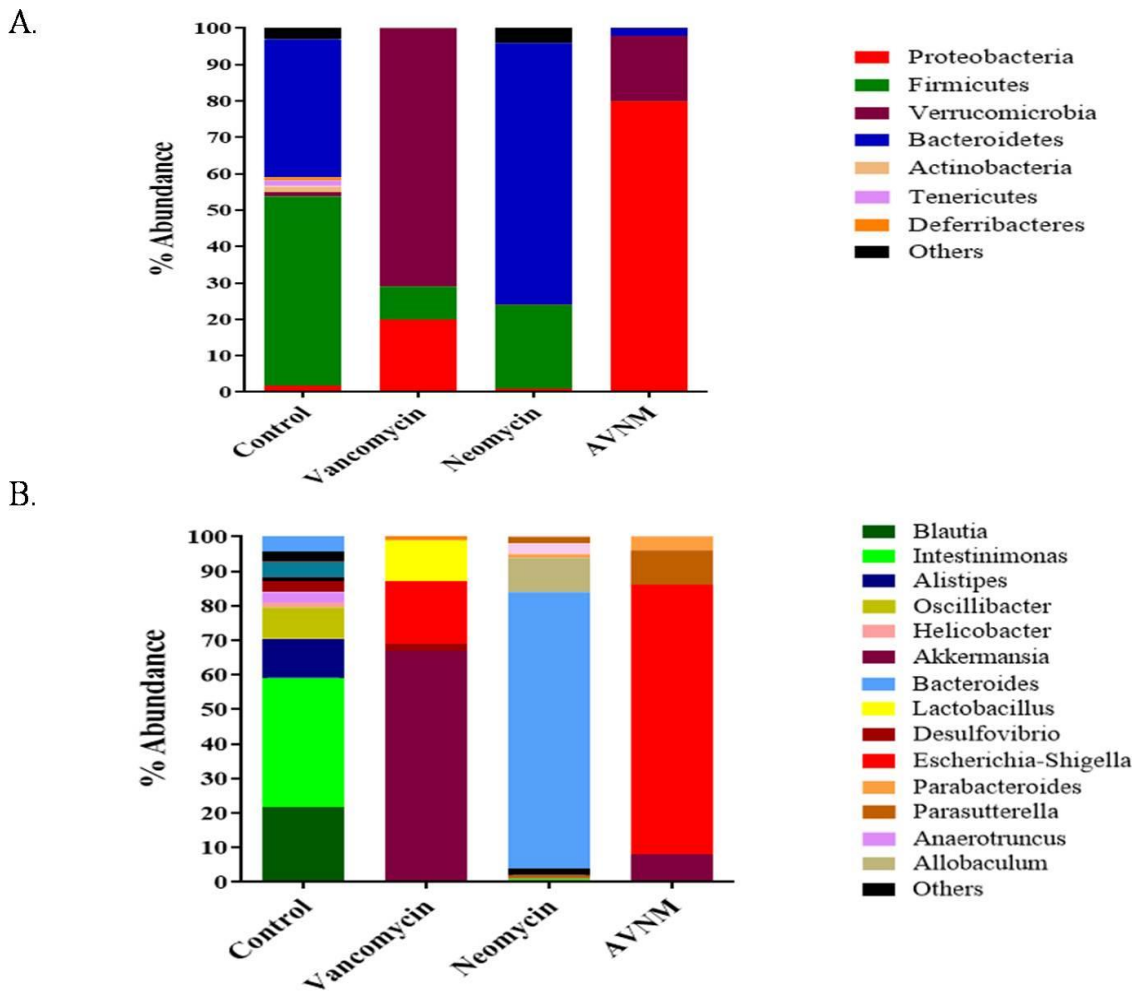


Figure 3.3.1: Alteration of the gut microbiota following antibiotic treatment. Percentage changes in the gut microbiota abundance A. phylum level B. genus level in the antibiotic-treated (vancomycin, Neomycin, AVNM) and control groups of mice.

Following treatment with vancomycin for seven consecutive days caused an increase in Verrucomicrobia (by 71%) and Proteobacteria (by 20%) with a concomitant decrease in Firmicutes and Bacteroidetes phyla (Table. 3.3.1). On the contrary, treatment with neomycin for seven days caused a significant increase in Bacteroidetes (by 72%) and a decrease in Firmicutes

like major phylum (by 23%) (Table. 3.3.1). Treatment with AVNM, in accordance, caused a significant increase in Proteobacteria (by 80%) and a decrease in essential phyla like Firmicutes and Bacteroidetes (Fig. 3.3.1A). Genus level analysis further validated the phylum level observation.

Genus level data showed that vancomycin treatment mainly caused an increase in the Akkermansia genus of Verrucomicrobia phylum (Fig. 3.3.1B). In contrast, neomycin treatment caused an increase in the Bacteroides genus of Bacteroidetes phylum. However, AVNM treatment mainly elevates Escherichia-Shigella genera of Proteobacteria phylum in the gut (Fig. 3.3.1B).

Other members of the phylum or genus shown in the figures depict the overall idea of composition and qualitative diversity of the gut microbiota. A detailed analysis of diversity is described below.

Alpha diversity of gut microbiota decreased following antibiotics treatment.

Measurement of diversity is crucial for understanding the extent of modulation of gut microbiota during antibiotic treatment (346,368). In the current study, the Shannon diversity index at the phylum level showed a decrease in gut microbiota diversity in all three groups of antibiotics-treated mice than the control group of mice.

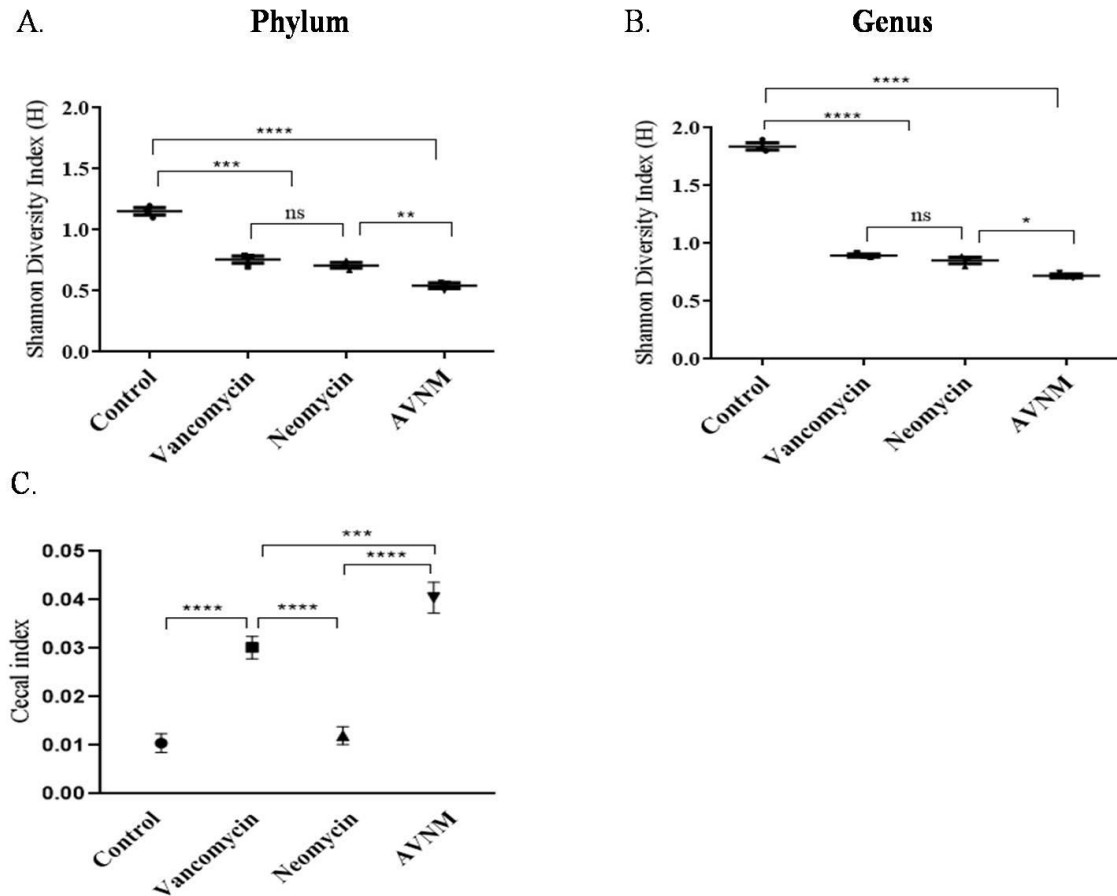


Figure 3.3.2: Effect of antibiotic treatment on the diversity of gut microbial composition.

Shannon diversity Index A. phylum B. genus level of the cecal sample in the control and antibiotic-treated mice C. weight of cecal content of control and antibiotic-treated mice. Two-way ANOVA calculated the statistical significance of diversity. ('***' corresponds to $P \leq 0.001$, '**' corresponds to $P \leq 0.01$, '*' corresponds to $P \leq 0.05$ level of significance). Error bars are one standard deviation of the mean value and determined from the average values of three biological replicates.

Vancomycin and neomycin treatment caused a similar extent of reduction in the diversity of gut microbiota. However, among the three antibiotic-treated groups, AVNM treatment caused a maximal decrease in gut microbial diversity (Fig 3.3.2A). The genus-level analysis of the data further validated the phylum level observations (Fig. 3.3.2B).

Alteration in the cecal index and bodyweight of mice during antibiotics treatment.

Alteration in the cecal size is usually a strong indication of the variation of bacterial abundance in the cecum of mice (317). In this study, the cecal index of the antibiotic-treated mice varied significantly compared to the control group of mice (Fig. 3.3.2C). It increased dramatically following vancomycin and AVNM treatment. AVNM treated group had the highest weight of cecal content among all groups of mice. However, the neomycin-treated group of mice showed no changes in the cecal weight compared to the control group of mice.

We had measured the bodyweight of control and antibiotics-treated mice from day zero to day seven of the experiment. Still, We could not find any significant difference between starting (day zero) and ending points (day seven) of the investigation (Table. 3.3.3). Fluid consumption (ml/day) of AVNM treated mice also didn't change significantly between day zero and day seven of treatment. However, we found a slight reduction in the body weight and fluid consumption of mice from day zero to day four of the experiment. On later days, it again came to nearly a similar level of day zero untreated mice.

The inflammatory response in the colon changed following antibiotics-mediated microbiota perturbation.

Gut microbiota composition and diversity regulated the expression of various Immune genes in the gut (78). Different immune genes were up or down-regulated depending on the antibiotic treatment groups.

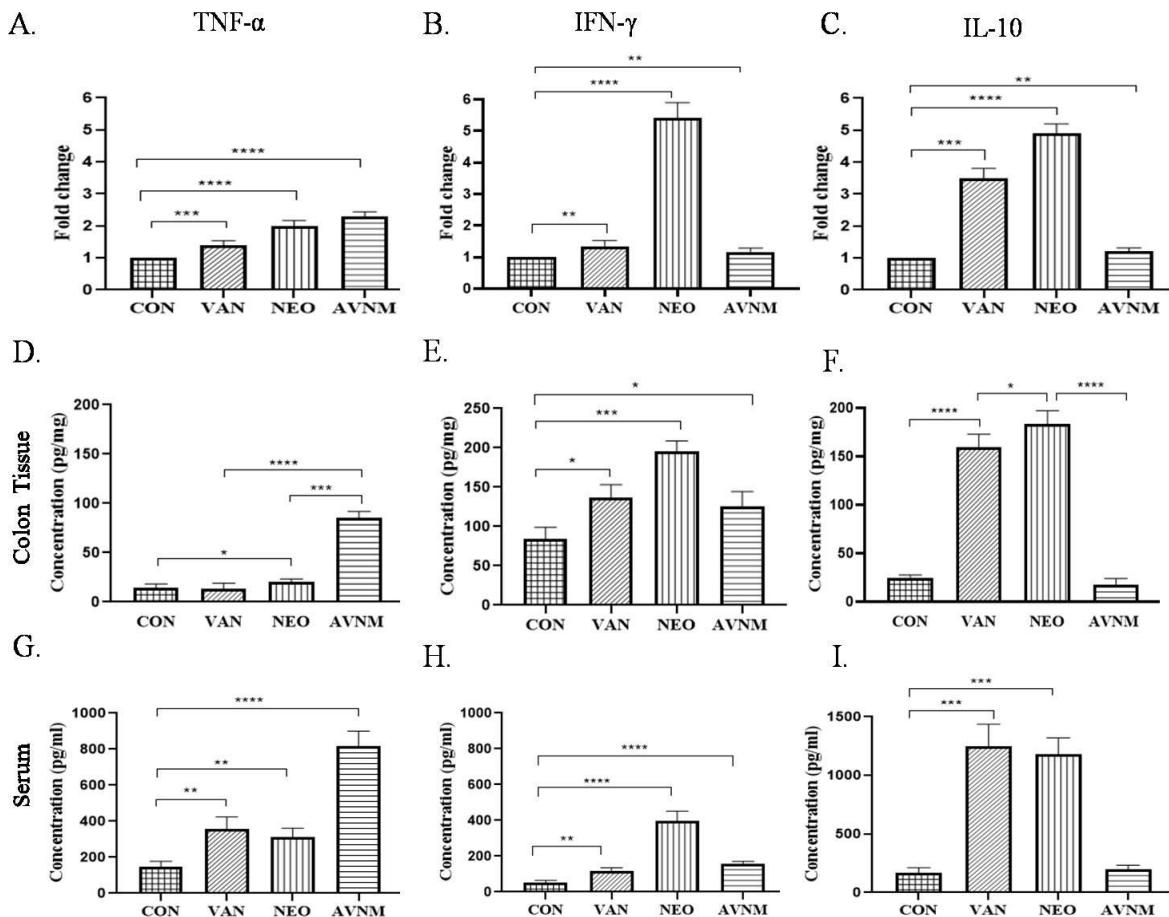


Figure 3.3.3: Transcriptional profile of different immune regulatory genes in the colon of mice following antibiotics. Changes in the expression of cytokine genes A. TNF α , B. IFN γ , C. IL10 at mRNA level following three antibiotics treatment (VAN, vancomycin; NEO, neomycin; AVNM treatment). Protein concentration was determined through ELISA in colon tissue, D. TNF α , E. IFN γ , F. IL10 and in serum, G. TNF α , H. IFN γ , I. IL10 following three antibiotics treatment.

Statistical significance was calculated by two-way ANOVA ('***' corresponds to $P \leq 0.001$, '**' corresponds to $P \leq 0.01$, '*' corresponds to $P \leq 0.05$ level of significance). Error bars are one standard deviation of the mean value and determined from the average values of four biological replicates.

Real-time PCR data showed variation in the expression of selected immune genes in the colon of mice post antibiotics treatment (Fig. 3.3.3A, B, and C). The vancomycin-treated group of mice showed an increase in IL-10 gene expression in the colon; however, we did not find any considerable changes in the expression of TNF- α and IFN- γ genes. While neomycin treated group of mice showed an increase in both IL-10 and IFN- γ expression in the colon. However, AVNM treatment caused a rise in TNF- α gene expression in the colon, whereas no significant changes were found in the expression of IL-10 and IFN- γ genes (Fig. 3.3.3A, B, and C).

We validated qRT-PCR results by measuring the expression of TNF- α , IFN- γ , and IL-10 genes in both colon tissue (Figures 3.3.3 D, E, and F) and serum sample of the host using ELISA (Figures 3.3.3 G, H, and I). ELISA results revealed that TNF- α level was the highest in the colon (Fig. 3.3.3D) and serum (Fig. 3.3.3G) of AVNM treated mice, whereas IL-10 level was more in both neomycin and vancomycin treated mice (Fig. 3.3.3F and 3.3.3I). IFN- γ concentration was highest in the serum of neomycin-treated mice (Fig. 3.3.3H). The ELISA data for immune genes were corroborated with the qRT-PCR results.

Alteration profiles of SCFA after antibiotics treatment

Antibiotic treatment can drastically alter the Short-chain fatty acids (SCFAs) level, which are essential regulators of host immune processes (100). Butyrate is mainly produced by the Firmicutes phylum, while acetate and propionate are mainly produced by the Bacteroidetes

phylum (100). Some earlier reports showed that *Akkermansiamuciniphila* also had acetate and propionate up to some extent in the gut (104).

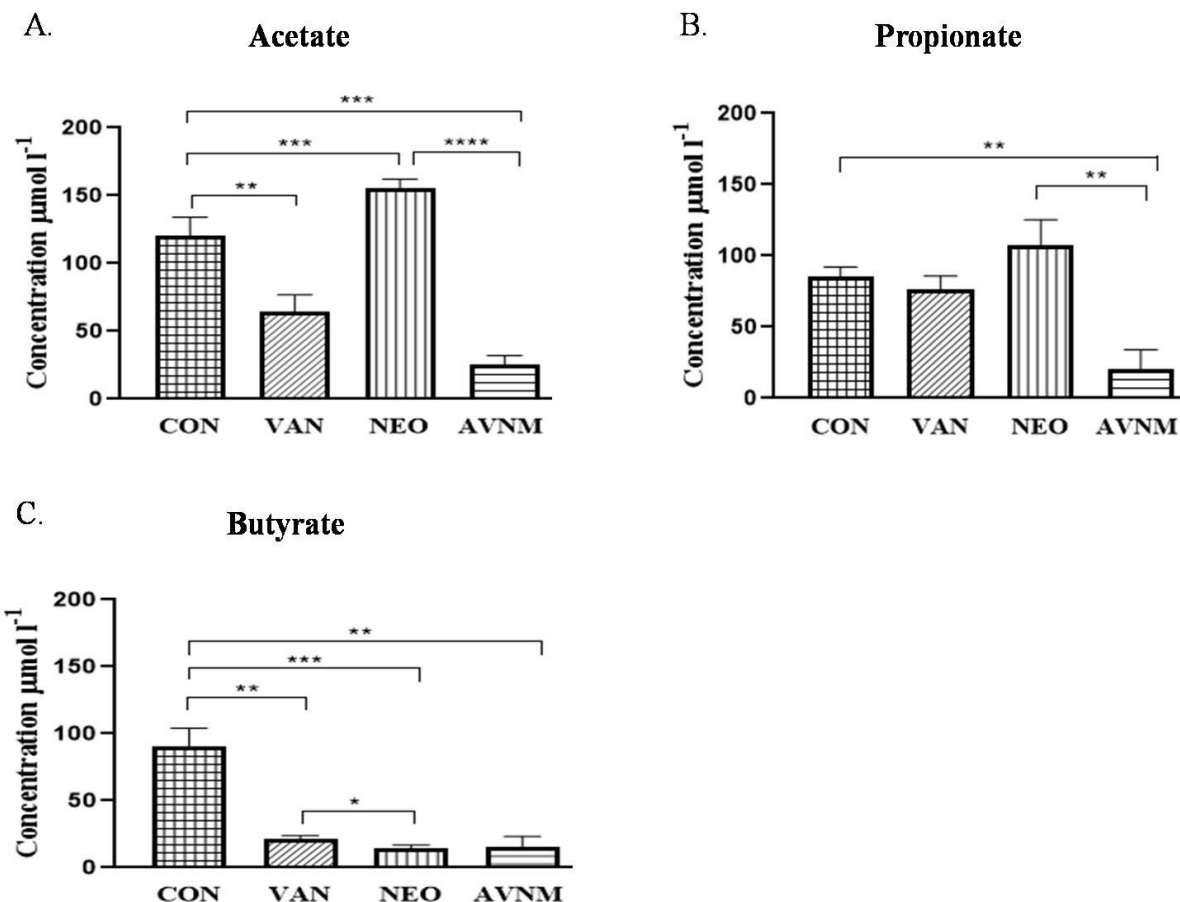


Figure3.3.4: The abundance of select metabolites in the serum of mice by chemometric 1H-NMR studies. The concentration of primary short-chain fatty acids A. acetate, B. butyrate, C. propionate of untreated control (con), vancomycin (VAN), neomycin (NEO), and AVNM treated mice. Statistical significance was calculated by two-way ANOVA ('***' corresponds to $P \leq 0.001$, '**' corresponds to $P \leq 0.01$, '*' corresponds to $P \leq 0.05$ level of significance). Error bars are the standard deviation of the mean value and determined from the average values of three biological replicates.

We measured the concentrations of SCFAs in the host serum using NMR based metabolomics study. Results revealed that neomycin treatment caused the highest increase in propionate and acetate level with a significant decrease in butyrate level compared to control mice (Fig. 3.3.4). Vancomycin-treated mice showed a reduction in acetate and butyrate levels compared to control mice, while we didn't find any significant alteration in the propionate level. However, AVNM treated mice showed the most significant decrease in all three SCFAs, such as acetate, propionate, and butyrate, compared to control and the other two antibiotics treated groups of mice (Fig. 3.3.4).

We also measured the abundance of acetate in the serum of both antibiotic-treated and control groups of mice using an acetate colorimetric assay kit (EOAC-100, San Francisco, USA). The results showed that the concentration of acetate through the colorimetric detection kit method for different groups of mice, like control (51.2 ± 4 μm), vancomycin (42 ± 6 μm), neomycin (60 ± 6.3 μm), and AVNM ($20\pm1.4\mu\text{m}$) showed nearly similar trends with NMR data.

Effects of various antibiotics on the proteobacteria level of the gut and its correlations with the anxiety level of the host.

Different antibiotics altered the Proteobacteria level of the gut to different extents. Neomycin-treated mice showed a decreased level of Proteobacteria phylum ($0.08\pm0.50\%$) compared to the control group of mice (1.8 ± 0.30 , whereas AVNM treatment caused a significant increase in the Proteobacteria abundance ($80\pm4\%$) compared to control (Fig. 3.3.5). We found a correlation between the Proteobacteria level of the gut and the altered behavior of the mice in different

stress-related tests (EPM, OF). The anxiety level (%) of the mice was calculated during other antibiotics treatment. Percent anxiety level was calculated using the formula: anxiety level (%) = [1- (time spent/total time)] ×100 in the EPM and OF test. Data revealed that Proteobacteria level in the gut was directly associated with the stress or anxiety level of the mice. Neomycin treatment showed significantly lower anxiety levels in mice, whereas AVNM treated mice showed the highest anxiety level in both stress tests.

Figure 3.3.5: Comparative relationship between anxiety and gut Proteobacteria level in mice.

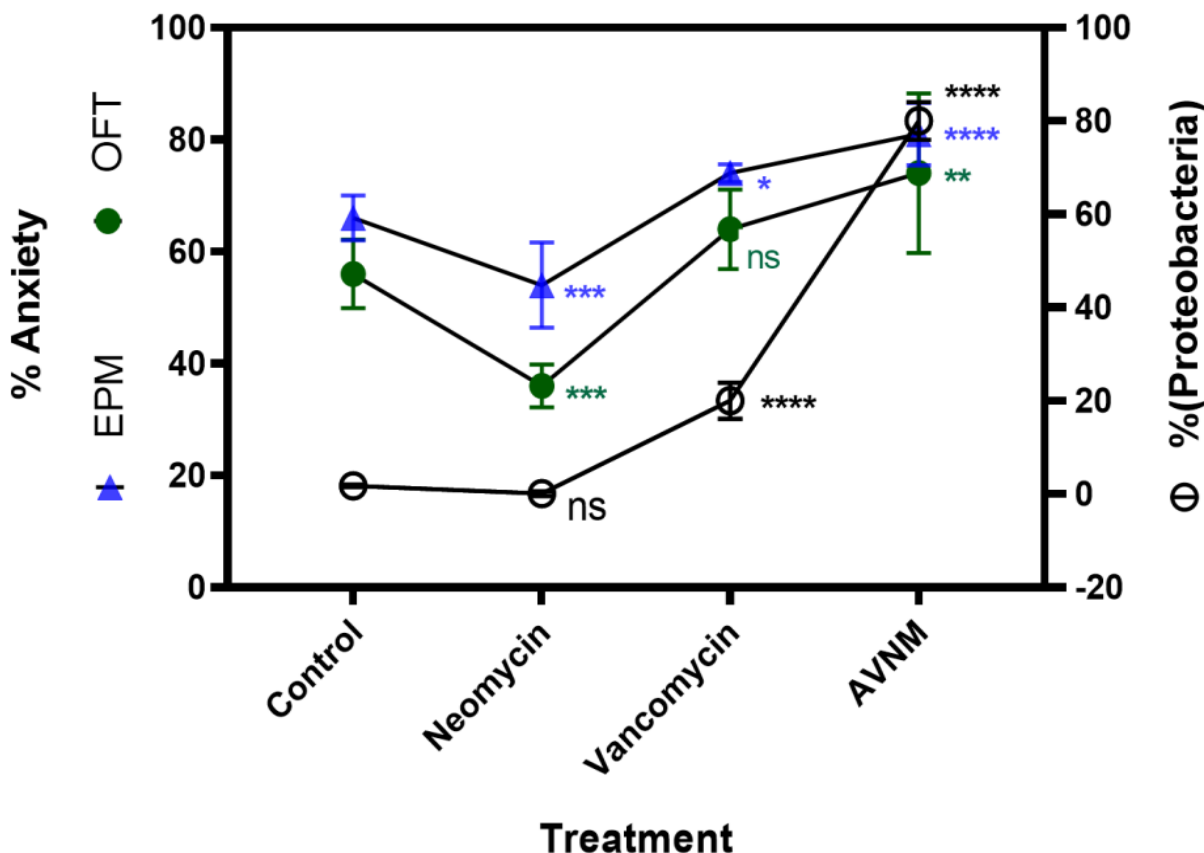


Figure 3.3.5: Association between the percentage of Proteobacteria present inside the gut and anxiety level of the mice was shown in the double y-axis graph. X-axis showed different antibiotic treatment conditions. Anxiety level was determined through EPM and OF tests. Statistical significance was determined by comparing the anxiety level of control groups with different antibiotics treated groups through one-way ANOVA and Proteobacteria percentage separately, where ('***' corresponds to $P \leq 0.001$, '**' corresponds to $P \leq 0.01$, '*' corresponds to $P \leq 0.05$ level of significance). Color codes were matched and shown in y-axis legends.

Table 3.3.1: Percent abundance of major phyla of gut microbes in the untreated control and different antibiotics treated mice.

Conditions	% Abundance			
	Firmicutes	Bacteroidetes	Proteobacteria	Verrucomicrobia
Control	52 (± 5)	38 (± 4)	1.8 (± 0.3)	1.2 (± 0.4)
Vancomycin	9 (± 2)	NIL	20 (± 4)	71 (± 6)
Neomycin	23 (± 4)	72 (± 5)	1 (± 0.5)	NIL
AVNM	NIL	2 (± 0.9)	80 (± 4)	18 (± 3)

Major groups of bacterial phyla present in the cecal content of mice are determined by metagenomic analysis (16s rRNA) at different conditions (vancomycin, neomycin, AVNM treated groups along with the time-matched control) of C57BL/6 mice. Means of percent abundance of various phyla with their respective standard deviations ($\pm SD$) are shown.

Table 3.3.2: Sequences of forward (_F) and reverse (_R) primers for PCR studies to confirm the expression of various genes used in this study.

Gene-specific for	The sequence of the primer used
<i>TNF-α</i>	F:5'-CCACGTCGTAGCAAACCACCAAAG-3' R:5'- TGCCC GGACTCCGCAAAGTCTAAG-3'
<i>IL-10</i>	F:5'-AGGCAGTGGAGCAGGTGAAGAGTG-3' R:5'-GCTCTCAAGTGTGGCCAGCCTAG-3'
<i>IFN-γ</i>	F:5'-TCAAGTGGCATAGATGTGGAAGAA R:5'-TGGCTTGCAGGATTTCATG-3'

Table3.3.3: Bodyweight of mice during antibiotic treatment.

	Control	Vancomycin	Neomycin	AVNM
0	26.43±0.3	25.36±0.38	27.4±0.9	26.77±0.55
1	26.4±0.36	25.17±0.28	27.28±0.75	26.2±0.46
2	26.36±0.32	25±0.62	26.81±0.16	25.8±0.75
3	26.5±0.4	24.85±0.58	27.1±0.75	25±0.3
4	26.58±0.23	24.7±0.5	27.26±0.54	25.9±0.37
5	26.37±0.29	25.13±0.35	27.2±0.25	26.34±0.43

6	26.42±0.18	25.41±0.39	27.5±0.3	26.61±0.58
7	26.51±0.25	26±0.7	28±0.5	26.5 ±0.65

Bodyweight of control and antibiotic-treated mice (Vancomycin, Neomycin, AVNM) from day zero to day seven were shown. Means of body weight (g) of mice on different days with their respective standard deviations (\pm SD) were represented.

Table 3.3.4:Daily Fluid consumption (ml/day) of mice during AVNM treatment.

Days	Control	AVNM
0	5.5±0.45	5.8±0.5
1	5.7±0.35	5.21±0.25
2	5.36±0.47	4.8±0.45
3	5.81±0.24	4.64±0.58
4	5.6±0.36	5±0.36
5	5.5±0.55	5.46±0.29
6	5.8±0.4	5.74±0.4
7	5.9±0.65	5.3±0.5

Daily fluid consumption kinetics for control and AVNM-treated mice from day zero to day seven were shown. Means of fluid consumption (ml/day) of mice with their respective standard deviations (\pm SD) were represented.

The bodyweight of the mice was measured from day to day seven of control and various antibiotic-treated groups (Table. 3.3.3). However, we didn't find any significant alteration in the bodyweight of mice between the initial and last days of antibiotics treatment. Similarly, the daily fluid consumption of AVNM treated mice also didn't change much after the addition of antibiotics in the drinking water bottle of mice (Table. 3.3.4).

3.3.3 Discussion:

The dysbiosis pattern of gut microbiota varied significantly among the different groups of antibiotic-treated mice. Treatment with both single and cocktail of antibiotics groups caused a considerable decrease in gut microbiota diversity. During antibiotic treatment, a significant increase in only one phylum replaced all other phyla, causing an overall reduction in gut microbiota diversity.

AVNM treatment was the most effective one to reduce the diversity of gut microbiota, therefore this cocktail was taken as one of the standard gut microbial depletion agents (282–284,370). Contrary to the literature (330,371), the current study showed that AVNM treatment did not deplete the gut microbiota completely or made pseudo-gnotobiotic mice. Though antibiotic-treated mice showed extensive gut microbiota depletion, some bacteria and other microorganisms were still left in the gut after antibiotic therapy. Antibiotic treatment also

promotes the outgrowth of resistant bacteria that make it different from germ-free mice free of all microorganisms (372,373). In this study, we found, AVNM treatment caused a significant elevation in the level of Proteobacteria phylum, which replaced all the other significant gut phyla microbes like Firmicutes and Bacteroidetes. Genus level data of AVNM treated mice showed a higher level of Proteobacteria phylum that mainly contained pathogenic Escherichia-Shigella bacteria.

A strong correlation was found between the altered abundance of the specific gut microbes and the expressions of various immune genes in the colon of mice. Increased Akkermansia, Bacteroidetes, Escherichia-Shigella-like genera, and decreased Clostridia like genus following antibiotics treatment caused significant modulation in the expression of various immune genes in the colon. Altered levels of Firmicutes and Bacteroidetes in the gut also differentially regulated the serum SCFA concentration in each antibiotic-treated group. Following vancomycin treatment, an increased abundance of Akkeremansia and Lactobacillus genera caused the increased expression of the anti-inflammatory IL-10 gene in the colon of mice. In comparison, no significant changes were found in the expression of pro-inflammatory genes like TNF- α and IFN- γ . Previous studies showed that the increased abundance of *Akkermansiamuciniphila* induced elevated anti-inflammatory cytokine genes in the gut (374). *A. muciniphila* produces SCFAs like acetate and propionate (100). In this study, the serum of vancomycin treated mice showed a comparatively lower concentration of butyrate than propionate and acetate, which could be a result of decreased Firmicutes (specifically intestinimonas) and increased *A.muciniphila* bacteria in the gut post vancomycin treatment.

Following neomycin treatment, a significant increase in the Bacteroides genus of Bacteroidetes phylum caused an increase in IFN- γ and IL-10 genes expression. It was already reported that the

increased abundance of *Bacteroides fragilis* caused alteration in the expression of various immune genes of the gut tissue (375–377). Some selected gram-negative bacteria in the gut stimulated the production of IL-10 cytokine (376). It is commonly known that bacteria from the Firmicutes phylum produce butyrate while the Bacteroidetes phylum produces acetate and propionate from dietary fibers (100). In this study, after neomycin treatment, a significant reduction of Firmicutes and elevation of Bacteroidetes phylum could be related to decreased butyrate with increased acetate and propionate concentration in the serum of mice

Following AVNM treatment, the dramatic increase in the Pathogenic Proteobacteria like *E.coli*, Shigella and a decrease in the Clostridia group of bacteria caused a rise in TNF- α gene expression. However, we didn't find any considerable alteration in the expression of IFN- γ and IL-10 genes. Previous reports showed that Firmicutes, specifically the Clostridium group present in the gut, produced short-chain fatty acids, and these SCFAs suppressed the LPS and pro-inflammatory cytokines (103,104). Some earlier reports showed a considerable increase in the *Escherichia coli* like pathogenic Proteobacteria caused the higher expression of pro-inflammatory cytokine genes in the gut (325,378,379). In the current study, due to a significant reduction in significant phyla like Firmicutes and Bacteroidetes, we found a substantial decrease in all three SCFAs (acetate, propionate, and butyrate) level in the serum of AVNM treated mice compared to control and other antibiotics treated groups.

Bacteria belong to the Intestinimonas genus (Firmicutes phylum), produces butyrate, and Bacteroidetes produce propionate in the gut (101,102). The production of these SCFAs in the gut suppresses the LPS and pro-inflammatory cytokines like TNF- α level. It enhances the release of anti-inflammatory cytokine like IL-10 in the colon (103,104). In the current study, AVNM treatment caused a decrease in the concentrations of all three SCFAs, which can be associated

with higher TNF- α and lower IL-10 levels in the colon of mice. In neomycin and vancomycin-treated mice, a higher level of propionate and acetate caused more anti-inflammatory cytokine-like IL10 compared to AVNM treated mice.

We aimed to study the effects of perturbation of gut microbiota through antibiotics commonly used for various medications in humans. We used the mice model to study the effect of those antibiotics. Though the cocktail of AVNM was an effective antibiotic mixture for maximum perturbation of gut microbiota, it has limited practical usage in the host during pathogen attack. Moreover, previous reports showed that AVNM can act as a positive control to deplete the maximum number of gut microbiota. However, our results showed that the AVNM cocktail did not deplete the gut microbiota completely; it only caused a decrease in healthy microbes and increased Proteobacteria level in the host.

In conclusion, the current study showed different antibiotic-induced alteration patterns of gut microbiota and their association with various cytokines and SCFA levels of the host.

Chapter 3.4: Effect of Cecal microbiota transplantation from younger to older mice following antibiotic-induced gut microbial dysbiosis.

3.4.1 Introduction: Our results, so far, revealed that following the withdrawal of antibiotics, the microbiota that was perturbed started to get restored. Restoration of microbiota to its original status is essential to maintain health. While the current results described in the preceding sections are mainly about the natural restoration, recently another mode of restoration of perturbed gut microbiota is by fecal microbiota transplantation (FMT). FMT is primarily used as one of the most effective ways to treat *Clostridium difficile* (CD) infection. CD-induced infection usually leads to Crohn's and colitis or inflammatory bowel disease (IBD). However, the efficiency of FMT for the restoration of perturbed gut microbiota following treatment with antibiotics or by other means is not well studied. Moreover, except for antibiotic treatment, gut microbiota diversity and composition also vary significantly with the host's aging. FMT is commonly used to treat *C. difficile* infection where antibiotics are ineffective (239,380). It was observed that after FMT treatment, the gut microbial composition of the recipient became similar to the gut microbial composition of the donor. An earlier report showed that after eating the poop of younger killifish by older killifish, the survival rate of older killifish increases by 41% than expected lifespan (381).

Our objective was to study the effect of cecal microbiota transplantation (CMT) from younger to older mice. We used CMT over FMT because cecal microbial content is an accurate representation of the gut microbiota, while the fecal matter is a minor and partial representation of gut microbiota. In humans, for ethical and practical reasons, FMT is used despite its limitations. In the current study, older BALB/c mice (23 weeks) received CMT from younger

BALB/c mice (3 weeks) following a cocktail of antibiotics (AVNM) treatment. Recipient mice were treated with AVNM to make them compatible to receive and accept the transplanted cecal matter from the younger mice. We compared the restoration efficiency of gut microbiota and selected host physiology (immune and metabolic response) of mice by treating either with CMT or without CMT following antibiotic treatment.

3.4.2 Results:

The composition and diversity of gut microbiota regulate the survivability of the host during pathogen attack by modulating the host's immune system. In this study, we checked the survivability following *Salmonella* challenge in mice a) with normal microbiota, b) with perturbed gut microbiota, c) with CMT, and d) without CMT procedure.

Survivability rate of mice at different doses of *Salmonella* challenge:

Salmonella enterica serovar Typhimurium (ST) is a potential Gram-negative pathogen which causes different systemic and gastrointestinal infection in mice. In this study, we standardized the effective ST dose for both BALB/c and C57BL/6 mice. Several earlier reports showed that three doses of ST mainly caused potential infection in mice, i.e. 10^7 CFU/ml, 10^8 CFU/ml, and 10^9 CFU/ml, per mice (382–384). Hence, in the current study, we selected these three doses of ST to challenge both strains of mice and kept them under observation for 15 days post- ST challenge to detect mice's mortality and survivability rate.

Among three different doses of ST, it was found that at the dose of 10^9 CFU/ml, all mice died within 8 days of *Salmonella* challenge in both BALB/c and C57BL/6 mice strains (Fig. 3.4.1A and 3.4.1B.). Whereas 10^7 doses did not cause any changes in the survivability rate of mice

compared to unchallenged control mice. 10^7 dose was too low to cause any difference while 10^9 dose was lethal

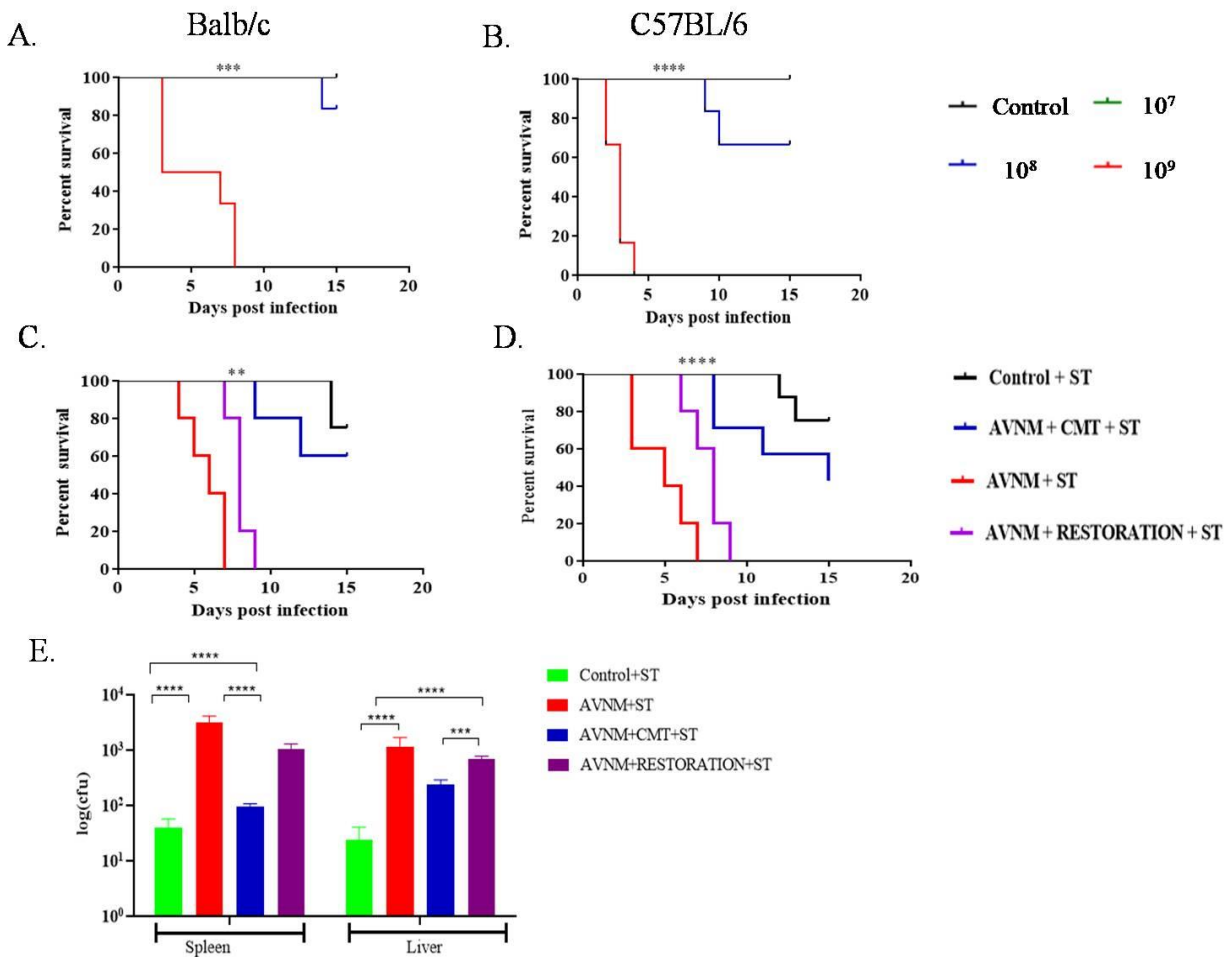


Figure3.4.1: The survivability rate of mice at different ST doses. Mice were challenged with Salmonella at 10^7 , 10^8 , 10^9 CFU/ mouse to select a suitable Salmonella dose. A. BALB/c, B. C57BL/6. Selected Salmonella dose at 10^8 CFU/mouse was challenged to control, AVNM treated, CMT or without CMT restored mice, C. BALB/c, D. C57BL/6. E. Salmonella CFU count in the spleen and liver of BALB/c mice at different conditions (control, AVNM treated, CMT treated, RESTORATION treated).

AVNM treated with CMT, and AVNM treated without CMT group) post-ST challenge. two-way ANOVA calculated statistical significance. ("****" corresponds to $P \leq 0.0001$, "****" corresponds to $P \leq 0.001$, "***" corresponds to $P \leq 0.01$ level of significance). Error bars are one standard deviation of the mean value and determined from the average values of seven biological replicates.

For mice showing 100% mortality. At 10^8 CFU/ml of ST, nearly 16% and 33% of mortality were observed in BALB/c and C57BL/6 mice, respectively, within 15 days following the challenge. Hence, 10^8 CFU/ml of ST dose was selected for further studies.

The selected dose (10^8 CFU/ml) of ST was challenged further to various groups of mice to see their survival rate. The response of mice to Salmonella challenge was studied following the alteration of gut microbiota through antibiotics perturbation and restoration (CMT and without CMT restoration).

Cecal microbiota transplantation rescues mice from Salmonella infection:

Susceptibility of the host towards different pathogens was dependent on the composition of gut microbiota (76,385). Gut microbiota regulates the colonization of Salmonella inside the host. The intestinal infection in mice through Salmonellawas not effective unless the gut microbiota is disturbed. The intact layer of commensal gut microbes gave protection against the colonization of Salmonella inside the host (384). Therefore, in this study, we wanted to see the effects of the Salmonella challenge after disrupting the intestinal microbiota through AVNM treatment and again colonizing the intestine with beneficial microbes through the CMT procedure.

The selected 10^8 CFU/ml dose of ST was challenged to all four groups, a) control,b) AVNM treated, c) AVNM+CMT, and d) AVNM-CMTof mice in both BALB/c and C57BL/6 strains

(Fig. 3.4.1C. and 3.4.1D.). Among the four groups of mice, control mice showed the lowest mortality, and the AVNM treated group of mice showed the highest mortality rate (100%) in both strains. After antibiotic treatment, when mice were challenged with ST, all mice died within 7 days. However, CMT followed by AVNM treatment lowered the mortality rate (33%) compared to without CMT restoration (66%) in BALB/c mice. This showed CMT restoration could protect the mice efficiently from salmonella infection compared to normal restoration following AVNM treatment (Fig. 3.4.1C and 3.4.1D). However, in the BALB/c mice, CMT treatment provided more effective protection against Salmonella challenge than C57BL/6 mice. The survival percentage of BALB/c mice was nearly 60%, whereas only 40% for C57BL/6 mice during 15 days of observation period following the ST challenge in CMTricipient mice. Because of the significantly higher survivability of BALB/c mice compared to the very low survivability of C57BL/6 mice irrespective of the ST dosage, we continued our further studies with BALB/c mice to understand the effects and roles of CMT.

It is known that ST colonizes mainly in the spleen and liver. We plated the spleen and liver of Salmonella challenged BALB/c mice of each group on Bismuth sulfite agar to see the colony-forming unit (Fig. 3.4.1E.). Results revealed that after AVNM treatment, higher numbers of colony-forming units of Salmonella were found on the plate whereas CMT treatment caused a significant decrease in the CFU count of ST (Fig. 3.4.1E.). Non-CMT (AVNM-CMT) group had a higher CFU of ST in both the liver and spleen of mice than CMT restoration.

As CMT gave better protection to mice during the Salmonella challenge, we wanted to check the constitution of gut microbiota following treatment with CMT. We compared the composition and restoration of gut microbiota in mice with and without CMT to establish the efficacy of CMT in the restoration process.

Cecal microbiota transplantation caused the effective restoration of gut microbial abundance and composition.

Transplantation of a healthy group of microbes to the intestine of mice caused significant improvement in the restoration process of gut microbiota following antibiotic treatment (236)

Metagenomic data of cecal samples showed that the untreated control group of young mice (3 weeks) mainly contained Firmicutes (60%) and Bacteroidetes (33%) with a meager amount of Proteobacteria (2%) (Fig. 3.4.2A).

Untreated older mice (23 weeks) showed higher Firmicutes (77%) and lowered Bacteroidetes (19%) compared to the control of older mice (Fig. 3.4.2B). When older mice treated with AVNM, Firmicutes and Bacteroidetes level decreased while Proteobacteria level increased significantly (90%) (Fig. 3.4.2C.).

CMT restored mice followed by AVNM treatment (Fig. 3.4.2D) caused more efficient recovery of gut microbiota than without or non-CMT (Fig. 3.4.2E) restored mice. Cecal microbiota composition of donor mice, i.e., young mice (Fig. 3.4.2A) and recipient CMT mice (Fig. 3.4.2D), showed a significant similarity successful transplantation of gut microbiota of donor mice in recipient mice.

Gut microbiota of Non-CMT restored mice (Fig. 3.4.2E.) still contained higher proteobacteria (15%) and fewer Firmicutes compared to its respective control group of mice (Fig. 3.4.2B.). However, CMT restoration following AVNM treatment caused a significant decrease in Proteobacteria and increased Firmicutes and Bacteroidetes.

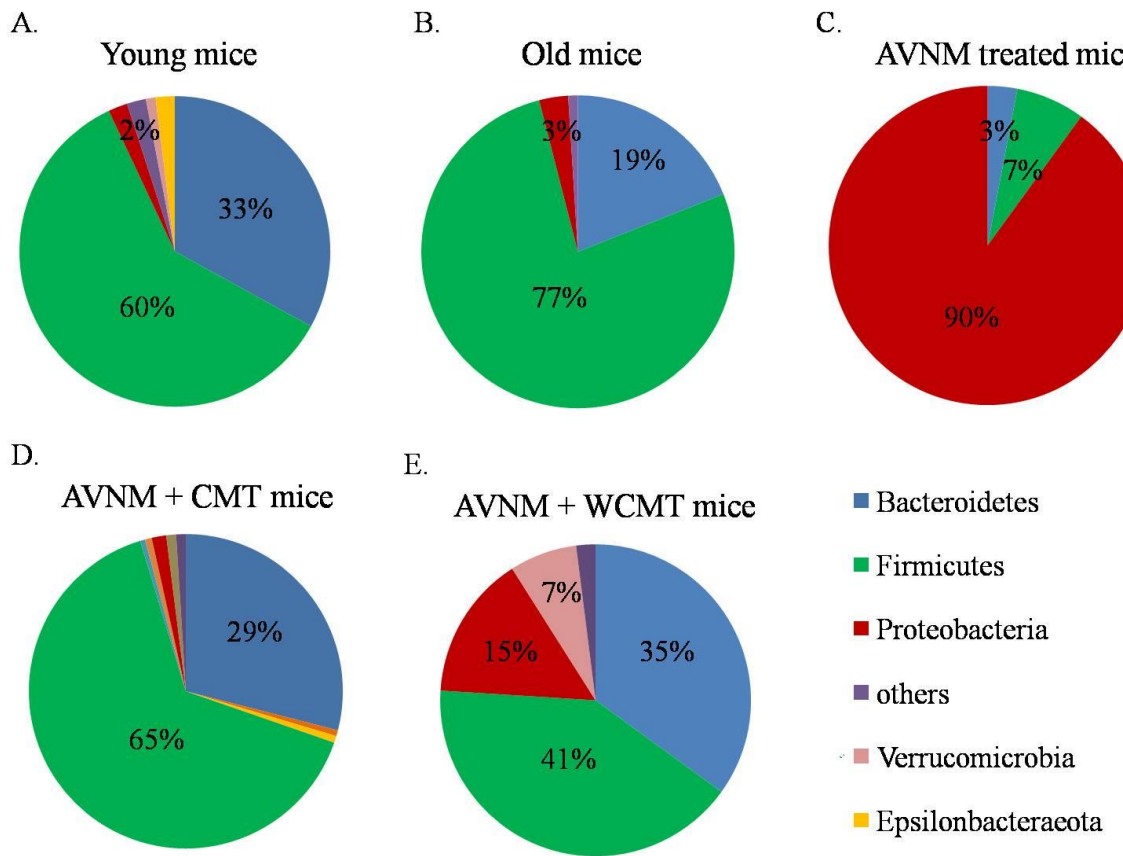


Figure3.4.2:Pie chart showing gut microbial composition at the phylum level, A. Young mice, B. Old mice, C. AVNM treated mice, restoration following AVNM treatment D. with CMT E. without CMT.

AVNM and CMT treatment caused alteration of the gut microbial diversity and cecal index of mice.

Treatment with antibiotics caused a significant alteration in the diversity of gut microbiota (344,386). We calculated the alpha diversity of gut microbiota using the Shannon methodology. Shannon diversity index showed that AVNM treatment caused a significant reduction in gut

microbial diversity than the control group of mice. CMT recipient group of mice following AVNM treatment (AVNM+CMT) showed a similar diversity index with its donor group of young control mice. Both CMT and without CMT restoration caused an increase in gut microbial diversity following AVNM treatment (Fig. 3.4.3A.).

Alteration in the cecal index (cecum weight/body weight) of the mice showed the altered abundance of bacteria present inside the cecum (317). Cecal size of mice increased significantly post AVNM treatment compared to the control group of mice (Fig. 3.4.3B.). The cecal index was highest for the AVNM treated group of mice compared to other groups. However, CMT restored mice (AVNM+CMT) showed more successful restoration of cecal size and significantly lowered the cecal index compared to without CMT (AVNM+WCMT) restored mice (Fig. 3.4.3C.).

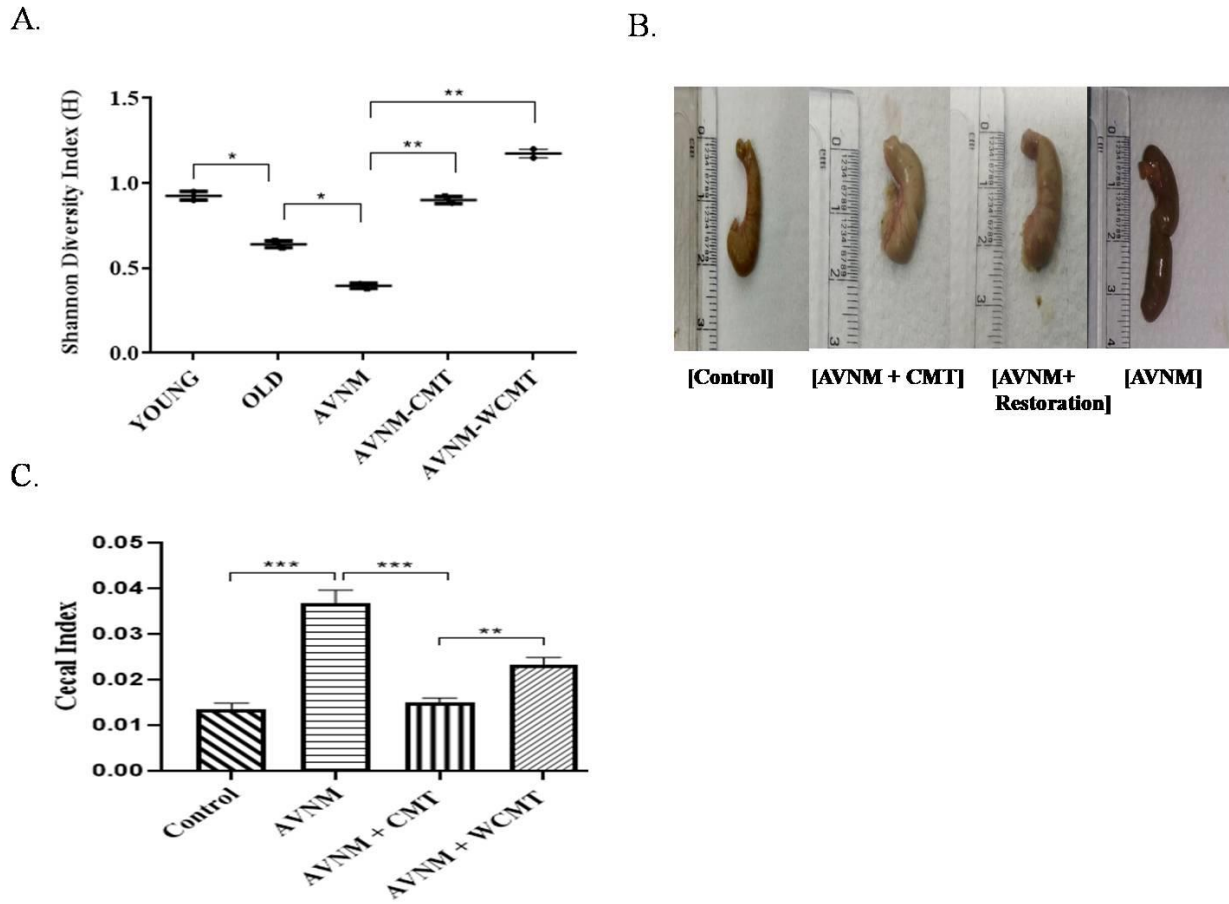


Figure 3.4.3: Gut microbial diversity and cecal index of mice at different conditions like young, old, AVNM treatment, CMT, or without CMT restoration. A. Shannon diversity index of gut microbiota at phylum level B. raw image representation of mice cecum C. Cecal index of mice.

Two-way ANOVA calculated statistical significance. ("***" corresponds to $P \leq 0.001$, "**" corresponds to $P \leq 0.01$, "*" corresponds to $P \leq 0.05$ level of significance). Error bars are one standard deviation of the mean value and determined from the average values of three biological replicates.

The inflammatory and tight junction gene expression altered in the colon post AVNM treatment and CMT restoration.

The host's immune response depends on the composition and diversity of the gut microbiota (39). The alteration of the gut microbiota through antibiotics or other perturbing agents caused considerable modulation in the immune response of the mice. In this study, as the composition of gut microbiota varied at different conditions, we wanted to check the effect of this altered gut microbiota on the expression of various pro-and anti-inflammatory genes. We checked the mRNA level expression of the TNF- α gene in the colon of both antibiotic-treated (AVNM) and restored (CMT and without CMT) groups of mice (Fig. 3.4.4A.). Results revealed that, after AVNM treatment, expression of the TNF- α gene increased significantly. However, CMT restoration caused a significant decrease in TNF- α level in the colon of mice following AVNM treatment. CMT restored group of mice showed a more successful reduction in the TNF- α level than the without CMT revived group of mice (Fig. 3.4.4A.). Expression of IL-10 and TGF- β gene decreased during AVNM treatment; however, CMT restoration following AVNM treatment caused a significant increase in the expression of both the anti-inflammatory genes (Figs. 3.4.4B. &3.4.4C.)

Expression of tight junction genes data showed that AVNM treatment caused a significant decrease in the expression of both Claudin-1 and Occludin genes in the colon of mice (Figs. 3.4.4D. &3.4.4E.). CMT restoration caused a considerable increase in the expression of Claudin-1 and Occludin genes in the colon of mice. CMT restored group of mice showed a more successful elevation of both tight junction protein genes than the without CMT restored group of mice (Figs. 3.4.4D. &3.4.4E.).

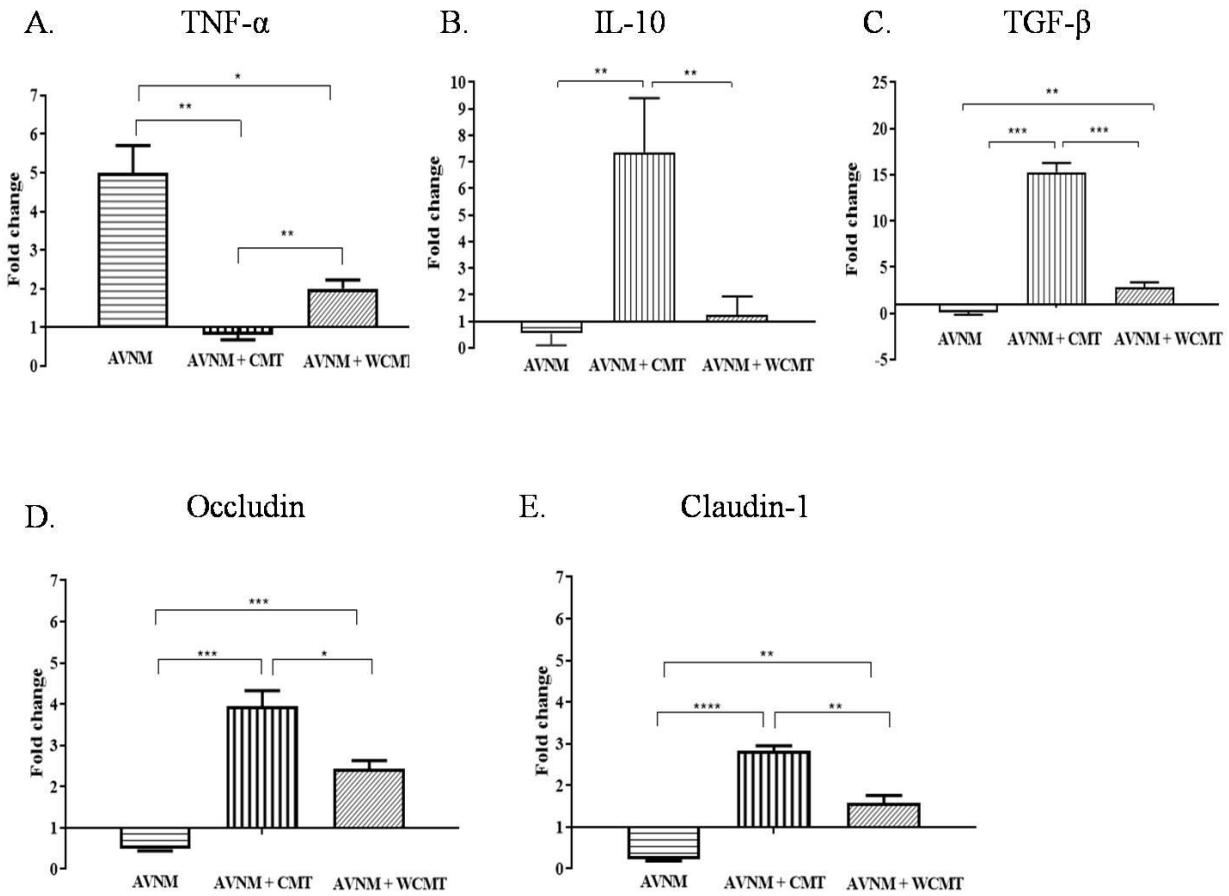


Figure 3.4.4: Expression of immune and tight junction protein genes in the colon of mice following antibiotic treatment and restoration period. Expression of A. TNF- α , B. IL-10, C. TGF- β , D. Occludin, and E. Claudin-1 genes at mRNA level in the colon of mice at various conditions AVNM treatment, with or without CMT restoration following antibiotic treatment.

Two-way ANOVA calculated statistical significance. ("****" corresponds to $P \leq 0.0001$, "****" corresponds to $P \leq 0.001$, "***" corresponds to $P \leq 0.01$, "**" corresponds to $P \leq 0.05$ level of significance). Error bars are one standard deviation of the mean value and determined from the average values of three biological replicates.

Metabolite level of serum altered following antibiotic treatment and CMT restoration.

Microbes resident in the gut could regulate the metabolite levels of the host. Antibiotics-induced disruption of gut microbiota altered the metabolic profile of the host (386,387). NMR-based metabolomics data of serum revealed that AVNM treatment mainly affected the aromatic amino acids pathway. We have measured the concentration of three aromatic amino acids (AAA), such as phenylalanine, tyrosine, and tryptophan. We found that AVNM treatment caused a significant increase in the above three aromatic amino acids in the serum. CMT restored and untreated control mice showed a reduced level of AAA in the serum.

Carbohydrate metabolism (glucose, starch, and sucrose) pathways were differentially affected in the AVNM treated and CMT restored mice. AVNM treated group of mice showed increased glucose and glucose- 6 phosphates with decreased glucose -1 phosphate level in the serum. While control and CMT were restored, the group showed higher level glucose-1 phosphate with comparatively lower glucose and glucose-6 phosphate level in the serum.

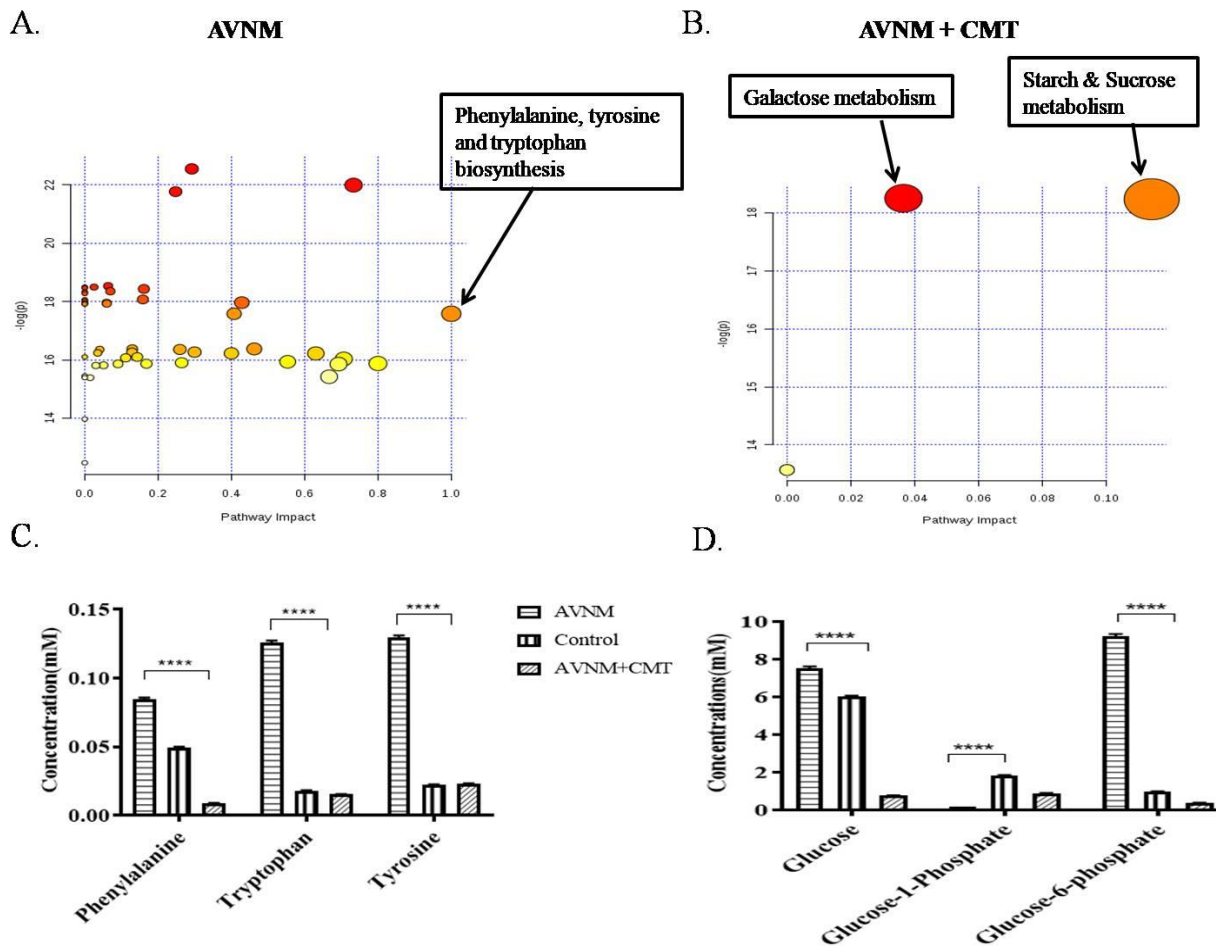


Figure3.4.5: Pathway analysis of different metabolites following antibiotic treatment and restoration period.Impacted pathways of various metabolites of mice at other conditions A. AVNM treatment B. CMT restoration following AVNM treatment.

Measurement of various aromatic amino acids and carbohydrates in the serum of control, AVNM treated and CMT restored mice, C.concentration of Phenylalanine, Tryptophan, Tyrosine, and D. Glucose, Glucose-1-Phosphate, and Glucose-6-phosphate.

Two-way ANOVA calculated statistical significance of panel C and D, where "****" corresponds to $P \leq 0.0001$ level of significance. Error bars are one standard deviation of the mean value and determined from the average values of three biological replicates.

3.4.3 Discussion:

AVNM treatment caused dysbiosis of gut microbes by decreasing major phyla like Firmicutes and Bacteroidetes while increasing pathogenic Proteobacteria. The genus-level data showed that mostly the E.coli and Shigella group of bacteria increased after AVNM treatment. It was well known that balanced gut microbes can protect the host from pathogens (2,76). In this study, the dysbiosis of gut microbiota increased the susceptibility of mice towards pathogens like Salmonella. Therefore the mortality rate was highest in the AVNM treated group of mice post salmonella challenge. However, CMT caused the more efficient restoration of gut microbiota compared to the non-CMT restoration group, which made CMT recipient mice more efficient survivors after the Salmonella challenge compared to other groups.

Several reports showed a higher level of pathogenic Proteobacteria caused increased inflammatory cytokines like TNF- α and decreased tight junction protein levels in the colon of mice genes (126,325,378,379). Firmicutes caused a decrease in the expression of inflammatory cytokines (103,104). The higher level of pathogenic Proteobacteria following AVNM treatment could be associated with the increased expression of pro-inflammatory cytokine genes like TNF- α and decreased expression of anti-inflammatory cytokine genes like IL-10, TGF- β , and tight junction genes like Claudin and Occludin. CMT restoration caused a significant reduction in the Proteobacteria level in the gut, resulting in lower expression of TNF- α and higher expression of

anti-inflammatory and tight junction genes of the colon. Though the restoration of gut microbiota also happened in the non-CMT group of mice, these mice still had higher Proteobacteria and lower Firmicutes level than the CMT restored group. Therefore, CMT restored mice were more efficient for alleviating the TNF- α gene expression and elevating the expression of tight junction protein genes in the colon compared to non-CMT group of mice.

It was reported that various microbes present inside the gut could efficiently metabolize multiple amino acids (102). However, in the current study, gut microbial dysbiosis following AVNM treatment caused the accumulation of AAA in the serum, resulting from the lower metabolism rate of these AAA. But, CMT restoration made the metabolites level nearly similar to control mice which showed successful restoration of gut microbiota through CMT.

Overall, the cecal microbiota transplantation caused the most effective restoration of gut microbiota following the antibiotic treatment in older mice, which gave various health-related beneficial effects to the mice like providing protection against Salmonella infection, decreasing the expression of pro-inflammatory genes, and increasing the expression of tight junction protein genes in the gut.

Chapter: 5

References

1. Guinane CM, Cotter PD. Role of the gut microbiota in health and chronic gastrointestinal disease: understanding a hidden metabolic organ. *Therap Adv Gastroenterol*. 2013;6(4):295–308.
2. Thursby E, Juge N. Introduction to the human gut microbiota. *Biochem J* [Internet]. 2017;474(11):1823–36. Available from: <http://www.ncbi.nlm.nih.gov/pubmed/28512250>
3. Kavvadia M, Santis GLD, Cascapera S, Lorenzo AD. Psychobiotics as integrative therapy for neuropsychiatric disorders with special emphasis on the microbiota-gut-brain axis. *Biomed Prev*. 2017;2(8).
4. Ray P, Pandey U, Aich P. Comparative analysis of beneficial effects of Vancomycin treatment on Th1-and Th2-biased mice and role of gut microbiota. *bioRxiv*. 2020;516898.
5. Hillman ET, Lu H, Yao T, Nakatsu CH. Microbial ecology along the gastrointestinal tract. *Microbes Environ*. 2017;ME17017.
6. Canny GO, McCormick BA. Bacteria in the intestine, helpful residents or enemies from within? *Infect Immun*. 2008;76(8):3360–73.
7. Anwar H, Irfan S, Hussain G, Faisal MN, Muzaffar H, Mustafa I, et al. Gut Microbiome: A New Organ System in Body. *Parasitol Microbiol Res*. 2019;10.
8. Golonka RM, Abokor AA, Ntambi JM, Vijay-Kumar M. Gut microbiota interaction in host lipid metabolism. In: *Lipid Signaling and Metabolism*. Elsevier; 2020. p. 321–43.
9. Wang B, Yao M, Lv L, Ling Z, Li L. The human microbiota in health and disease. *Engineering*. 2017;3(1):71–82.

10. Frank DN, Amand ALS, Feldman RA, Boedeker EC, Harpaz N, Pace NR. Molecular-phylogenetic characterization of microbial community imbalances in human inflammatory bowel diseases. *Proc Natl Acad Sci.* 2007;104(34):13780–5.
11. Jandhyala SM, Talukdar R, Subramanyam C, Vuyyuru H, Sasikala M, Reddy DN. Role of the normal gut microbiota. *World J Gastroenterol WJG.* 2015;21(29):8787.
12. Micah H, Claire F-L, Rob K. The human microbiome project: exploring the microbial part of ourselves in a changing world. *Nature.* 2007;449(7164):804–10.
13. Bilen M, Dufour J-C, Lagier J-C, Cadoret F, Daoud Z, Dubourg G, et al. The contribution of culturomics to the repertoire of isolated human bacterial and archaeal species. *Microbiome.* 2018;6(1):1–11.
14. Hugon P, Dufour J-C, Colson P, Fournier P-E, Sallah K, Raoult D. A comprehensive repertoire of prokaryotic species identified in human beings. *Lancet Infect Dis.* 2015;15(10):1211–9.
15. King CH, Desai H, Sylvetsky AC, LoTempio J, Ayanyan S, Carrie J, et al. Baseline human gut microbiota profile in healthy people and standard reporting template. *PLoS One.* 2019;14(9):e0206484.
16. Malla MA, Dubey A, Kumar A, Yadav S, Hashem A, Abd_Allah EF. Exploring the human microbiome: The potential future role of next-generation sequencing in disease diagnosis and treatment. *Front Immunol.* 2019;9:2868.
17. Fricker AM, Podlesny D, Fricke WF. What is new and relevant for sequencing-based microbiome research? A mini-review. *J Adv Res.* 2019;19:105–12.

18. Goodfellow M, Sutcliffe I, Chun J. New approaches to prokaryotic systematics. Academic Press; 2014.
19. Kho ZY, Lal SK. The human gut microbiome—a potential controller of wellness and disease. *Front Microbiol*. 2018;9:1835.
20. Wakita Y, Shimomura Y, Kitada Y, Yamamoto H, Ohashi Y, Matsumoto M. Taxonomic classification for microbiome analysis, which correlates well with the metabolite milieu of the gut. *BMC Microbiol*. 2018;18(1):188.
21. Rinninella E, Raoul P, Cintoni M, Franceschi F, Miggiano GAD, Gasbarrini A, et al. What is the healthy gut microbiota composition? A changing ecosystem across age, environment, diet, and diseases. *Microorganisms*. 2019;7(1):14.
22. Hossain MI, Islam R, Mimi SI, Jewel ZA, Haider UA. Gut Microbiota Gut Microbiota: Succinct Overview of Impacts on Human Physique and Current Research Status with Future Aspects. *Int J Adv Life Sci Res*. 2020;3(2):1–10.
23. Stephen AM, Cummings JH. The microbial contribution to human faecal mass. *J Med Microbiol*. 1980;13(1):45–56.
24. Lozupone CA, Stombaugh JI, Gordon JI, Jansson JK, Knight R. Diversity, stability and resilience of the human gut microbiota. *Nature*. 2012;489(7415):220–30.
25. Nguyen TLA, Vieira-Silva S, Liston A, Raes J. How informative is the mouse for human gut microbiota research? *Dis Model Mech*. 2015;8(1):1–16.
26. Hugenholtz F, de Vos WM. Mouse models for human intestinal microbiota research: a critical evaluation. *Cell Mol Life Sci*. 2018;75(1):149–60.

27. Turner P V. The role of the gut microbiota on animal model reproducibility. *Anim Model Exp Med.* 2018;1(2):109–15.
28. Franklin CL, Ericsson AC. Microbiota and reproducibility of rodent models. *Lab Anim (NY).* 2017;46(4):114.
29. Gurung M, Li Z, You H, Rodrigues R, Jump DB, Morgun A, et al. Role of gut microbiota in type 2 diabetes pathophysiology. *EBioMedicine.* 2020;51:102590.
30. Hörmannsperger G, Schaubeck M, Haller D. Intestinal microbiota in animal models of inflammatory diseases. *ILAR J.* 2015;56(2):179–91.
31. Casteleyn C, Rekecki A, Van der Aa A, Simoens P, Van den Broeck W. Surface area assessment of the murine intestinal tract as a prerequisite for oral dose translation from mouse to man. *Lab Anim.* 2010;44(3):176–83.
32. Treuting PM, Arends MJ, Dintzis SM. Lower gastrointestinal tract. In: Comparative Anatomy and Histology. Elsevier; 2018. p. 213–28.
33. Pei Z, Bini EJ, Yang L, Zhou M, Francois F, Blaser MJ. Bacterial biota in the human distal esophagus. *Proc Natl Acad Sci.* 2004;101(12):4250–5.
34. Justesen T, Nielsen OH, Jacobsen IE, Lave J, Rasmussen SN. The normal cultivable microflora in upper jejunal fluid in healthy adults. *Scand J Gastroenterol.* 1984;19(2):279–82.
35. Andersson AF, Lindberg M, Jakobsson H, Bäckhed F, P. I. Nyrén, and L. Engstrand. 2008. Comparative analysis of human gut microbiota by barcoded pyrosequencing. *PLoS One.* 3:e2836.

36. Blaser MJ. Hypothesis: the changing relationships of Helicobacter pylori and humans: implications for health and disease. *J Infect Dis.* 1999;179(6):1523–30.
37. Swidsinski A, Loening-Baucke V, Lochs H, Hale LP. Spatial organization of bacterial flora in normal and inflamed intestine: a fluorescence in situ hybridization study in mice. *World J Gastroenterol WJG.* 2005;11(8):1131.
38. Wahlgren M, Axenstrand M, Håkansson Å, Marefati A, Lomstein Pedersen B. In vitro methods to study colon release: State of the art and an outlook on new strategies for better in-vitro biorelevant release media. *Pharmaceutics.* 2019;11(2):95.
39. Cahill F, Ji Y, Wadden D, Amini P, Randell E, Vasdev S, et al. The gut microbiota shapes intestinal immune responses during health and disease. *Front Microbiol [Internet].* 2016 May;7(1):333–6. Available from: <https://www.ncbi.nlm.nih.gov/pubmed/18178854>
40. Sun L, Jia H, Li J, Yu M, Yang Y, Tian D, et al. Cecal Gut Microbiota and Metabolites Might Contribute to the Severity of Acute Myocardial Ischemia by Impacting the Intestinal Permeability, Oxidative Stress and Energy Metabolism. *Front Microbiol.* 2019;10:1745.
41. Galperin MY. Genome diversity of spore-forming Firmicutes. *Microbiol Spectr.* 2013;1(2):TBS-0015.
42. Kim S, Covington A, Pamer EG. The intestinal microbiota: antibiotics, colonization resistance, and enteric pathogens. *Immunol Rev.* 2017;279(1):90–105.
43. Medvecky M, Cejkova D, Polansky O, Karasova D, Kubasova T, Cizek A, et al. Whole genome sequencing and function prediction of 133 gut anaerobes isolated from chicken

caecum in pure cultures. *BMC Genomics*. 2018;19(1):561.

44. Gibiino G, Lopetuso LR, Scaldaferri F, Rizzatti G, Binda C, Gasbarrini A. Exploring Bacteroidetes: metabolic key points and immunological tricks of our gut commensals. *Dig Liver Dis*. 2018;50(7):635–9.
45. Flint HJ, Duncan SH. Bacteroides and prevotella. 2014;
46. Gupta RS. The phylogeny of proteobacteria: relationships to other eubacterial phyla and eukaryotes. *FEMS Microbiol Rev*. 2000;24(4):367–402.
47. Rizzatti G, Lopetuso LR, Gibiino G, Binda C, Gasbarrini A. Proteobacteria: a common factor in human diseases. *Biomed Res Int*. 2017;2017.
48. Shin N-R, Whon TW, Bae J-W. Proteobacteria: microbial signature of dysbiosis in gut microbiota. *Trends Biotechnol*. 2015;33(9):496–503.
49. Schlesner H, Jenkins C, Staley JT. The phylum Verrucomicrobia: a phylogenetically heterogeneous bacterial group. *Prokaryotes*. 2006;7:881–96.
50. Dubourg G, Lagier J-C, Armougom F, Robert C, Audoly G, Papazian L, et al. High-level colonisation of the human gut by Verrucomicrobia following broad-spectrum antibiotic treatment. *Int J Antimicrob Agents*. 2013;41(2):149–55.
51. Lee K-C, Webb RI, Janssen PH, Sangwan P, Romeo T, Staley JT, et al. Phylum Verrucomicrobia representatives share a compartmentalized cell plan with members of bacterial phylum Planctomycetes. *BMC Microbiol*. 2009;9(1):5.
52. Binda C, Lopetuso LR, Rizzatti G, Gibiino G, Cennamo V, Gasbarrini A. Actinobacteria:

a relevant minority for the maintenance of gut homeostasis. *Dig Liver Dis.* 2018;50(5):421–8.

53. Anandan R, Dharumadurai D, Manogaran GP. An introduction to actinobacteria. In: *Actinobacteria-Basics and Biotechnological Applications*. Intechopen; 2016.
54. Walker RW, Clemente JC, Peter I, Loos RJF. The prenatal gut microbiome: are we colonized with bacteria in utero? *Pediatr Obes.* 2017;12:3–17.
55. Nuriel-Ohayon M, Neuman H, Koren O. Microbial changes during pregnancy, birth, and infancy. *Front Microbiol.* 2016;7:1031.
56. Dominguez-Bello MG, Costello EK, Contreras M, Magris M, Hidalgo G, Fierer N, et al. Delivery mode shapes the acquisition and structure of the initial microbiota across multiple body habitats in newborns. *Proc Natl Acad Sci.* 2010;107(26):11971–5.
57. Mueller NT, Bakacs E, Combellick J, Grigoryan Z, Dominguez-Bello MG. The infant microbiome development: mom matters. *Trends Mol Med.* 2015;21(2):109–17.
58. Neu J, Rushing J. Cesarean versus vaginal delivery: long-term infant outcomes and the hygiene hypothesis. *Clin Perinatol.* 2011;38(2):321–31.
59. Rutayisire E, Huang K, Liu Y, Tao F. The mode of delivery affects the diversity and colonization pattern of the gut microbiota during the first year of infants' life: a systematic review. *BMC Gastroenterol.* 2016;16(1):86.
60. Stewart CJ, Ajami NJ, O'Brien JL, Hutchinson DS, Smith DP, Wong MC, et al. Temporal development of the gut microbiome in early childhood from the TEDDY study. *Nature.* 2018;562(7728):583–8.

61. Hill CJ, Lynch DB, Murphy K, Ulaszewska M, Jeffery IB, O'Shea CA, et al. Evolution of gut microbiota composition from birth to 24 weeks in the INFANTMET Cohort. *Microbiome*. 2017;5(1):4.
62. Odamaki T, Kato K, Sugahara H, Hashikura N, Takahashi S, Xiao J, et al. Age-related changes in gut microbiota composition from newborn to centenarian: a cross-sectional study. *BMC Microbiol*. 2016;16(1):1–12.
63. Mohammadkhah AI, Simpson EB, Patterson SG, Ferguson JF. Development of the gut microbiome in children, and lifetime implications for obesity and cardiometabolic disease. *Children*. 2018;5(12):160.
64. Nagpal R, Mainali R, Ahmadi S, Wang S, Singh R, Kavanagh K, et al. Gut microbiome and aging: Physiological and mechanistic insights. *Nutr Heal aging*. 2018;4(4):267–85.
65. Novakovic M, Rout A, Kingsley T, Kirchoff R, Singh A, Verma V, et al. Role of gut microbiota in cardiovascular diseases. *World J Cardiol*. 2020;12(4):110.
66. Horwitz DA, Fahmy TM, Piccirillo CA, La Cava A. Rebalancing immune homeostasis to treat autoimmune diseases. *Trends Immunol*. 2019;40(10):888–908.
67. Tourneur E, Chassin C. Neonatal immune adaptation of the gut and its role during infections. *Clin Dev Immunol*. 2013;2013.
68. Marcabal A, Sonnenburg JL. Human milk oligosaccharide consumption by intestinal microbiota. *Clin Microbiol Infect*. 2012;18:12–5.
69. Marcabal A, Barboza M, Froehlich JW, Block DE, German JB, Lebrilla CB, et al. Consumption of human milk oligosaccharides by gut-related microbes. *J Agric Food*

- Chem. 2010;58(9):5334–40.
70. Belkaid Y, Hand TW. Role of the microbiota in immunity and inflammation. *Cell*. 2014;157(1):121–41.
71. Quintana-Hayashi MP, Padra M, Padra JT, Benktander J, Lindén SK. Mucus-pathogen interactions in the gastrointestinal tract of farmed animals. *Microorganisms*. 2018;6(2):55.
72. Kasarelo K, Sajdel-Sulkowska EM. Developmental significance of early gut-associated lymphoid tissue (GALT)-microbiota interactions in health and disease: creating balance between tolerance and inflammation in children. *Open J Pediatr Child Heal*. 2019;4(1):40–6.
73. Sommer F, Bäckhed F. The gut microbiota—masters of host development and physiology. *Nat Rev Microbiol*. 2013;11(4):227–38.
74. Weng M, Walker WA. The role of gut microbiota in programming the immune phenotype. *J Dev Orig Health Dis*. 2013;4(3):203–14.
75. Wu H-J, Wu E. The role of gut microbiota in immune homeostasis and autoimmunity. *Gut Microbes*. 2012;3(1):4–14.
76. Pickard JM, Zeng MY, Caruso R, Núñez G. Gut microbiota: Role in pathogen colonization, immune responses, and inflammatory disease. *Immunol Rev*. 2017;279(1):70–89.
77. Kamada N, Seo S-U, Chen GY, Núñez G. Role of the gut microbiota in immunity and inflammatory disease. *Nat Rev Immunol*. 2013;13(5):321–35.

78. Round JL, Mazmanian SK. The gut microbiota shapes intestinal immune responses during health and disease. *Nat Rev Immunol*. 2009;9(5):313.
79. Ferreira CM, Vieira AT, Vinolo MAR, Oliveira FA, Curi R, Martins F dos S. The central role of the gut microbiota in chronic inflammatory diseases. *J Immunol Res*. 2014;2014.
80. Kamada N, Núñez G. Regulation of the immune system by the resident intestinal bacteria. *Gastroenterology*. 2014;146(6):1477–88.
81. Ohkubo T, Tsuda M, Suzuki S, El Borai N, Yamamura M. Peripheral Blood Neutrophils of Germ-Free Rats Modified by In Vivo Granulocyte–Colony-Stimulating Factor and Exposure to Natural Environment. *Scand J Immunol*. 1999;49(1):73–7.
82. Forestier Catherine Sandre, Françoise AG. Influence of microbial flora on macrophages. *Microb Ecol Health Dis*. 2000;12(2):128–37.
83. Wolf AJ, Underhill DM. Peptidoglycan recognition by the innate immune system. *Nat Rev Immunol*. 2018;18(4):243.
84. Schwarzer M, Hermanova P, Srutkova D, Golias J, Hudcovic T, Zwicker C, et al. Germ-free mice exhibit mast cells with impaired functionality and gut homing and do not develop food allergy. *Front Immunol*. 2019;10:205.
85. Kunii J, Takahashi K, Kasakura K, Tsuda M, Nakano K, Hosono A, et al. Commensal bacteria promote migration of mast cells into the intestine. *Immunobiology*. 2011;216(6):692–7.
86. Karmarkar D, Rock KL. Microbiota signalling through MyD88 is necessary for a systemic neutrophilic inflammatory response. *Immunology*. 2013;140(4):483–92.

87. Takiishi T, Fenero CIM, Câmara NOS. Intestinal barrier and gut microbiota: shaping our immune responses throughout life. *Tissue Barriers*. 2017;5(4):e1373208.
88. Caballero S, Pamer EG. Microbiota-mediated inflammation and antimicrobial defense in the intestine. *Annu Rev Immunol*. 2015;33:227–56.
89. Van Wijk F, Cheroutre H. Mucosal T cells in gut homeostasis and inflammation. *Expert Rev Clin Immunol*. 2010;6(4):559–66.
90. Chaplin DD. Overview of the immune response. *J Allergy Clin Immunol*. 2010;125(2):S3–23.
91. Troy EB, Kasper DL. Beneficial effects of *Bacteroides fragilis* polysaccharides on the immune system. *Front Biosci a J virtual Libr*. 2010;15:25.
92. Faith JJ, Ahern PP, Ridaura VK, Cheng J, Gordon JI. Identifying gut microbe–host phenotype relationships using combinatorial communities in gnotobiotic mice. *Sci Transl Med*. 2014;6(220):220ra11-220ra11.
93. Geuking MB, Cahenzli J, Lawson MAE, Ng DCK, Slack E, Hapfelmeier S, et al. Intestinal bacterial colonization induces mutualistic regulatory T cell responses. *Immunity*. 2011;34(5):794–806.
94. Atarashi K, Tanoue T, Shima T, Imaoka A, Kuwahara T, Momose Y, et al. Induction of colonic regulatory T cells by indigenous Clostridium species. *Science* (80-). 2011;331(6015):337–41.
95. Franchi L, Muñoz-Planillo R, Núñez G. Sensing and reacting to microbes through the inflammasomes. *Nat Immunol*. 2012;13(4):325–32.

96. Cerutti A, Cols M, Puga I. Marginal zone B cells: virtues of innate-like antibody-producing lymphocytes. *Nat Rev Immunol*. 2013;13(2):118–32.
97. Macpherson AJ, Uhr T. Induction of protective IgA by intestinal dendritic cells carrying commensal bacteria. *Science (80-)*. 2004;303(5664):1662–5.
98. Lazar V, Ditu L, Pircalabioru G, Gheorghe I, Curutiu C, Holban AM, et al. Aspects of gut microbiota and immune system interactions in infectious diseases, immunopathology and cancer. *Front Immunol*. 2018;9:1830.
99. Mestre L, Carrillo-Salinas FJ, Mecha M, Feliú A, Guaza C. Gut microbiota, cannabinoid system and neuroimmune interactions: new perspectives in multiple sclerosis. *Biochem Pharmacol*. 2018;157:51–66.
100. Venegas DP, Marjorie K, Landskron G, González MJ, Quera R, Dijkstra G, et al. Short Chain Fatty Acids (SCFAs)-mediated gut epithelial and immune regulation and its relevance for Inflammatory Bowel Diseases. *Front Immunol*. 2019;10.
101. Bui TPN, Ritari J, Boeren S, De Waard P, Plugge CM, De Vos WM. Production of butyrate from lysine and the Amadori product fructoselysine by a human gut commensal. *Nat Commun*. 2015;6:10062.
102. Neis EPJG, Dejong CHC, Rensen SS. The role of microbial amino acid metabolism in host metabolism. *Nutrients*. 2015;7(4):2930–46.
103. Vinolo MAR, Rodrigues HG, Nachbar RT, Curi R. Regulation of inflammation by short chain fatty acids. *Nutrients*. 2011;3(10):858–76.
104. Morrison DJ, Preston T. Formation of short chain fatty acids by the gut microbiota and

- their impact on human metabolism. *Gut Microbes*. 2016;7(3):189–200.
105. Steimle A, Autenrieth IB, Frick J-SS. Structure and function: Lipid A modifications in commensals and pathogens. *Int J Med Microbiol*. 2016 Aug;306(5):290–301.
106. Akira S, Hemmi H. Recognition of pathogen-associated molecular patterns by TLR family. *Immunol Lett*. 2003;85(2):85–95.
107. Rallabhandi P, Awomoyi A, Thomas KE, Phalipon A, Fujimoto Y, Fukase K, et al. Differential activation of human TLR4 by Escherichia coli and Shigella flexneri 2a lipopolysaccharide: combined effects of lipid A acylation state and TLR4 polymorphisms on signaling. *J Immunol [Internet]*. 2008 Jan;180(2):1139–47. Available from: <https://www.ncbi.nlm.nih.gov/pubmed/18178854>
108. Zarrinpar A, Chaix A, Xu ZZ, Chang MW, Marotz CA, Saghatelian A, et al. Antibiotic-induced microbiome depletion alters metabolic homeostasis by affecting gut signaling and colonic metabolism. *Nat Commun [Internet]*. 2018;9(1):2872. Available from: <https://doi.org/10.1038/s41467-018-05336-9>
109. Haller D. The Gut Microbiome in Health and.
110. Kim CH, Park J, Kim M. Gut microbiota-derived short-chain fatty acids, T cells, and inflammation. *Immune Netw*. 2014;14(6):277–88.
111. Inan MS, Rasoulpour RJ, Yin L, Hubbard AK, Rosenberg DW, Giardina C. The luminal short-chain fatty acid butyrate modulates NF-κB activity in a human colonic epithelial cell line. *Gastroenterology*. 2000;118(4):724–34.
112. Liu T, Li J, Liu Y, Xiao N, Suo H, Xie K, et al. Short-chain fatty acids suppress

lipopolysaccharide-induced production of nitric oxide and proinflammatory cytokines through inhibition of NF-κB pathway in RAW264.7 cells. *Inflammation*. 2012;35(5):1676–84.

113. Wang X, Zhang A, Miao J, Sun H, Yan G, Wu F, et al. Gut microbiota as important modulator of metabolism in health and disease. *RSC Adv*. 2018;8(74):42380–9.
114. Gillis CC, Hughes ER, Spiga L, Winter MG, Zhu W, de Carvalho TF, et al. Dysbiosis-associated change in host metabolism generates lactate to support *Salmonella* growth. *Cell Host Microbe*. 2018;23(1):54–64.
115. Rivière A, Selak M, Lantin D, Leroy F, De Vuyst L. Bifidobacteria and butyrate-producing colon bacteria: importance and strategies for their stimulation in the human gut. *Front Microbiol*. 2016;7:979.
116. Louis P, Flint HJ. Diversity, metabolism and microbial ecology of butyrate-producing bacteria from the human large intestine. *FEMS Microbiol Lett*. 2009;294(1):1–8.
117. Louis P, Flint HJ. Formation of propionate and butyrate by the human colonic microbiota. *Environ Microbiol*. 2017;19(1):29–41.
118. Kelly CJ, Colgan SP. Breathless in the gut: implications of luminal O₂ for microbial pathogenicity. *Cell Host Microbe*. 2016;19(4):427–8.
119. Rivera-Chávez F, Zhang LF, Faber F, Lopez CA, Byndloss MX, Olsan EE, et al. Depletion of butyrate-producing Clostridia from the gut microbiota drives an aerobic luminal expansion of *Salmonella*. *Cell Host Microbe*. 2016;19(4):443–54.
120. Byndloss MX, Olsan EE, Rivera-Chávez F, Tiffany CR, Cevallos SA, Lokken KL, et al.

Microbiota-activated PPAR- γ signaling inhibits dysbiotic Enterobacteriaceae expansion.
Science (80-). 2017;357(6351):570–5.

121. Pryde SE, Duncan SH, Hold GL, Stewart CS, Flint HJ. The microbiology of butyrate formation in the human colon. *FEMS Microbiol Lett.* 2002;217(2):133–9.
122. Vital M, Howe AC, Tiedje JM. Revealing the bacterial butyrate synthesis pathways by analyzing (meta) genomic data. *MBio.* 2014;5(2).
123. Chelakkot C, Ghim J, Ryu SH. Mechanisms regulating intestinal barrier integrity and its pathological implications. *Exp Mol Med.* 2018;50(8):1–9.
124. Wang H-B, Wang P-Y, Wang X, Wan Y-L, Liu Y-C. Butyrate enhances intestinal epithelial barrier function via up-regulation of tight junction protein Claudin-1 transcription. *Dig Dis Sci.* 2012;57(12):3126–35.
125. Davie JR. Inhibition of histone deacetylase activity by butyrate. *J Nutr.* 2003;133(7):2485S-2493S.
126. Al-Sadi R, Guo S, Ye D, Ma TY. TNF- α modulation of intestinal epithelial tight junction barrier is regulated by ERK1/2 activation of Elk-1. *Am J Pathol.* 2013;183(6):1871–84.
127. Rios-Arce ND, Collins FL, Schepper JD, Steury MD, Raehtz S, Mallin H, et al. Epithelial barrier function in gut-bone signaling. In: Understanding the Gut-Bone Signaling Axis. Springer; 2017. p. 151–83.
128. Lee SH. Intestinal permeability regulation by tight junction: implication on inflammatory bowel diseases. *Intest Res.* 2015;13(1):11–8.

129. Ray P, Das D, Pandey U, Aich P. Comparative metagenomic analysis following treatment with vancomycin in C57BL/6 and BALB/c mice to elucidate host immunity and behavior. *bioRxiv*. 2020;
130. Singh RK, Chang H-W, Yan D, Lee KM, Ucmak D, Wong K, et al. Influence of diet on the gut microbiome and implications for human health. *J Transl Med*. 2017;15(1):73.
131. Blacher E, Levy M, Tatirovsky E, Elinav E. Microbiome-modulated metabolites at the interface of host immunity. *J Immunol*. 2017;198(2):572–80.
132. Fan Y, Pedersen O. Gut microbiota in human metabolic health and disease. *Nat Rev Microbiol*. 2020;1–17.
133. Schott EM, Farnsworth CW, Grier A, Lillis JA, Soniwala S, Dadourian GH, et al. Targeting the gut microbiome to treat the osteoarthritis of obesity. *JCI insight*. 2018;3(8).
134. Qin J, Li Y, Cai Z, Li S, Zhu J, Zhang F, et al. A metagenome-wide association study of gut microbiota in type 2 diabetes. *Nature*. 2012;490(7418):55–60.
135. Liu S, Qin P, Wang J. High-fat diet alters the intestinal microbiota in streptozotocin-induced type 2 diabetic mice. *Microorganisms*. 2019;7(6):176.
136. Hamada D, Maynard R, Schott E, Drinkwater CJ, Ketz JP, Kates SL, et al. Suppressive effects of insulin on tumor necrosis factor-dependent early osteoarthritic changes associated with obesity and type 2 diabetes mellitus. *Arthritis Rheumatol*. 2016;68(6):1392–402.
137. Lee J-H, Li X, O’Sullivan DJ. Transcription analysis of a lantibiotic gene cluster from *Bifidobacterium longum* DJO10A. *Appl Environ Microbiol*. 2011;77(17):5879–87.

138. Smith MI, Yatsunenko T, Manary MJ, Trehan I, Mkakosya R, Cheng J, et al. Gut microbiomes of Malawian twin pairs discordant for kwashiorkor. *Science* (80-). 2013;339(6119):548–54.
139. Million M, Diallo A, Raoult D. Gut microbiota and malnutrition. *Microb Pathog*. 2017;106:127–38.
140. Mata LJ, Jiménez F, Cordón M, Rosales R, Prera E, Schneider RE, et al. Gastrointestinal flora of children with protein—calorie malnutrition. *Am J Clin Nutr*. 1972;25(10):1118–26.
141. Brunt EM, Kleiner DE, Wilson LA, Belt P, Neuschwander-Tetri BA, (CRN) NCRN. Nonalcoholic fatty liver disease (NAFLD) activity score and the histopathologic diagnosis in NAFLD: distinct clinicopathologic meanings. *Hepatology*. 2011;53(3):810–20.
142. Jiang W, Wu N, Wang X, Chi Y, Zhang Y, Qiu X, et al. Dysbiosis gut microbiota associated with inflammation and impaired mucosal immune function in intestine of humans with non-alcoholic fatty liver disease. *Sci Rep*. 2015;5:8096.
143. Zhu L, Baker SS, Gill C, Liu W, Alkhouri R, Baker RD, et al. Characterization of gut microbiomes in nonalcoholic steatohepatitis (NASH) patients: a connection between endogenous alcohol and NASH. *Hepatology*. 2013;57(2):601–9.
144. Del Chierico F, Nobili V, Vernocchi P, Russo A, De Stefanis C, Gnani D, et al. Gut microbiota profiling of pediatric nonalcoholic fatty liver disease and obese patients unveiled by an integrated meta-omics-based approach. *Hepatology*. 2017;65(2):451–64.
145. Jie Z, Xia H, Zhong S-L, Feng Q, Li S, Liang S, et al. The gut microbiome in

atherosclerotic cardiovascular disease. *Nat Commun.* 2017;8(1):1–12.

146. Sokol H, Pigneur B, Watterlot L, Lakhdari O, Bermúdez-Humarán LG, Gratadoux J-J, et al. *Faecalibacterium prausnitzii* is an anti-inflammatory commensal bacterium identified by gut microbiota analysis of Crohn disease patients. *Proc Natl Acad Sci.* 2008;105(43):16731–6.
147. Cui X, Ye L, Li J, Jin L, Wang W, Li S, et al. Metagenomic and metabolomic analyses unveil dysbiosis of gut microbiota in chronic heart failure patients. *Sci Rep.* 2018;8(1):1–15.
148. Wang Z, Klipfell E, Bennett BJ, Koeth R, Levison BS, DuGar B, et al. Gut flora metabolism of phosphatidylcholine promotes cardiovascular disease. *Nature.* 2011;472(7341):57–63.
149. Horta-Baas G, Romero-Figueroa M del S, Montiel-Jarquín AJ, Pizano-Zárate ML, García-Mena J, Ramírez-Durán N. Intestinal dysbiosis and rheumatoid arthritis: a link between gut microbiota and the pathogenesis of rheumatoid arthritis. *J Immunol Res.* 2017;2017.
150. Alam MT, Amos GCA, Murphy ARJ, Murch S, Wellington EMH, Arasaradnam RP. Microbial imbalance in inflammatory bowel disease patients at different taxonomic levels. *Gut Pathog.* 2020;12(1):1–8.
151. Khan I, Ullah N, Zha L, Bai Y, Khan A, Zhao T, et al. Alteration of gut microbiota in inflammatory bowel disease (IBD): Cause or consequence? IBD treatment targeting the gut microbiome. *Pathogens.* 2019;8(3):126.
152. Martin AM, Sun EW, Rogers GB, Keating DJ. The influence of the gut microbiome on

host metabolism through the regulation of gut hormone release. *Front Physiol.* 2019;10:428.

153. Yano JM, Yu K, Donaldson GP, Shastri GG, Ann P, Ma L, et al. Indigenous bacteria from the gut microbiota regulate host serotonin biosynthesis. *Cell.* 2015;161(2):264–76.
154. Akiba Y, Inoue T, Kaji I, Higashiyama M, Narimatsu K, Iwamoto K, et al. Short-chain fatty acid sensing in rat duodenum. *J Physiol.* 2015;593(3):585–99.
155. Martin AM, Lumsden AL, Young RL, Jessup CF, Spencer NJ, Keating DJ. The nutrient-sensing repertoires of mouse enterochromaffin cells differ between duodenum and colon. *Neurogastroenterol Motil.* 2017;29(6):e13046.
156. Bellono NW, Bayrer JR, Leitch DB, Castro J, Zhang C, O'Donnell TA, et al. Enterochromaffin cells are gut chemosensors that couple to sensory neural pathways. *Cell.* 2017;170(1):185–98.
157. Lund ML, Egerod KL, Engelstoft MS, Dmytriyeva O, Theodorsson E, Patel BA, et al. Enterochromaffin 5-HT cells—A major target for GLP-1 and gut microbial metabolites. *Mol Metab.* 2018;11:70–83.
158. Sun EW, De Fontgalland D, Rabbitt P, Hollington P, Sposato L, Due SL, et al. Mechanisms controlling glucose-induced GLP-1 secretion in human small intestine. *Diabetes.* 2017;66(8):2144–9.
159. Grøndahl MF, Keating DJ, Vilsbøll T, Knop FK. Current therapies that modify glucagon secretion: what is the therapeutic effect of such modifications? *Curr Diab Rep.* 2017;17(12):128.

160. Holst JJ. The physiology of glucagon-like peptide 1. *Physiol Rev.* 2007;87(4):1409–39.
161. Olivares M, Neyrinck AM, Pötgens SA, Beaumont M, Salazar N, Cani PD, et al. The DPP-4 inhibitor vildagliptin impacts the gut microbiota and prevents disruption of intestinal homeostasis induced by a Western diet in mice. *Diabetologia.* 2018;61(8):1838–48.
162. Olivares M, Schüppel V, Hassan AM, Beaumont M, Neyrinck AM, Bindels LB, et al. The potential role of the dipeptidyl peptidase-4-like activity from the gut microbiota on the host health. *Front Microbiol.* 2018;9:1900.
163. Bala V, Rajagopal S, Kumar DP, Nalli AD, Mahavadi S, Sanyal AJ, et al. Release of GLP-1 and PYY in response to the activation of G protein-coupled bile acid receptor TGR5 is mediated by Epac/PLC- \square pathway and modulated by endogenous H2S. *Front Physiol.* 2014;5:420.
164. Tolhurst G, Heffron H, Lam YS, Parker HE, Habib AM, Diakogiannaki E, et al. Short-chain fatty acids stimulate glucagon-like peptide-1 secretion via the G-protein-coupled receptor FFAR2. *Diabetes.* 2012;61(2):364–71.
165. Chimerel C, Emery E, Summers David K, Keyser U, Gribble Fiona M, Reimann F. Bacterial metabolite indole modulates incretin secretion from intestinal enteroendocrine L cells. *Cell Rep* 9 (4): 1202–1208. 2014.
166. Dumont Y, Fournier A, St-Pierre S, Quirion R. Characterization of neuropeptide Y binding sites in rat brain membrane preparations using [¹²⁵I][Leu31, Pro34] peptide YY and [¹²⁵I] peptide YY3-36 as selective Y1 and Y2 radioligands. *J Pharmacol Exp Ther.*

1995;272(2):673–80.

167. Cahill F, Ji Y, Wadden D, Amini P, Randell E, Vasdev S, et al. The association of serum total peptide YY (PYY) with obesity and body fat measures in the coding study. *PLoS One*. 2014;
168. Larraufie P, Martin-Gallausiaux C, Lapaque N, Dore J, Gribble FM, Reimann F, et al. SCFAs strongly stimulate PYY production in human enteroendocrine cells. *Sci Rep*. 2018;8(1):74.
169. Hawkesworth S, Moore SE, Fulford AJC, Barclay GR, Darboe AA, Mark H, et al. Evidence for metabolic endotoxemia in obese and diabetic Gambian women. *Nutr Diabetes*. 2013;3(8):e83.
170. Boutagy NE, McMillan RP, Frisard MI, Hulver MW. Metabolic endotoxemia with obesity: Is it real and is it relevant? *Biochimie*. 2016;124:11–20.
171. Fujio-Vejar S, Vasquez Y, Morales P, Magne F, Vera-Wolf P, Ugalde JA, et al. The gut microbiota of healthy chilean subjects reveals a high abundance of the phylum verrucomicrobia. *Front Microbiol*. 2017;8:1221.
172. Plovier H, Everard A, Druart C, Depommier C, Van Hul M, Geurts L, et al. A purified membrane protein from *Akkermansia muciniphila* or the pasteurized bacterium improves metabolism in obese and diabetic mice. *Nat Med*. 2017;23(1):107.
173. FUJISAKA S, USUI I, NAWAZ A, IGARASHI Y, KADO T, OKABE K, et al. Bofutsushosan Improves Gut Barrier Function with a Bloom of *Akkermansia Muciniphila* and Improves Glucose Metabolism in Diet-Induced Obese Mice. *Diabetes*. 2018

May;67(Supplement 1):1990--P.

174. Foster JA, Rinaman L, Cryan JF. Stress & the gut-brain axis: regulation by the microbiome. *Neurobiol Stress*. 2017;7:124–36.
175. Carabotti M, Scirocco A, Maselli MA, Severi C. The gut-brain axis: interactions between enteric microbiota, central and enteric nervous systems. *Ann Gastroenterol Q Publ Hell Soc Gastroenterol*. 2015;28(2):203.
176. Martin CR, Osadchiy V, Kalani A, Mayer EA. The brain-gut-microbiome axis. *Cell Mol Gastroenterol Hepatol*. 2018;6(2):133–48.
177. Wang Y, Kasper LH. The role of microbiome in central nervous system disorders. *Brain Behav Immun*. 2014;38:1–12.
178. Smith SM, Vale WW. The role of the hypothalamic-pituitary-adrenal axis in neuroendocrine responses to stress. *Dialogues Clin Neurosci*. 2006;8(4):383.
179. Sudo N. Role of gut microbiota in brain function and stress-related pathology. *Biosci microbiota, food Heal*. 2019;6–19.
180. Luczynski P, McVey Neufeld K-A, Oriach CS, Clarke G, Dinan TG, Cryan JF. Growing up in a bubble: using germ-free animals to assess the influence of the gut microbiota on brain and behavior. *Int J Neuropsychopharmacol*. 2016;19(8).
181. Bendtsen KMB, Krych L, Sørensen DB, Pang W, Nielsen DS, Josefson K, et al. Gut microbiota composition is correlated to grid floor induced stress and behavior in the BALB/c mouse. *PLoS One*. 2012;7(10):e46231.

182. Clarke G, Grenham S, Scully P, Fitzgerald P, Moloney RD, Shanahan F, et al. The microbiome-gut-brain axis during early life regulates the hippocampal serotonergic system in a sex-dependent manner. *Mol Psychiatry*. 2013;18(6):666.
183. Sudo N, Chida Y, Aiba Y, Sonoda J, Oyama N, Yu X, et al. Postnatal microbial colonization programs the hypothalamic–pituitary–adrenal system for stress response in mice. *J Physiol*. 2004;558(1):263–75.
184. Asano Y, Hiramoto T, Nishino R, Aiba Y, Kimura T, Yoshihara K, et al. Critical role of gut microbiota in the production of biologically active, free catecholamines in the gut lumen of mice. *Am J Physiol Liver Physiol*. 2012;303(11):G1288–95.
185. Goehler LE, Park SM, Opitz N, Lyte M, Gaykema RPA. *Campylobacter jejuni* infection increases anxiety-like behavior in the holeboard: possible anatomical substrates for viscerosensory modulation of exploratory behavior. *Brain Behav Immun*. 2008;22(3):354–66.
186. Reis DJ, Ilardi SS, Punt SEW. The anxiolytic effect of probiotics: A systematic review and meta-analysis of the clinical and preclinical literature. *PLoS One*. 2018;13(6):e0199041.
187. McGaughey KD, Yilmaz-Swenson T, Elsayed NM, Cruz DA, Rodriguez RM, Kritzer MD, et al. Relative abundance of *Akkermansia* spp. and other bacterial phylotypes correlates with anxiety-and depressive-like behavior following social defeat in mice. *Sci Rep*. 2019;9(1):1–11.
188. Ried K, Travica N, Sali A. The effect of Kyolic aged garlic extract on gut microbiota,

inflammation, and cardiovascular markers in hypertensives: The GarGIC Trial. *Front Nutr.* 2018;5:122.

189. Ahmed F, Kerna NA, Tulp OL. Managing the F: B Ratio in DM; A Review of the Role of Firmicutes and Bacteroidetes in Diabetes Mellitus.
190. Bercik P, Denou E, Collins J, Jackson W, Lu J, Jury J, et al. The intestinal microbiota affect central levels of brain-derived neurotropic factor and behavior in mice. *Gastroenterology.* 2011;141(2):599–609.
191. Park AJ, Collins J, Blennerhassett PA, Ghia JE, Verdu EF, Bercik P, et al. Altered colonic function and microbiota profile in a mouse model of chronic depression. *Neurogastroenterol Motil.* 2013;25(9):733--e575.
192. Li K, Nakajima M, Ibañez-Tallon I, Heintz N. A cortical circuit for sexually dimorphic oxytocin-dependent anxiety behaviors. *Cell.* 2016;167(1):60–72.
193. Kunze WA, Mao Y, Wang B, Huizinga JD, Ma X, Forsythe P, et al. Lactobacillus reuteri enhances excitability of colonic AH neurons by inhibiting calcium-dependent potassium channel opening. *J Cell Mol Med.* 2009;13(8b):2261–70.
194. Fröhlich EE, Farzi A, Mayerhofer R, Reichmann F, Jačan A, Wagner B, et al. Cognitive impairment by antibiotic-induced gut dysbiosis: Analysis of gut microbiota-brain communication. *Brain Behav Immun.* 2016/02/23. 2016 Aug;56:140–55.
195. Ait-Belgnaoui A, Durand H, Cartier C, Chaumaz G, Eutamene H, Ferrier L, et al. Prevention of gut leakiness by a probiotic treatment leads to attenuated HPA response to an acute psychological stress in rats. *Psychoneuroendocrinology.* 2012;37(11):1885–95.

196. Zareie M, Johnson-Henry K, Jury J, Yang P-C, Ngan B-Y, McKay DM, et al. Probiotics prevent bacterial translocation and improve intestinal barrier function in rats following chronic psychological stress. *Gut*. 2006;55(11):1553–60.
197. Ma N, Ma X. Dietary amino acids and the gut-microbiome-immune axis: physiological metabolism and therapeutic prospects. *Compr Rev Food Sci Food Saf*. 2019;18(1):221–42.
198. Dai Z, Wu Z, Hang S, Zhu W, Wu G. Amino acid metabolism in intestinal bacteria and its potential implications for mammalian reproduction. *MHR Basic Sci Reprod Med*. 2015;21(5):389–409.
199. Macfarlane GT, Macfarlane S. Bacteria, colonic fermentation, and gastrointestinal health. *J AOAC Int*. 2012;95(1):50–60.
200. Libao-Mercado AJO, Zhu CL, Cant JP, Lapierre H, Thibault J-N, Seve B, et al. Dietary and endogenous amino acids are the main contributors to microbial protein in the upper gut of normally nourished pigs. *J Nutr*. 2009;139(6):1088–94.
201. Durbán A, Abellán JJ, Jiménez-Hernández N, Ponce M, Ponce J, Sala T, et al. Assessing gut microbial diversity from feces and rectal mucosa. *Microb Ecol*. 2011;61(1):123–33.
202. Probert HM, Gibson GR. Bacterial biofilms in the human gastrointestinal tract. *Curr Issues Intest Microbiol*. 2002;3(2):23–7.
203. Thakur AK, Shakya A, Husain GM, Emerald M, Kumar V. Gut-microbiota and mental health: current and future perspectives. *J Pharmacol Clin Toxicol*. 2014;2(1):1016.
204. Morton ER, Lynch J, Froment A, Lafosse S, Heyer E, Przeworski M, et al. Variation in

rural African gut microbiota is strongly correlated with colonization by Entamoeba and subsistence. *PLoS Genet.* 2015;11(11):e1005658.

205. Falony G, Joossens M, Vieira-Silva S, Wang J, Darzi Y, Faust K, et al. Population-level analysis of gut microbiome variation. *Science* (80-). 2016;352(6285):560–4.
206. Khan CM. The dynamic interactions between *Salmonella* and the microbiota, within the challenging niche of the gastrointestinal tract. *Int Sch Res Not.* 2014;2014.
207. Lange K, Buerger M, Stallmach A, Bruns T. Effects of antibiotics on gut microbiota. *Dig Dis.* 2016;34(3):260–8.
208. Willing BP, Russell SL, Finlay BB. Shifting the balance: Antibiotic effects on host-microbiota mutualism. Vol. 9, *Nature Reviews Microbiology*. 2011. p. 233–43.
209. Li M, Bauer LL, Chen X, Wang M, Kuhlenschmidt TB, Kuhlenschmidt MS, et al. Microbial composition and in vitro fermentation patterns of human milk oligosaccharides and prebiotics differ between formula-fed and sow-reared piglets. *J Nutr.* 2012;142(4):681–9.
210. Yatsunenko T, Rey FE, Manary MJ, Trehan I, Dominguez-Bello MG, Contreras M, et al. Human gut microbiome viewed across age and geography. *Nature*. 2012;486(7402):222–7.
211. Smith EA, Macfarlane GT. Enumeration of amino acid fermenting bacteria in the human large intestine: effects of pH and starch on peptide metabolism and dissimilation of amino acids. *FEMS Microbiol Ecol.* 1998;25(4):355–68.
212. Romond M-B, Ais A, Guillemot F, Bounouader R, Cortot A, Romond C. Cell-free whey

- from milk fermented with *Bifidobacterium breve* C50 used to modify the colonic microflora of healthy subjects. *J Dairy Sci.* 1998;81(5):1229–35.
213. Meddah ATT, Yazourh A, Desmet I, Risbourg B, Verstraete W, Romond MB. The regulatory effects of whey retentate from bifidobacteria fermented milk on the microbiota of the Simulator of the Human Intestinal Microbial Ecosystem (SHIME). *J Appl Microbiol.* 2001;91(6):1110–7.
214. Dominika Š, Arjan N, Karyn RP, Henryk K. The study on the impact of glycated pea proteins on human intestinal bacteria. *Int J Food Microbiol.* 2011;145(1):267–72.
215. David LA, Maurice CF, Carmody RN, Gootenberg DB, Button JE, Wolfe BE, et al. Diet rapidly and reproducibly alters the human gut microbiome. *Nature.* 2014;505(7484):559–63.
216. Reddy BS, Weisburger JH, Wynder EL. Effects of high risk and low risk diets for colon carcinogenesis on fecal microflora and steroids in man. *J Nutr.* 1975;105(7):878–84.
217. Cotillard A, Kennedy SP, Kong LC, Prifti E, Pons N, Le Chatelier E, et al. Dietary intervention impact on gut microbial gene richness. *Nature.* 2013;500(7464):585–8.
218. De Filippo C, Cavalieri D, Di Paola M, Ramazzotti M, Poulet JB, Massart S, et al. Impact of diet in shaping gut microbiota revealed by a comparative study in children from Europe and rural Africa. *Proc Natl Acad Sci.* 2010;107(33):14691–6.
219. Rytter MJH, Kolte L, Briand A, Friis H, Christensen VB. The immune system in children with malnutrition—a systematic review. *PLoS One.* 2014;9(8):e105017.
220. Rolhion N, Chassaing B. When pathogenic bacteria meet the intestinal microbiota. *Philos*

Trans R Soc B Biol Sci. 2016;371(1707):20150504.

221. Bassis CM, Theriot CM, Young VB. Alteration of the murine gastrointestinal microbiota by tigecycline leads to increased susceptibility to Clostridium difficile infection. *Antimicrob Agents Chemother*. 2014;58(5):2767–74.
222. Contijoch EJ, Britton GJ, Yang C, Mogno I, Li Z, Ng R, et al. Gut microbiota density influences host physiology and is shaped by host and microbial factors. *Elife*. 2019 Jan;8.
223. HayGlass KT, Nashed B, Haile S, Marshall AJ, Thomas W. C57Bl/6 and BALB/c mice do not represent default Th1 and Th2 strains in allergen-driven immune responses. *J Allergy Clin Immunol*. 2005;115(2):S258.
224. Tabrett A, Horton MW. The influence of host genetics on the microbiome. *F1000Research*. 2020;9.
225. Shoji H, Miyakawa T. Increased depression-related behavior during the postpartum period in inbred BALB/c and C57BL/6 strains. *Mol Brain*. 2019;12(1):1–20.
226. Fransen F, Zagato E, Mazzini E, Fosso B, Manzari C, El Aidy S, et al. BALB/c and C57BL/6 mice differ in polyreactive IgA abundance, which impacts the generation of antigen-specific IgA and microbiota diversity. *Immunity*. 2015;43(3):527–40.
227. Watanabe H, Numata K, Ito T, Takagi K, Matsukawa A. Innate immune response in Th1- and Th2-dominant mouse strains. *Shock*. 2004;
228. Ray P, Pandey U, Aich P. Comparative analysis of beneficial effects of Vancomycin treatment on Th1- and Th2-biased mice and role of gut microbiota [Internet]. bioRxiv; 2019. Available from: <https://doi.org/10.1101/516898>

229. Pradhan B, Guha D, Naik AK, Banerjee A, Tambat S, Chawla S, et al. Probiotics L. acidophilus and B. clausii Modulate Gut Microbiota in Th1-and Th2-Biased Mice to Ameliorate *Salmonella Typhimurium*-Induced Diarrhea. *Probiotics Antimicrob Proteins*. 2018;1–18.
230. Ferreira BL, Ferreira ÉR, de Brito M V, Salu BR, Oliva ML V, Mortara RA, et al. BALB/c and C57BL/6 mice cytokine responses to *Trypanosoma cruzi* infection are independent of parasite strain infectivity. *Front Microbiol*. 2018;9:553.
231. Palleja A, Mikkelsen KH, Forslund SK, Kashani A, Allin KH, Nielsen T, et al. Recovery of gut microbiota of healthy adults following antibiotic exposure. *Nat Microbiol*. 2018;3(11):1255.
232. MacPherson CW, Mathieu O, Tremblay J, Champagne J, Nantel A, Girard S-A, et al. Gut bacterial microbiota and its resistome rapidly recover to basal state levels after short-term amoxicillin-clavulanic acid treatment in healthy adults. *Sci Rep*. 2018;8(1):1–14.
233. Dethlefsen L, Relman DA. Incomplete recovery and individualized responses of the human distal gut microbiota to repeated antibiotic perturbation. *Proc Natl Acad Sci*. 2011;108(Supplement 1):4554–61.
234. Isaac S, Scher JU, Djukovic A, Jiménez N, Littman DR, Abramson SB, et al. Short-and long-term effects of oral vancomycin on the human intestinal microbiota. *J Antimicrob Chemother*. 2016;72(1):128–36.
235. Grazul H, Kanda LL, Gondek D. Impact of probiotic supplements on microbiome diversity following antibiotic treatment of mice. *Gut Microbes*. 2016;7(2):101–14.

236. Seekatz AM, Aas J, Gessert CE, Rubin TA, Saman DM, Bakken JS, et al. Recovery of the gut microbiome following fecal microbiota transplantation. *MBio*. 2014;5(3).
237. Smits LP, Bouter KEC, de Vos WM, Borody TJ, Nieuwdorp M. Therapeutic potential of fecal microbiota transplantation. *Gastroenterology*. 2013;145(5):946–53.
238. Gupta S, Allen-Vercoe E, Petrof EO. Fecal microbiota transplantation: in perspective. *Therap Adv Gastroenterol*. 2016;9(2):229–39.
239. Rohlke F, Stollman N. Fecal microbiota transplantation in relapsing *Clostridium difficile* infection. *Therap Adv Gastroenterol*. 2012;5(6):403–20.
240. Shahinas D, Silverman M, Sittler T, Chiu C, Kim P, Allen-Vercoe E, et al. Toward an understanding of changes in diversity associated with fecal microbiome transplantation based on 16S rRNA gene deep sequencing. *MBio*. 2012;3(5).
241. Willing B, Halfvarson J, Dicksved J, Rosenquist M, Järnerot G, Engstrand L, et al. Twin studies reveal specific imbalances in the mucosaassociated microbiota of patients with ileal Crohn’s disease. *Inflamm Bowel Dis*. 2009;15(5):653–60.
242. Varela E, Manichanh C, Gallart M, Torrejón A, Borruel N, Casellas F, et al. Colonisation by *Faecalibacterium prausnitzii* and maintenance of clinical remission in patients with ulcerative colitis. *Aliment Pharmacol Ther*. 2013;38(2):151–61.
243. Rosa CP, Pereira JA, Cristina de Melo Santos N, Brancaglion GA, Silva EN, Tagliati CA, et al. Vancomycin-induced gut dysbiosis during *Pseudomonas aeruginosa* pulmonary infection in a mice model. *J Leukoc Biol*. 2020;107(1):95–104.
244. Hansen CHF, Krych L, Nielsen DS, Vogensen FK, Hansen LH, Sørensen SJ, et al. Early

- life treatment with vancomycin propagates *Akkermansia muciniphila* and reduces diabetes incidence in the NOD mouse. *Diabetologia*. 2012;55(8):2285–94.
245. Basolo A, Hohenadel M, Ang QY, Piaggi P, Heinitz S, Walter M, et al. Effects of underfeeding and oral vancomycin on gut microbiome and nutrient absorption in humans. *Nat Med*. 2020;26(4):589–98.
246. Xu X, Fukui H, Ran Y, Tomita T, Oshima T, Watari J, et al. Alteration of GLP-1/GPR43 expression and gastrointestinal motility in dysbiotic mice treated with vancomycin. *Sci Rep*. 2019;9(1):1–10.
247. Tulstrup MV-L, Christensen EG, Carvalho V, Linninge C, Ahrné S, Højberg O, et al. Antibiotic treatment affects intestinal permeability and gut microbial composition in Wistar rats dependent on antibiotic class. *PLoS One*. 2015;10(12):e0144854.
248. Reijnders D, Goossens GH, Hermes GDA, Smidt H, Zoetendal EG, Blaak EE. Short-term microbiota manipulation and forearm substrate metabolism in obese men: A randomized, double-blind, placebo-controlled trial. *Obes Facts*. 2018;11(4):318–26.
249. Sun L, Zhang X, Zhang Y, Zheng K, Xiang Q, Chen N, et al. Antibiotic-Induced Disruption of Gut Microbiota Alters Local Metabolomes and Immune Responses. *Front Cell Infect Microbiol* [Internet]. 2019 Apr;9:99. Available from: <https://www.ncbi.nlm.nih.gov/pubmed/31069173>
250. Taylor MR, Flannigan KL, Rahim H, Mohamud A, Lewis IA, Hirota SA, et al. Vancomycin relieves mycophenolate mofetil–induced gastrointestinal toxicity by eliminating gut bacterial β-glucuronidase activity. *Sci Adv*. 2019;5(8):eaax2358.

251. Uribe-Herranz M, Rafail S, Beghi S, Gil-de-Gómez L, Verginadis I, Bittinger K, et al. Gut microbiota modulate dendritic cell antigen presentation and radiotherapy-induced antitumor immune response. *J Clin Invest.* 2019;130(1).
252. Yang X, Feng H, Zhan X, Zhang C, Cui R, Zhong L, et al. Early-life vancomycin treatment promotes airway inflammation and impairs microbiome homeostasis. *Aging (Albany NY).* 2019;11(7):2071.
253. Thorpe CM, Kane A V, Chang J, Tai A, Vickers RJ, Snydman DR. Enhanced preservation of the human intestinal microbiota by ridinilazole, a novel *Clostridium difficile*-targeting antibacterial, compared to vancomycin. *PLoS One.* 2018;13(8):e0199810.
254. van Opstal E, Kolling GL, Moore JH, Coquery CM, Wade NS, Loo WM, et al. Vancomycin treatment alters humoral immunity and intestinal microbiota in an aged mouse model of *Clostridium difficile* infection. *J Infect Dis.* 2016;214(1):130–9.
255. Džunková M, D'Auria G, Xu H, Huang J, Duan Y, Moya A, et al. The monoclonal antitoxin antibodies (actoxumab–bezlotoxumab) treatment facilitates normalization of the gut microbiota of mice with *Clostridium difficile* infection. *Front Cell Infect Microbiol.* 2016;6:119.
256. Wang Q, Qian L, Jiang S, Cai C, Ma D, Gao P, et al. Safety evaluation of neo transgenic pigs by studying changes in gut microbiota using high-throughput sequencing technology. *PLoS One.* 2016;11(3):e0150937.
257. Zhao L, Huang Y, Lu L, Yang W, Huang T, Lin Z, et al. Saturated long-chain fatty acid-producing bacteria contribute to enhanced colonic motility in rats. *Microbiome.*

2018;6(1):1–16.

258. Jovicic N, Jeftic I, Jovanovic I, Radosavljevic G, Arsenijevic N, Lukic ML, et al. Differential immunometabolic phenotype in Th1 and Th2 dominant mouse strains in response to high-fat feeding. *PLoS One*. 2015;
259. Leo S, Lazarevic V, Girard M, Gaïa N, Schrenzel J, de Lastours V, et al. Metagenomic Characterization of Gut Microbiota of Carriers of Extended-Spectrum Beta-Lactamase or Carbapenemase-Producing Enterobacteriaceae Following Treatment with Oral Antibiotics and Fecal Microbiota Transplantation: Results from a Multicenter Randomized Microorganisms. 2020;8(6):941.
260. Le Bastard Q, Ward T, Sidiropoulos D, Hillmann BM, Chun CL, Sadowsky MJ, et al. Fecal microbiota transplantation reverses antibiotic and chemotherapy-induced gut dysbiosis in mice. *Sci Rep*. 2018;8(1):1–11.
261. Kabbani TA, Pallav K, Dowd SE, Villafuerte-Galvez J, Vanga RR, Castillo NE, et al. Prospective randomized controlled study on the effects of *Saccharomyces boulardii* CNCM I-745 and amoxicillin-clavulanate or the combination on the gut microbiota of healthy volunteers. *Gut Microbes*. 2017;8(1):17–32.
262. Lavelle A, Hoffmann TW, Pham H-P, Langella P, Guédon E, Sokol H. Baseline microbiota composition modulates antibiotic-mediated effects on the gut microbiota and host. *Microbiome*. 2019;7(1):1–13.
263. Bulow C, Langdon A, Hink T, Wallace M, Reske KA, Patel S, et al. Impact of amoxicillin-clavulanate followed by autologous fecal microbiota transplantation on fecal

microbiome structure and metabolic potential. *MSphere*. 2018;3(6).

264. Schumann A, Nutten S, Donnicola D, Comelli EM, Mansourian R, Cherbut C, et al. Neonatal antibiotic treatment alters gastrointestinal tract developmental gene expression and intestinal barrier transcriptome. *Physiol Genomics*. 2005;23(2):235–45.
265. Soler C, Goossens T, Bermejo A, Migura-García L, Cusco A, Francino O, et al. Digestive microbiota is different in pigs receiving antimicrobials or a feed additive during the nursery period. *PLoS One*. 2018;13(5):e0197353.
266. Korry BJ, Cabral DJ, Belenky P. Metatranscriptomics Reveals Antibiotic-Induced Resistance Gene Expression in the Murine Gut Microbiota. *Front Microbiol*. 2020;11:322.
267. Stewardson AJ, Gaia N, Francois P, Malhotra-Kumar S, Delemont C, de Tejada BM, et al. Collateral damage from oral ciprofloxacin versus nitrofurantoin in outpatients with urinary tract infections: a culture-free analysis of gut microbiota. *Clin Microbiol Infect*. 2015;21(4):344-e1.
268. Dethlefsen L, Huse S, Sogin ML, Relman DA. The pervasive effects of an antibiotic on the human gut microbiota, as revealed by deep 16S rRNA sequencing. *PLoS Biol*. 2008;6(11):e280.
269. Ju T, Shoblak Y, Gao Y, Yang K, Fouhse J, Finlay BB, et al. Initial gut microbial composition as a key factor driving host response to antibiotic treatment, as exemplified by the presence or absence of commensal *Escherichia coli*. *Appl Environ Microbiol*. 2017;83(17).
270. Arnold CE, Isaiah A, Pilla R, Lidbury J, Coverdale JS, Callaway TR, et al. The cecal and

fecal microbiomes and metabolomes of horses before and after metronidazole administration. PLoS One. 2020;15(5):e0232905.

271. Pélassier M-A, Vasquez N, Balamurugan R, Pereira E, Dossou-Yovo F, Suau A, et al. Metronidazole effects on microbiota and mucus layer thickness in the rat gut. FEMS Microbiol Ecol. 2010;73(3):601–10.
272. Shmalberg JW, Montalbano C, Morelli G, Buckley GJ. A randomized double blinded placebo-controlled clinical trial of a probiotic or metronidazole for acute canine diarrhea. Front Vet Sci. 2019;6:163.
273. Dodiya HB, Frith M, Sidebottom A, Cao Y, Koval J, Chang E, et al. Synergistic depletion of gut microbial consortia, but not individual antibiotics, reduces amyloidosis in APPPS1-21 Alzheimer's transgenic mice. Sci Rep. 2020;10(1):1–10.
274. Manickam R, Oh HYP, Tan CK, Paramalingam E, Wahli W. Metronidazole causes skeletal muscle atrophy and modulates muscle chronometabolism. Int J Mol Sci. 2018;19(8):2418.
275. Yoon H, Schaubeck M, Lagkouvardos I, Blesl A, Heinzlmeir S, Hahne H, et al. Increased pancreatic protease activity in response to antibiotics impairs gut barrier and triggers colitis. Cell Mol Gastroenterol Hepatol. 2018;6(3):370–88.
276. Zhao Z, Cheng W, Qu W, Shao G, Liu S. Antibiotic Alleviates Radiation-Induced Intestinal Injury by Remodeling Microbiota, Reducing Inflammation, and Inhibiting Fibrosis. ACS omega. 2020;5(6):2967–77.
277. Newton DF, Macfarlane S, Macfarlane GT. Effects of antibiotics on bacterial species

composition and metabolic activities in chemostats containing defined populations of human gut microorganisms. *Antimicrob Agents Chemother*. 2013;57(5):2016–25.

278. Lankelma JM, Cranendonk DR, Belzer C, De Vos AF, De Vos WM, Van Der Poll T, et al. Antibiotic-induced gut microbiota disruption during human endotoxemia: a randomised controlled study. *Gut*. 2017;66(9):1623–30.
279. Gao H, Shu Q, Chen J, Fan K, Xu P, Zhou Q, et al. Antibiotic exposure has sex-dependent effects on the gut microbiota and metabolism of short-chain fatty acids and amino acids in mice. *Msystems*. 2019;4(4).
280. Lankelma JM, Belzer C, Hoogendijk AJ, De Vos AF, De Vos WM, Van Der Poll T, et al. Antibiotic-induced gut microbiota disruption decreases TNF- α release by mononuclear cells in healthy adults. *Clin Transl Gastroenterol*. 2016;7(8):e186.
281. Cho Y, Abu-Ali G, Tashiro H, Kasahara DI, Brown TA, Brand JD, et al. The microbiome regulates pulmonary responses to ozone in mice. *Am J Respir Cell Mol Biol*. 2018;59(3):346–54.
282. Nakamura YK, Metea C, Karstens L, Asquith M, Gruner H, Moscibrocki C, et al. Gut microbial alterations associated with protection from autoimmune uveitis. *Invest Ophthalmol Vis Sci*. 2016;57(8):3747–58.
283. Jena PK, Sheng L, Liu H-X, Kalanetra KM, Mirsoian A, Murphy WJ, et al. Western diet–induced dysbiosis in farnesoid X receptor knockout mice causes persistent hepatic inflammation after antibiotic treatment. *Am J Pathol*. 2017;187(8):1800–13.
284. Kaur K, Saxena A, Debnath I, O’Brien JL, Ajami NJ, Auchtung TA, et al.

Antibiotic-mediated bacteriome depletion in ApcMin/+ mice is associated with reduction in mucus-producing goblet cells and increased colorectal cancer progression. *Cancer Med.* 2018;7(5):2003–12.

285. Yao H, Fan C, Lu Y, Fan X, Xia L, Li P, et al. Alteration of gut microbiota affects expression of adiponectin and resistin through modifying DNA methylation in high-fat diet-induced obese mice. *Genes Nutr.* 2020;15(1):1–14.
286. Swidsinski A, Loening-Baucke V, Schulz S, Manowsky J, Verstraelen H, Swidsinski S. Functional anatomy of the colonic bioreactor: Impact of antibiotics and *Saccharomyces boulardii* on bacterial composition in human fecal cylinders. *Syst Appl Microbiol.* 2016;39(1):67–75.
287. Card RM, Mafura M, Hunt T, Kirchner M, Weile J, Rashid M-U, et al. Impact of ciprofloxacin and clindamycin administration on gram-negative bacteria isolated from healthy volunteers and characterization of the resistance genes they harbor. *Antimicrob Agents Chemother.* 2015;59(8):4410–6.
288. Monira S, Nakamura S, Gotoh K, Izutsu K, Watanabe H, Alam NH, et al. Metagenomic profile of gut microbiota in children during cholera and recovery. *Gut Pathog.* 2013;5(1):1.
289. Choo JM, Kanno T, Zain NMM, Leong LEX, Abell GCJ, Keeble JE, et al. Divergent relationships between fecal microbiota and metabolome following distinct antibiotic-induced disruptions. *MspHERE.* 2017;2(1):e00005-17.
290. Jačan A, Kashofer K, Zenz G, Fröhlich EE, Reichmann F, Hassan AM, et al. Synergistic

and antagonistic interactions between antibiotics and synbiotics in modifying the murine fecal microbiome. *Eur J Nutr.* 2020;59(5):1831–44.

291. Chen C-Y, Hsu K-C, Yeh H-Y, Ho H-C. Visualizing the effects of antibiotics on the mouse colonic mucus layer. *Tzu-chi Med J.* 2019;32(2):145.
292. Staley C, Kelly CR, Brandt LJ, Khoruts A, Sadowsky MJ. Complete microbiota engraftment is not essential for recovery from recurrent *Clostridium difficile* infection following fecal microbiota transplantation. *MBio.* 2016;7(6).
293. Mason KL, Downward JRE, Mason KD, Falkowski NR, Eaton KA, Kao JY, et al. Candida albicans and bacterial microbiota interactions in the cecum during recolonization following broad-spectrum antibiotic therapy. *Infect Immun.* 2012;80(10):3371–80.
294. Warn P, Thommes P, Sattar A, Corbett D, Flattery A, Zhang Z, et al. Disease progression and resolution in rodent models of *Clostridium difficile* infection and impact of antitoxin antibodies and vancomycin. *Antimicrob Agents Chemother.* 2016;60(11):6471–82.
295. Osman M-A, Neoh H, Ab Mutalib N-S, Chin S-F, Jamal R. 16S rRNA gene sequencing for deciphering the colorectal cancer gut microbiome: Current protocols and workflows. *Front Microbiol.* 2018;9:767.
296. Yang B, Wang Y, Qian P-Y. Sensitivity and correlation of hypervariable regions in 16S rRNA genes in phylogenetic analysis. *BMC Bioinformatics.* 2016;17(1):1–8.
297. Chakravorty S, Helb D, Burday M, Connell N, Alland D. A detailed analysis of 16S ribosomal RNA gene segments for the diagnosis of pathogenic bacteria. *J Microbiol Methods.* 2007;69(2):330–9.

298. Mitreva M. The Microbiome in infectious diseases. In: Infectious diseases. Elsevier; 2017. p. 68–74.
299. Fuks G, Elgart M, Amir A, Zeisel A, Turnbaugh PJ, Soen Y, et al. Combining 16S rRNA gene variable regions enables high-resolution microbial community profiling. *Microbiome*. 2018;6(1):1–13.
300. Janda JM, Abbott SL. 16S rRNA gene sequencing for bacterial identification in the diagnostic laboratory: pluses, perils, and pitfalls. *J Clin Microbiol*. 2007;45(9):2761–4.
301. Clarridge JE. Impact of 16S rRNA gene sequence analysis for identification of bacteria on clinical microbiology and infectious diseases. *Clin Microbiol Rev*. 2004;17(4):840–62.
302. Lau SKP, Teng JLL, Ho C-C, Woo PCY. Gene amplification and sequencing for bacterial identification. In: Methods in Microbiology. Elsevier; 2015. p. 433–64.
303. Alzu’bi A, Zhou L, Watzlaf V. Personal genomic information management and personalized medicine: challenges, current solutions, and roles of HIM professionals. *Perspect Heal Inf Manag*. 2014;11(Spring).
304. Ray P, Aich P. Effects of gut microbiota perturbation on Th1-and Th2-biased mice following treatment with Vancomycin. *bioRxiv*. 2019;516898.
305. Erikstrup LT, Aarup M, Hagemann-Madsen R, Dagnaes-Hansen F, Kristensen B, Olsen KEP, et al. Treatment of Clostridium difficile infection in mice with vancomycin alone is as effective as treatment with vancomycin and metronidazole in combination. *BMJ open Gastroenterol*. 2015;2(1):e000038.
306. Patel S, Preuss C V, Bernice F. Vancomycin. StatPearls. StatPearls Publishing; 2019.

307. Dekker JP, Frank KM. *Salmonella, Shigella, and Yersinia*. Vol. 35, *Clinics in Laboratory Medicine*. W.B. Saunders; 2015. p. 225–46.
308. Dhaliwal A. DNA extraction and purification. *Mater Methods*. 2013;3:191.
309. Mysara M, Njima M, Leys N, Raes J, Monsieurs P. From reads to operational taxonomic units: an ensemble processing pipeline for MiSeq amplicon sequencing data. *Gigascience*. 2017;6(2):1–10.
310. Caporaso JG, Kuczynski J, Stombaugh J, Bittinger K, Bushman FD, Costello EK, et al. QIIME allows analysis of high-throughput community sequencing data. *Nat Methods*. 2010;7(5):335.
311. DeSantis TZ, Hugenholtz P, Keller K, Brodie EL, Larsen N, Piceno YM, et al. NAST: A multiple sequence alignment server for comparative analysis of 16S rRNA genes. *Nucleic Acids Res*. 2006;34(WEB. SERV. ISS.):394–9.
312. DeSantis TZ, Hugenholtz P, Larsen N, Rojas M, Brodie EL, Keller K, et al. Greengenes, a chimera-checked 16S rRNA gene database and workbench compatible with ARB. *Appl Environ Microbiol*. 2006;72(7):5069–72.
313. Pradhan B, Guha D, Ray P, Das D, Aich P. Comparative Analysis of the Effects of Two Probiotic Bacterial Strains on Metabolism and Innate Immunity in the RAW 264.7 Murine Macrophage Cell Line. *Probiotics Antimicrob Proteins*. 2016;
314. Ghosh A, Mukherjee R, Aich P, Naik AK, Chakraborty S, Mukhopadhyay S, et al. Lactobacillus rhamnosus GG reverses mortality of neonatal mice against *Salmonella* challenge. *Toxicol Res (Camb)*. 2019;

315. Cruickshank-Quinn C, Zheng LK, Quinn K, Bowler R, Reisdorph R, Reisdorph N. Impact of blood collection tubes and sample handling time on serum and plasma metabolome and lipidome. *Metabolites*. 2018;8(4):88.
316. Shi Y, Kellingray L, Zhai Q, Le Gall G, Narbad A, Zhao J, et al. Structural and functional alterations in the microbial community and immunological consequences in a mouse model of antibiotic-induced dysbiosis. *Front Microbiol*. 2018;9.
317. Woting A, Blaut M. Small Intestinal Permeability and Gut-Transit Time Determined with Low and High Molecular Weight Fluorescein Isothiocyanate-Dextrans in C3H Mice. *Nutrients*. 2018;10(6):685.
318. Andrikopoulos S, Blair AR, Deluca N, Fam BC, Proietto J. Evaluating the glucose tolerance test in mice. *Am J Physiol Metab*. 2008;295(6):E1323–32.
319. Dhatt GS, Agarwal MM, Othman Y, Nair SC. Performance of the Roche Accu-Chek active glucose meter to screen for gestational diabetes mellitus using fasting capillary blood. *Diabetes Technol Ther*. 2011;13(12):1229–33.
320. Xia J, Sinelnikov I V, Han B, Wishart DS. MetaboAnalyst 3.0—making metabolomics more meaningful. *Nucleic Acids Res*. 2015;43(W1):W251--W257.
321. Xia J, Wishart DS. Web-based inference of biological patterns, functions and pathways from metabolomic data using MetaboAnalyst. *Nat Protoc*. 2011;6(6):743.
322. Hapfelmeier S, Stecher B, Barthel M, Kremer M, Müller AJ, Heikenwalder M, et al. The *Salmonella* pathogenicity island (SPI)-2 and SPI-1 type III secretion systems allow *Salmonella* serovar typhimurium to trigger colitis via MyD88-dependent and MyD88-

independent mechanisms. *J Immunol*. 2005;174(3):1675–85.

323. Zhou Y, Zhi F. Lower level of bacteroides in the gut microbiota is associated with inflammatory bowel disease: a meta-analysis. *Biomed Res Int*. 2016;2016.
324. Holzheimer RG. Antibiotic Induced Endotoxin Release and Clinical Sepsis: a Review. *J Chemother*. 2014;
325. Walf AA, Frye CA. The use of the elevated plus maze as an assay of anxiety-related behavior in rodents. *Nat Protoc*. 2007;2(2):322.
326. Desbonnet L, Garrett L, Clarke G, Kiely B, Cryan JF, Dinan TG. Effects of the probiotic *Bifidobacterium infantis* in the maternal separation model of depression. *Neuroscience*. 2010;170(4):1179–88.
327. Seibenhener ML, Wooten MC. Use of the open field maze to measure locomotor and anxiety-like behavior in mice. *J Vis Exp JoVE*. 2015;(96).
328. Rodrigues RR, Greer RL, Dong X, DSouza KN, Gurung M, Wu JY, et al. Antibiotic-induced alterations in gut microbiota are associated with changes in glucose metabolism in healthy mice. *Front Microbiol*. 2017;8:2306.
329. Reikvam DH, Erofeev A, Sandvik A, Grcic V, Jahnsen FL, Gaustad P, et al. Depletion of murine intestinal microbiota: Effects on gut mucosa and epithelial gene expression. *PLoS One*. 2011;
330. Hawk CT, Leary SL, Morris TH. Formulary for laboratory animals. Vol. 19. Iowa State University Press Ames, IA; 1999.

331. Miglioli PA, Allerberger F, Calabrò GB, Gaion RM. Effects of daily oral administration of rifaximin and neomycin on faecal aerobic flora in rats. *Pharmacol Res.* 2001;44(5):373–5.
332. Jernberg C, Löfmark S, Edlund C, Jansson JK. Long-term impacts of antibiotic exposure on the human intestinal microbiota. *Microbiology.* 2010;156(11):3216–23.
333. Fujisaka S, Ussar S, Clish C, Devkota S, Dreyfuss JM, Sakaguchi M, et al. Antibiotic effects on gut microbiota and metabolism are host dependent. *J Clin Invest.* 2016;126(12):4430–43.
334. Dunlop SP, Hebden J, Campbell E, Naesdal J, Olbe L, Perkins AC, et al. Abnormal intestinal permeability in subgroups of diarrhea-predominant irritable bowel syndromes. *Am J Gastroenterol.* 2006;101(6):1288.
335. Bosi E, Molteni L, Radaelli MG, Folini L, Fermo I, Bazzigaluppi E, et al. Increased intestinal permeability precedes clinical onset of type 1 diabetes. *Diabetologia.* 2006;49(12):2824–7.
336. Pepin J. Vancomycin for the treatment of *Clostridium difficile* infection: for whom is this expensive bullet really magic? *Clin Infect Dis.* 2008;46(10):1493–8.
337. Tang J, Hu J, Kang L, Deng Z, Wu J, Pan J. The use of vancomycin in the treatment of adult patients with methicillin-resistant *Staphylococcus aureus* (MRSA) infection: a survey in a tertiary hospital in China. *Int J Clin Exp Med.* 2015;8(10):19436.
338. Bernard L, Vaudaux P, Vuagnat A, Stern R, Rohner P, Pittet D, et al. Effect of vancomycin therapy for osteomyelitis on colonization by methicillin-resistant

Staphylococcus aureus: lack of emergence of glycopeptide resistance. *Infect Control Hosp Epidemiol.* 2003;24(9):650–4.

339. Christiansen CB, Gabe MBN, Svendsen B, Dragsted LO, Rosenkilde MM, Holst JJ. The impact of short chain fatty acids on GLP-1 and PYY secretion from the isolated perfused rat colon. *Am J Physiol Liver Physiol.* 2018;
340. Turner JR. Intestinal mucosal barrier function in health and disease. *Nat Rev Immunol.* 2009;9(11):799.
341. Ulluwishewa D, Anderson RC, McNabb WC, Moughan PJ, Wells JM, Roy NC. Regulation of tight junction permeability by intestinal bacteria and dietary components. *J Nutr.* 2011;141(5):769–76.
342. Sekirov I, Tam NM, Jogova M, Robertson ML, Li Y, Lupp C, et al. Antibiotic-induced perturbations of the intestinal microbiota alter host susceptibility to enteric infection. *Infect Immun.* 2008;76(10):4726–36.
343. Sun L, Zhang X, Zhang Y, Zheng K, Xiang Q, Chen N, et al. Antibiotic-induced disruption of gut microbiota alters local metabolomes and immune responses. *Front Cell Infect Microbiol.* 2019;9(APR).
344. Wahid HH, Dorian CL, Chin PY, Hutchinson MR, Rice KC, Olson DM, et al. Toll-like receptor 4 is an essential upstream regulator of on-time parturition and perinatal viability in mice. *Endocrinology.* 2015;156(10):3828–41.
345. Vrieze A, Out C, Fuentes S, Jonker L, Reuling I, Koote RS, et al. Impact of oral vancomycin on gut microbiota, bile acid metabolism, and insulin sensitivity. *J Hepatol.*

2014 Apr;60(4):824–31.

346. Khan TJ, Hasan MN, Azhar EI, Yasir M. Association of gut dysbiosis with intestinal metabolites in response to antibiotic treatment. *Hum Microbiome J*. 2019;
347. Dao MC, Everard A, Aron-Wisnewsky J, Sokolovska N, Prifti E, Verger EO, et al. Akkermansia muciniphila and improved metabolic health during a dietary intervention in obesity: relationship with gut microbiome richness and ecology. *Gut*. 2016;65(3):426–36.
348. Segain JP, De La Blétiere DR, Bourreille A, Leray V, Gervois N, Rosales C, et al. Butyrate inhibits inflammatory responses through NFκB inhibition: implications for Crohn’s disease. *Gut*. 2000;47(3):397–403.
349. Maier E, Anderson RC, Roy NC. Understanding how commensal obligate anaerobic bacteria regulate immune functions in the large intestine. *Nutrients*. 2014;7(1):45–73.
350. Lyte M, Li W, Opitz N, Gaykema RPA, Goehler LE. Induction of anxiety-like behavior in mice during the initial stages of infection with the agent of murine colonic hyperplasia *Citrobacter rodentium*. *Physiol Behav*. 2006;89(3):350–7.
351. Desbonnet L, Clarke G, Shanahan F, Dinan TG, Cryan JF. Microbiota is essential for social development in the mouse. *Mol Psychiatry*. 2014;19(2):146.
352. Heijtz RD, Wang S, Anuar F, Qian Y, Björkholm B, Samuelsson A, et al. Normal gut microbiota modulates brain development and behavior. *Proc Natl Acad Sci*. 2011;108(7):3047–52.
353. Neufeld K-AM, Kang N, Bienenstock J, Foster JA. Effects of intestinal microbiota on anxiety-like behavior. *Commun Integr Biol*. 2011;4(4):492–4.

354. Yu H, Chen Z. The role of BDNF in depression on the basis of its location in the neural circuitry. *Acta Pharmacol Sin.* 2011;32(1):3.
355. Knoop KA, McDonald KG, Kulkarni DH, Newberry RD. Antibiotics promote inflammation through the translocation of native commensal colonic bacteria. *Gut* [Internet]. 2016 Jul;65(7):1100 LP-- 1109. Available from: <http://gut.bmjjournals.org/content/65/7/1100.abstract>
356. Kelly JR, Kennedy PJ, Cryan JF, Dinan TG, Clarke G, Hyland NP. Breaking down the barriers: the gut microbiome, intestinal permeability and stress-related psychiatric disorders. *Front Cell Neurosci.* 2015;9:392.
357. Dantzer R, O'Connor JC, Freund GG, Johnson RW, Kelley KW. From inflammation to sickness and depression: when the immune system subjugates the brain. *Nat Rev Neurosci.* 2008;9(1):46.
358. Suliman S, Hemmings SMJ, Seedat S. Brain-Derived Neurotrophic Factor (BDNF) protein levels in anxiety disorders: systematic review and meta-regression analysis. *Front Integr Neurosci.* 2013;7:55.
359. Neufeld KM, Kang N, Bienenstock J, Foster JA. Reduced anxiety-like behavior and central neurochemical change in germ-free mice. *Neurogastroenterol Motil.* 2011;23(3):255--e119.
360. Huo R, Zeng B, Zeng L, Cheng K, Li B, Luo Y, et al. Microbiota modulate anxiety-like behavior and endocrine abnormalities in hypothalamic-pituitary-adrenal axis. *Front Cell Infect Microbiol.* 2017;7:489.

361. Dantzer R, Konsman J-P, Bluthé R-M, Kelley KW. Neural and humoral pathways of communication from the immune system to the brain: parallel or convergent? *Auton Neurosci*. 2000;85(1–3):60–5.
362. Donaldson GP, Lee SM, Mazmanian SK. Gut biogeography of the bacterial microbiota. *Nat Rev Microbiol*. 2016;14(1):20.
363. Petra AI, Panagiotidou S, Hatziagelaki E, Stewart JM, Conti P, Theoharides TC. Gut-microbiota-brain axis and its effect on neuropsychiatric disorders with suspected immune dysregulation. *Clin Ther*. 2015;37(5):984–95.
364. Saunders PR, Santos J, Hanssen NPM, Yates D, Groot JA, Perdue MH. Physical and psychological stress in rats enhances colonic epithelial permeability via peripheral CRH. *Dig Dis Sci*. 2002;47(1):208–15.
365. Contijoch EJ, Britton GJ, Yang C, Mogno I, Li Z, Ng R, et al. Gut microbiota density influences host physiology and is shaped by host and microbial factors. *Elife*. 2018;8:277095.
366. Maldonado RF, Sa-Correia I, Valvano MA. Lipopolysaccharide modification in Gram-negative bacteria during chronic infection. *FEMS Microbiol Rev*. 2016;40(4):480–93.
367. Mosca A, Leclerc M, Hugot JP. Gut Microbiota Diversity and Human Diseases: Should We Reintroduce Key Predators in Our Ecosystem? *Front Microbiol* [Internet]. 2016 Mar;7:455. Available from: <https://www.ncbi.nlm.nih.gov/pubmed/27065999>
368. Hakansson A, Molin G. Gut microbiota and inflammation. *Nutrients*. 2011.
369. Ochoa-Repáraz J, Mielcarz DW, Ditrio LE, Burroughs AR, Foureau DM, Haque-Begum

S, et al. Role of gut commensal microflora in the development of experimental autoimmune encephalomyelitis. *J Immunol.* 2009;183(10):6041–50.

370. Gancarčíková S, Popper M, Hrčková G, Maďar M, Mudroňová D, Sopková D, et al. Antibiotic-treated SPF mice as a gnotobiotic model. In: *Antibiotic Use in Animals*. IntechOpen; 2017.
371. Kennedy EA, King KY, Baldridge MT. Mouse microbiota models: comparing germ-free mice and antibiotics treatment as tools for modifying gut bacteria. *Front Physiol.* 2018;9:1534.
372. Rakoff-Nahoum S, Paglino J, Eslami-Varzaneh F, Edberg S, Medzhitov R. Recognition of commensal microflora by toll-like receptors is required for intestinal homeostasis. *Cell.* 2004;118(2):229–41.
373. Lindenberg F, Krych L, Fielden J, Kot W, Frøkiær H, van Galen G, et al. Expression of immune regulatory genes correlate with the abundance of specific Clostridiales and Verrucomicrobia species in the equine ileum and cecum. *Sci Rep.* 2019;9(1):1–10.
374. Cohen-Poradosu R, McLoughlin RM, Lee JC, Kasper DL. *Bacteroides fragilis*–stimulated interleukin-10 contains expanding disease. *J Infect Dis.* 2011;204(3):363–71.
375. Hessle C, Andersson B, Wold AE. Gram-positive bacteria are potent inducers of monocytic interleukin-12 (IL-12) while gram-negative bacteria preferentially stimulate IL-10 production. *Infect Immun.* 2000;68(6):3581–6.
376. Johansson MA, Saghafian-Hedengren S, Haileselassie Y, Roos S, Troye-Blomberg M, Nilsson C, et al. Early-life gut bacteria associate with IL-4–, IL-10– and IFN- γ production

at two years of age. PLoS One. 2012;7(11).

377. Qi H, Gao Y, Li Y, Wei J, Su X, Zhang C, et al. Induction of Inflammatory Macrophages in the Gut and Extra-Gut Tissues by Colitis-Mediated Escherichia coli. iScience. 2019;21:474–89.
378. Jones-Hall YL, Nakatsu CH. The Intersection of TNF, IBD and the Microbiome. Gut Microbes. 2016;7(1):58–62.
379. Liubakka A, Vaughn BP. Clostridium difficile infection and fecal microbiota transplant. AACN Adv Crit Care. 2016;27(3):324–37.
380. Smith P, Willemse D, Popkes M, Metge F, Gandiwa E, Reichard M, et al. Regulation of life span by the gut microbiota in the short-lived African turquoise killifish. Elife. 2017;6:1–26.
381. Wickham ME, Brown NF, Provias J, Finlay BB, Coombes BK. Oral infection of mice with *Salmonella enterica* var *Typhimurium* causes meningitis and infection of the brain. BMC Infect Dis. 2007;7(1):65.
382. Chaudhuri D, Roy Chowdhury A, Biswas B, Chakravortty D. *Salmonella typhimurium* infection leads to colonization of the mouse brain and is not completely cured with antibiotics. Front Microbiol. 2018;9:1632.
383. Nilsson OR, Kari L, Steele-Mortimer O. Highly reproducible murine model of oral *Salmonella* infection via inoculated food. BioRxiv. 2019;593442.
384. Ubeda C, Djukovic A, Isaac S. Roles of the intestinal microbiota in pathogen protection. Clin Transl Immunol. 2017;6(2).

385. Reijnders D, Goossens GH, Hermes GDA, Neis EPJG, van der Beek CM, Most J, et al. Effects of Gut Microbiota Manipulation by Antibiotics on Host Metabolism in Obese Humans: A Randomized Double-Blind Placebo-Controlled Trial. *Cell Metab.* 2016;
386. Cani PD, Delzenne NM. The role of the gut microbiota in energy metabolism and metabolic disease. *Curr Pharm Des.* 2009;15(13):1546–58.
387. Korach-Rechtman H, Freilich S, Gerassy-Vainberg S, Buhnik-Rosenblau K, Danin-Poleg Y, Bar H, et al. Murine genetic background has a stronger impact on the composition of the gut microbiota than maternal inoculation or exposure to unlike exogenous microbiota. *Appl Environ Microbiol.* 2019;85(18):e00826-19.
388. Thangaraju M, Cresci GA, Liu K, Ananth S, Gnanaprakasam JP, Browning DD, et al. GPR109A is a G-protein–coupled receptor for the bacterial fermentation product butyrate and functions as a tumor suppressor in colon. *Cancer Res.* 2009;69(7):2826–32.
389. Koido S, Ohkusa T, Kajiura T, Shinozaki J, Suzuki M, Saito K, et al. Long-term alteration of intestinal microbiota in patients with ulcerative colitis by antibiotic combination therapy. *PLoS One.* 2014;9(1):e86702.
390. Willing BP, Dicksved J, Halfvarson J, Andersson AF, Lucio M, Zheng Z, et al. A pyrosequencing study in twins shows that gastrointestinal microbial profiles vary with inflammatory bowel disease phenotypes. *Gastroenterology.* 2010;139(6):1844–54.
391. Zhang Q, Wu Y, Wang J, Wu G, Long W, Xue Z, et al. Accelerated dysbiosis of gut microbiota during aggravation of DSS-induced colitis by a butyrate-producing bacterium. *Sci Rep.* 2016;6(1):1–11.

Abbreviations

AAA	Aromatic Amino Acid
ANOVA	Analysis of variance
AVNM	Ampicillin, Vancomycin, Neomycin, Metronidazole
BDNF	Brain-derived neurotrophic factor
CD	Crohn's disease
CFU	Colony Forming Unit
CMT	Cecal Microbiota Transplantation
CMT	Cecal microbiota Transplantation
CRH	Corticotropin releasing hormone
CRHBP	Corticotropin-releasing factor-binding protein
DCS	Dendritic cells
E.coli	<i>Escherichia coli</i>
EC cells	Enterochromaffin cells
ELISA	Enzyme-Linked Immunoassay
EMB	Eosin Methylene Blue
EPM	Elevated Plus Maze

F/B ratio Firmicutes to Bacteroidetes ratio

FFAR2 Free fatty acid receptor

FITC Fluorescein isothiocyanate

FMT Fecal Microbiota Transplantation

FST Forced Swim test

GALT Gut-associated lymphoid tissue

gDNA Genomic DNA

GF mice Germ-free mice

GI tract Gastrointestinal tract

GLP-1 Glucagon-like peptide 1

GPCR G protein-coupled receptor

HPA axis Hypothalamic-pituitary-adrenal axis

IBD Inflammatory Bowel Disease

IECs Intestinal epithelium cells

IL Interleukin

IgA Immunoglobulin- A

LAL Limulus amebocyte lysate

LP	Lamina propria
LPS	Lipopolysaccharide
MAMPs	Microbial associated molecular patterns
NGS	Next-generation sequence
NMR	Nuclear Magnetic Resonance
OFT	Open Field Test
OGTT	Oral Glucose Tolerance Test
OTU	Operational taxonomic unit
PBS	Phosphate-buffered Saline
PCI	Phenol-chloroform isoamyl alcohol
PPAR- γ	Peroxisome proliferator receptor- γ
PSA	Polysaccharide A
PYY	Peptide YY
RCF	Relative centrifugal force
SCFA	Short-chain fatty acids
SDS	Sodium dodecyl sulfate
SFB	Segmented Filamentous Bacteria

SPF Specific pathogen-free

ST *Salmonella Typhimurium*

TGF- β Transforming growth factor-beta

TLR Toll-Like receptor

T_{reg} T regulatory cells

V1 region Variable regions

Thesis Highlight

Name of the Student: Pratikshya Ray

Name of the CI/OCC: National Institute of Science Education and Research

Enrolment No.: LIFE11201404008

Thesis Title: Effects of perturbation of gut microbiota on host physiology: In C57BL/6 and BALB/c mice models

Discipline: Life Sciences

Sub-Area of Discipline: Microbiome and Immunity

Date of viva voce: 17th May 2021

Gut, in mammals, harbors a large number of diverse microbiota which plays a major role in maintaining the health and homeostasis of the host. An effective way to understand the role of gut microbiota in the host is to perturb the gut microbial population. We used some commonly available antibiotics such as vancomycin, neomycin, and AVNM cocktail to perturb the gut microbiota and understand the altered host response in terms of metabolic, innate immune profile, and behavioral changes in mice. The study was performed in both Th2-(BALB/c) and Th1- (C57BL/6) biased mice models. The restoration patterns of the gut microbiota were also observed by cecal microbiota transplantation. The current study established that initial doses of vancomycin increased pathogenic bacteria but the continued doses of vancomycin provided significant health-related benefits to the host by increasing beneficial microbes of Verrucomicrobia phylum (*A. muciniphila*) more in C57BL/6 (Th1) than BALB/c (Th2) mice. Results revealed that each type of antibiotic treatment followed certain time-dependent perturbation patterns of gut microbiota. These alteration patterns varied significantly between C57BL/6 and BALB/c mice models. A strong correlation was observed between the dysbiosis pattern of gut microbes with the expression of different immune regulatory genes and the stress level of the host. We also found that during antibiotic treatments, the alteration in the abundance of four major phyla, i.e., Firmicutes, Bacteroidetes, Proteobacteria, and Verrucomicrobia mainly affected the metabolism of glucose, aromatic amino acid, and short-chain fatty acids of the host. The further result revealed that the restoration pattern of gut microbiota varied between two strains of mice and maximum gut microbes restored efficiently within 15days following the termination of antibiotics treatment. Cecal microbiota transplantation (CMT) restored both the diversity and composition of gut microbiota more efficiently following antibiotic treatment compared to non-CMT recipient mice.

Fig.1. showing the antibiotic-induced perturbation and restoration of gut microbiota and its effect on host physiology.

